สกว
TRF

สำนักงานคณะกรรมการการอุดมศึกษา

รายงานวิจัยฉบับสมบูรณ์

โครงการ การพัฒนาวัสดุประกอบแต่งพอลิเบนซอกซาซีนดัดแปรด้วยอนุภาคยางระดับนาโนเมตร สำหรับวัสดุต้านทานการสึกหรอ

โดย ผู้ช่วยศาสตราจารย์ ดร.จันจิรา จับศิลป์ และคณะ

31 สิงหาคม 2558

สัญญาเลขที่ MRG5580101

รายงานวิจัยฉบับสมบูรณ์

โครงการ การพัฒนาวัสดุประกอบแต่งพอลิเบนซอกซาซีนดัดแปรด้วยอนุภาคยางระดับนาโนเมตร สำหรับวัสดุต้านทานการสึกหรอ

โดย ผู้ช่วยศาสตราจารย์ ดร.จันจิรา จับศิลป์ และคณะ
ภาควิชาวิศวกรรมเคมี คณะวิศวกรรมศาสตร์
มหาวิทยาลัยศรีนครินทรวิโรฒ

สนับสนุนโดยสำนักงานกองทุนสนับสนุนการวิจัย

Acknowledgements

This research is supported by a New Researcher's Grant of Thailand Research Fund-Commission on Higher Education (MRG5580101) and Matching Fund, Strategic Wisdom and Research Institute, Srinakharinwirot University 2012-2014 (Contact Grants No. 411/2555). The authors also greatly acknowledged the National Research University Project, Office of Higher Education Commission, Thailand (WCU028-AM-57). Additional funding is from the Matsumae International Foundation (2012), Japan. Thai Polycarbonate Co., Ltd. (TPCC) for bisphenol-A supply is also gratefully acknowledged.

บทคัดย่อ

รหัสโครงการ : MRG5580101

ชื่อโครงการ : การพัฒนาวัสดุประกอบแต่งพอลิเบนซอกซาซีนดัดแปรด้วยอนุภาคยางระดับนาโนเมตร สำหรับวัสดุต้านทานการสึกหรอ

ชื่อนักวิจัย : ผู้ช่วยศาสตราจารย์ ดร. จันจิรา จับศิลป์
ภาควิชาวิศวกรรมเคมี คณะวิศวกรรมศาสตร์ มหาวิทยาลัยศรีนครินทรวิโรฒ
โทรศัพท์ 02-649-5000 ต่อ 22119, 092-025-0820

E-mail Address: chanchira@g.swu.ac.th

ระยะเวลาโครงการ : 2 กรกฎาคม 2555 ถึง 1 กรกฎาคม 2557

งานวิจัยนี้ศึกษาผลของปริมาณยางเหลวชนิดอะมีนเทอร์มิเนตเทตบิวทาไดอีน-อะไครโลไนไตร์ลต่อสมบัติต่างๆ ของพอลิเบนซอกซาซีนโคพอลิเมอร์และพอลิเบนซอกซาซีนคอมพอสิท สำหรับระบบยางเหลวอะมีนเทอร์มิเนตเทตบิวทาไดอีน-อะไครโลไนไตร์ล-พอลิเบนซอกซาซีนโคพอลิเมอร์ เวลาในการเกิดเจลและอุณหภูมิการบ่มของเบนซอกซาซีนเรซินจะมีค่าลดลงเมื่อปริมาณยางเหลวอะมีนเทอร์มิเนตเทตบิวทาไดอีน-อะไครโลไนไตร์ลเพิ่มขึ้น อีกทั้งการเติมยางเหลวอะมีนเทอร์มิเนตเทตบิวทาไดอีน-อะไครโลไนไตร์ลที่ปริมาณ 1-5 เปอร์เซ็นต์โดยน้ำหนัก ในพอลิเบนซอกซาซีน ส่งผลให้สมบัติการเสียดทาน เช่น ค่าสัมประสิทธิ์การเสียดทานและอัตราการสูญเสียมวลจำเพาะของพอลิเบนซอกซีนลดลง นอกจากนี้การเติมยางเหลวอะมีนเทอร์มิเนตเทตบิวทาไดอีน-อะไครโลไนไตร์ลที่ปริมาณ 1-5 เปอร์เซ็นต์โดยน้ำหนัก ส่งผลให้พอลิเบนซอกซาซีนโคพอลิเมอร์มีค่าสตรอเรจมอดุลัสและอุณหภูมิการเปลี่ยนสถานะคล้ายแก้วที่คงที่ ในขณะที่พอลิเบนซอกซาซีนช่วยให้พอลิเบนซาซีนโคพอลิเมอร์มีความเสถียรทางความร้อนที่ดี สำหรับวัสดุยางเหลวอะมีนเทอร์มิเนตเทตบิวทาไดอีน-อะไครโลไนไตร์ล-พอลิเบนซอกซาซีนคอมพอสิท พบว่า การเติมยางเหลวอะมีนเทอร์มิเนตเทตบิวทาไดอีน-อะไครโลไนไตร์ลในพอลิเบนซอกซาซีนคอมพอสิท ส่งผลให้ชิ้นงานคอมพอสิทมีสมบัติการเสียดทานและสมบัติทางกลที่ดีขึ้นเมื่อเทียบกับสมบัติการเสียดทานและสมบัติทางกลของพอลิเบนซอกซา-ซีนคอมพอสิทที่ไม่ได้ทำการดัดแปรด้วยยางเหลวอะมีนเทอร์มิเนตเทตบิวทาไดอีน-อะไครโลไนไตร์ล ซึ่งการเติมยางเหลวอะมีนเทอร์มิเนตเทตบิวทาไดอีน-อะไครโลไนไตร์ลในปริมาณ 5 เปอร์เซ็นต์โดยน้ำหนัก ในพอลิเบนซอกซาซีนคอมพอสิท ส่งผลให้ชิ้นงานพอลิเบนซอกซาซีนคอมพอสิทมีค่าสัมประสิทธิ์การเสียดทานลดลงอย่างเห็นได้ชัด โดยมีค่าเท่ากับ 0.15 ในขณะที่ค่าสัมประสิทธิ์การเสียดทานของพอลิเบนซอกซาซีนคอมพอสิทที่ไม่ได้ทำการดัดแปรมีค่าเท่ากับ 0.28 นอกจากนี้กลไกการขัดสีของชิ้นงานยางเหลวอะมีนเทอร์มิเนตเทตบิวทาไดอีน-อะไครโลไนไตร์ล-พอลิเบนซอกซาซีนคอมพอสิทสามารถสังเกตได้จากพื้นผิวของชิ้นงานที่ผ่านการขัดสี ดังนั้นวัสดุพอลิเบนซอกซาซีนคอมพอสิทที่ดัดแปรด้วยยางเหลวอะมีนเทอร์มิเนตเทตบิวทาไดอีน-อะไครโลไนไตร์ล จึงสามารถนำไปประยุกต์ใช้ในงานที่ต้องการค่าสัมประสิทธิ์การเสียดทานค่อนข้างต่ำ ความต้านทานต่อการขัดสีได้ดี และค่ามอดุลัสและความเสถียรทางความร้อนที่ดี

คำหลัก : ยาง การขัดสี การหล่อลื่น โคพอลิเมอร์ คอมพอสิท เทอร์โมเซต

Abstract

Project Code : MRG5580101

Project Title : Development of nano powdered rubber-modified polybenzoxazine composites for friction materials

Investigator : Asst. Prof. Dr. Chanchira Jubsilp
Department of Chemical Engineering, Faculty of Engineering
Srinakharinwirot University

E-mail Address : chanchira@g.swu.ac.th, chanchira@swu.ac.th

Project Period : 2 July 2012 to 1 July 2014

Effects of amine terminated butadiene–acrylonitrile (ATBN) on properties of bisphenol-A/aniline based polybenzoxazine (PBA-a) and their composites were investigated. ATBN systematically decreased gel time and lowered curing temperature of the benzoxazine resin (BA-a). The inclusion of the ATBN at 5wt% was found to decrease friction coefficient and improve wear resistance of the obtained PBA-a/ATBN copolymers. Storage modulus and glass transition temperature of the PBA-a was maintained with an addition of the ATBN in the range of 1-5% by weight. An increase of the PBA-a content can impart thermal stability of the copolymers. The PBA-a/ATBN-based self-lubricating composites were observed to provide substantial enhancement in their tribological properties, i.e. fiction coefficient (0.36 for 5wt% ATBN modified polybenzoxazine and 0.38 for polybenzoxazine) and mechanical properties. The plausible wear mechanism of the composites was also investigated based on their worn surface morphology. The obtained PBA-a/ATBN self-lubricating composites are highly attractive for bearing material applications that require low friction coefficient, high wear resistance, and high modulus with good thermal stability.

Keywords: rubber; friction; lubrication; copolymers; composites; thermosets

Executive Summary

Nowadays, a wide range of friction and wear materials serving industries with products suitable for a variety of applications including self-lubricating materials, industrial equipment, automotive and aerospace has been investigated. In some cases, it has to be accepted that, frictional force sometimes needs to be increased for safety reason such as in automobile brakes, friction clutches and tires on icy roadways, while the reduction of friction and wear, in many cases, is still the primary objective such as in coating, engineered bearing materials, and other engineering applications. Polymers and their composites are finding ever increasing usage for numerous industrial applications replacing traditional metallic materials, particularly in sliding/rolling components such as bearings, rollers, gears, cams, wheels, piston rings and clutches where their self lubricating properties (low friction coefficient) are exploited to avoid the need for oil or grease lubrication with its attendant problems of contamination.

Therefore, this research studied effects of liquid amine terminated butadiene–acrylonitrile (ATBN) on rheological, cure kinetics, triboligical, thermal and mechanical properties of bisphenol-A/aniline based polybenzoxazine (PBA-a) and their composites for self-lubricating materials. Liquid ATBN systematically decreased gel time, lowered curing temperature and curing activation energy of the benzoxazine resin (BA-a). The inclusion of the ATBN at 5wt% was found to decrease friction coefficient and improve wear resistance of the obtained PBA-a/ATBN copolymers. The coefficient of friction for the copolymer was 0.36, while that of polybenzoxazine showed 0.38. Storage modulus (E') and glass transition temperature (T_g) of the PBA-a was maintained with an addition of the ATBN in the range of 1-5wt%, i.e. E'= 4.5-5.2 GPa and T_gs = 168-172°C. An increase of the PBA-a content can impart thermal stability of the copolymers Furthermore, the PBA-a/ATBN-based self-lubricating composites are observed to provide substantial enhancement in their tribological and mechanical properties. It was found that the ATBN-modified polybenzoxazine based self-lubricating composites showed a significantly low friction coefficient value and specific wear rate at the optimal ATBN content of 5wt%, i.e. 0.15 and 6.07×10^{-5} mm^3/Nm, respectively. The mechanical and thermal properties of the composites are still maintained with an addition of ATBN content at less than 10 wt%, i.e. T_g ~ 190°C, σ_f ~ 47.6 MPa and E_f = 5.9 GPa. In addition, the ether bonds formed between the polybenzoxazine and the ATBN is attributed to the significant improvement on thermal and mechanical properties of the resulting polybenzoxazine/ATBN based self-lubricating composites.

Contents

Page

Introduction

1.1 General Introduction

Nowadays, a wide range of friction and wear materials serving industries with products suitable for a variety of applications including self-lubricating materials, industrial equipment, automotive and aerospace industries has been investigated [1-4]. Moreover, polymers and their composites can be used to replace traditional metallic-based self-lubricating materials, particularly in sliding/rolling components such as bearings, rollers, and gears where their self lubricating properties (low friction coefficient) are exploited to avoid the need for oil or grease lubrication with its attendant problems of contamination. However, in the case of the polymer-based self-lubricating materials, temperature ranges, dimensional stability, and load limitations are in general less than the metallic-based self-lubricating materials, but the materials are remarkably versatile and economical. Typically, the most commonly used polymer for the polymer-based self-lubricating material, i.e. bearings is phenolics. However, these resins have various limitations, most notably when used in sufficient concentration to impart strength; the material may become too rigid or brittle for the applications. Therefore, modifications have been made to phenolics to address these limitations including the modification of the phenolic with such moieties as cashew nut shell liquid, epoxy, and various rubbers. In addition, poor shelf life, evolution of harmful volatiles during processing, and shrinkage in final products along with voids are the major problems of the phenolics. In order to overcome those problems, the alternative resins, i.e. benzoxazine resins were synthesized in the present work to replace currently used phenolics.

Benzoxazine resins, new types of phenolics, have been synthesized from phenol, formaldehyde, and amine to yield a relatively clean precursor, without the need of solvent elimination or monomer purification. After the ring-opening polymerization of benzoxazine monomers, polybenzoxazine overcomes many shortcomings of traditional phenolics such as using acid or base catalyst, and releasing condensation by-products, meanwhile it can retain good thermal properties, and flame retardancy of phenolics. Besides, they have a very low melt viscosity, dimensional stability, fast development of mechanical properties as a function of curing conversion, low water absorption, and low dielectric constant [5]. Polybenzoxazines have been used as a matrix for highly filled composites [6, 7]. In addition, polybenzoxazines are used automotive [8], electronic packaging [9], and aerospace industries [5]. Moreover, an ability of benzoxazine resins to blend with various other resins or polymers results in new resins with a broad range of applications [5, 10, 11]. For example, blending between benzoxazine resins and epoxy resins, polyurethanes, and dianhydrides [12-16] was considered to be a potentially effective measure to enhance thermal or mechanical properties as well as flammability of the polymers. Furthermore, thermosetting copolymers based on benzoxazine resins and rubbers such as amine-terminated acrylonitrile-butadiene (ATBN), and epoxy-terminated liquid nitrile rubber (ETBN) have been reported to provide various useful characteristics [17, 18]. As an example, the combination of *N*-alkyl benzoxazine resin with ATBN resulted in a significant enhancement of the fracture toughness properties of the polybenzoxazine. The cause of these particular responses is attributed to secondary molecular interactions between the toughening additive and the structural molecules of the polybenzoxazine network. In addition, the presence of rubbery particles creates stress concentration, which acts as initiation sites for plastic shear deformation of the binder/matrix and cavitation of the rubber particles. Consequently, this characteristic provides an additional energy dissipation mechanism.

Although previous studies have found that the liquid rubber can improve the toughness of the polybenzoxazine [17, 18], there is very little or no information about the effect of the liquid rubber on the rheology, cure kinetics, tribological behaviors of the polymer for self-lubricating polymer composites. Therefore, in this work, those behaviors of outstanding liquid rubber-modified polybenzoxazine composites including liquid rubber-modified polybenzoxazine filled with a fiber base, a friction modifier and filler will be investigated in order to design tribosystems and select materials based on the wear map. A better understanding of wear rate, varieties of wear modes and wear mechanisms will be provided within the scope of this study.

1.2 Objectives of This Research

1.2.1 To develop nano powdered rubber-modified polybenzoxazine composites for friction materials.

1.2.2 To systematically investigate the effect of nano powdered rubber contents on curing behaviors of the nano powdered rubber-modified polybenzoxazine.

1.2.3 To study the effect of nano powdered rubber contents on thermomechanical and tribological properties of the nano powdered rubber-modified polybenzoxazine.

1.2.4 To evaluate the effect of on the thermal, mechanical and some important tribological properties of the resulting nano powdered rubber-modified polybenzoxazine composites.

1.2.5 To determine the interfacial bonding between nano powdered rubber-modified polybenzoxazine and a fiber base or a friction modifier, or a filler.

Theory

2.1 Types of Thermosetting Polymers

During the past decades, thermosetting polymers are well established in areas where thermoplastics cannot compete because of either properties or costs. For example, phenolics constitute a first option when fire resistance is required because they are self-extinguishing and exhibit low smoke emission. Urea-formaldehyde polymers for wood agglomerates and melamine-formaldehyde for furniture coatings give products of good quality at low costs. Unsaturated polyesters are extensively used to produce structural part with glass-fiber reinforcement. In addition, epoxies, cyanate, esters, and polyimide are employed for aeronautical and electronic applications where their excellent properties cannot be matched by thermoplastics. However, in the case of phenolic resins, these resins have various limitations; most notably when used in sufficient concentration to impart strength the material may become too rigid or brittle for the applications. In addition, poor shelf life, evolution of harmful volatiles during processing, need of inclusion of curing agent before dispatching to the market, shrinkage in final products along with voids are the major problems of the phenolics. In order to overcome those problems, a newly developed thermosetting resin with interesting properties, polybenzoxazine, was investigated in recent years.

2.2 Benzoxazine Resin [5, 10]

Recently introduced benzoxazine resins overcome almost all drawbacks of conventional phenolic resins, Furthermore, the materials exhibit a number of special properties that have been rarely observed in other commonly used polymers. The resin chemistry is based on a ring-opening polymerization of benzoxazine precursors. The material offers superb molecular design flexibility, while performance properties can be tailored and optimized to meet specific application requirements. The benzoxazine resin can be synthesized from phenolic derivatives, primary amine, and aldehyde. Benzoxazine resin can be classified into a monofuctional and a bifunctional type depending on a type of phenol used as shown in Fig. 2.1 and Fig. 2.2.

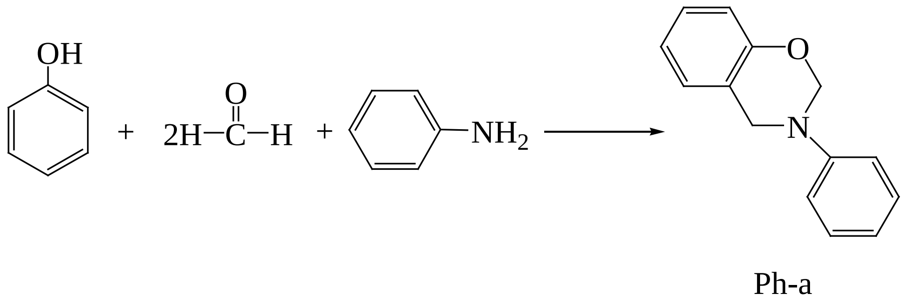

Fig. 2.1 Synthesis of phenol-aniline type benzoxazine monomer.

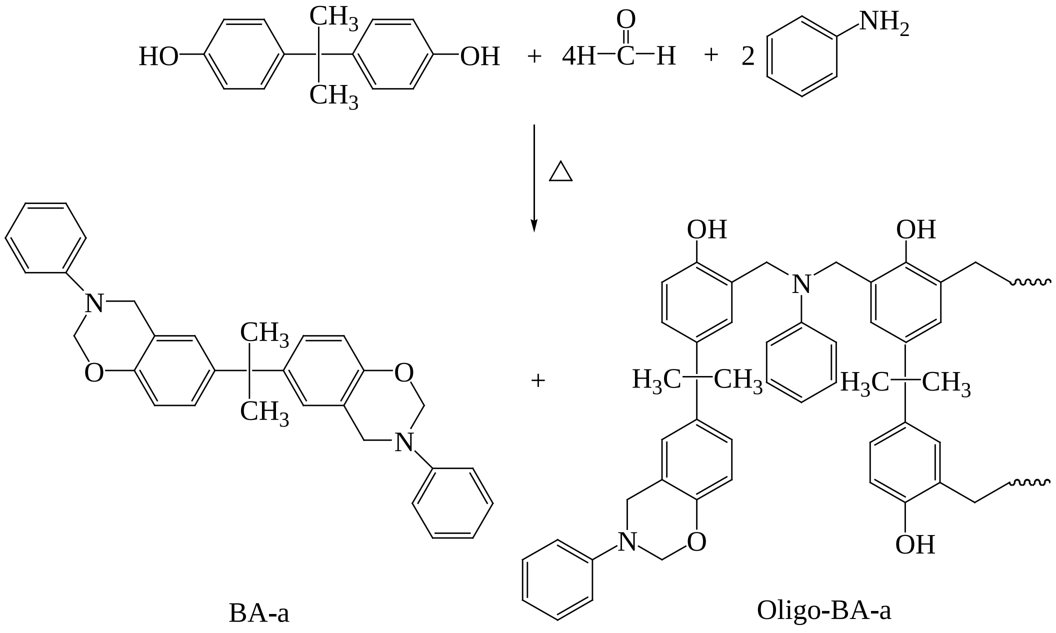

Fig. 2.2 Synthesis of bisphenol A and aniline based benzoxazine (BA-a) monomer.

The polymerization occurs by a simple ring-opening addition reaction and did not yield any reaction by-product. Benzoxazine resins cure without the aid of any strong acid catalysts required by traditional phenolic materials. Various polymerization mechanisms proposed in the literature as can be seen in Fig. 2.3.

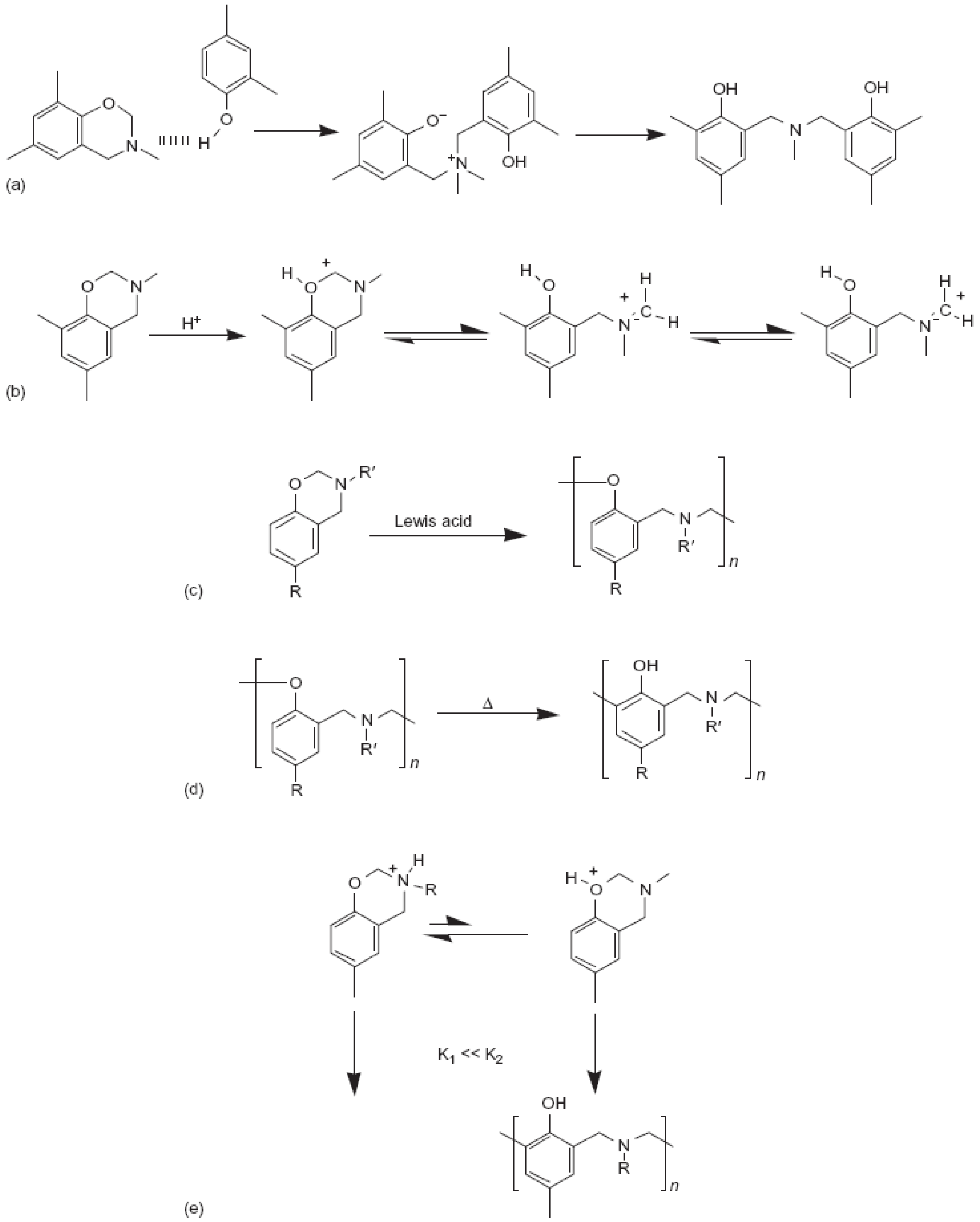

Fig. 2.3 Various polymerization mechanisms proposed in the literature.

Benzoxazine is a single benzene ring fused to another six-membered heterocycle group containing one oxygen atom and a single nitrogen atom, called an oxazine ring. The oxazine ring is the reactive site for curing of the benzoxazine. There are a number of possible isomers of benzoxazine depending on the relative positions of the two heteroatoms and the degree of oxidation of this oxazine ring system. Benzoxazine may be synthesized as monofunctional or difunctional. The latter can produce crosslinked structures. The polymerization of monofunctional benzoxazine produces only linear oligomeric phenolic structure. However, difunctional benzoxazine monomers are tetrafunctional in terms of reactive sites and can be polymerized to form crosslinked networks, resulting in phenolic materials with substantial mechanical integrity. The polybenzoxazines overcome many of the traditional shortcomings of conventional novolak and resole type phenolic resins, while retaining their benefits. Table 2.1 compares the properties of polybenzoxazine with those of the state-of-the-art matrices.

Table 2.1 Comparison of the physical and mechanical properties of cross-linked polybenzoxazine with an epoxy and phenolic resin.

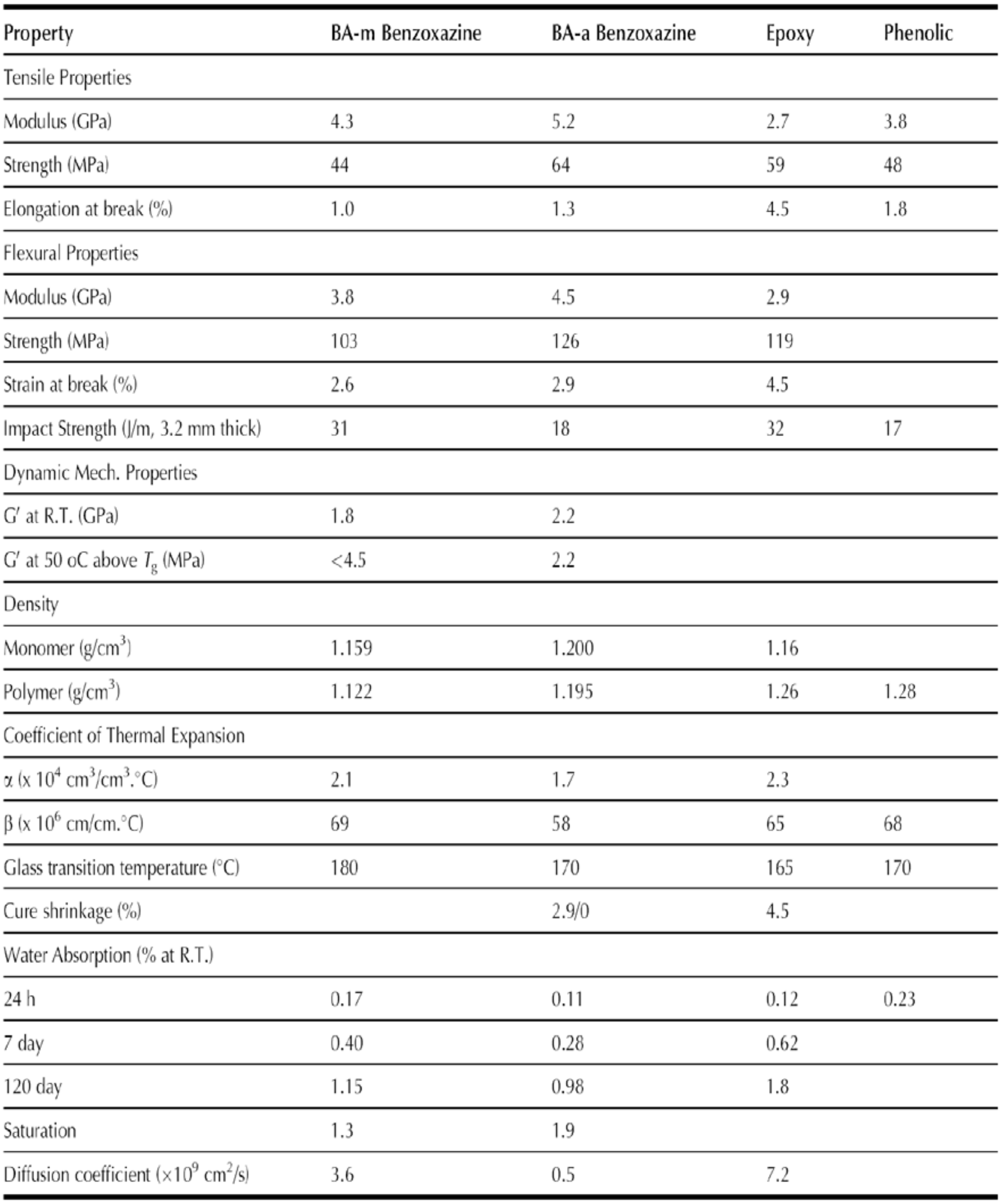

Property	BA-m Benzoxazine	BA-a Benzoxazine	Epoxy	Phenolic
Tensile Properties				
Modulus (GPa)	4.3	5.2	2.7	3.8
Strength (MPa)	44	64	59	48
Elongation at break (%)	1.0	1.3	4.5	1.8
Flexural Properties				
Modulus (GPa)	3.8	4.5	2.9	
Strength (MPa)	103	126	119	
Strain at break (%)	2.6	2.9	4.5	
Impact Strength (J/m, 3.2 mm thick)	31	18	32	17
Dynamic Mech. Properties				
G′ at R.T. (GPa)	1.8	2.2		
G′ at 50 oC above T_g (MPa)	<4.5	2.2		
Density				
Monomer (g/cm^3)	1.159	1.200	1.16	
Polymer (g/cm^3)	1.122	1.195	1.26	1.28
Coefficient of Thermal Expansion				
α (x 10^4 cm^3/cm^3.°C)	2.1	1.7	2.3	
β (x 10^6 cm/cm.°C)	69	58	65	68
Glass transition temperature (°C)	180	170	165	170
Cure shrinkage (%)		2.9/0	4.5	
Water Absorption (% at R.T.)				
24 h	0.17	0.11	0.12	0.23
7 day	0.40	0.28	0.62	
120 day	1.15	0.98	1.8	
Saturation	1.3	1.9		
Diffusion coefficient ($\times$10^9 cm^2/s)	3.6	0.5	7.2	

The physical and mechanical properties feature a wide range. The balance material properties of these resins such as good thermal, chemical, electrical, mechanical, and physical properties make the polybenzoxazine family an attractive option in many existing applications. In addition, these new materials possess high glass transition temperatures, high char yield, high moduli, low water absorption despite the large amount of hydroxyl groups in the backbone structure, excellent resistance to chemicals and UV light, low melt viscosities compared to conventional phenolics, near-zero volumetric shrinkage or expansion upon polymerization and relatively low coefficients of thermal expansion. The polybenzoxazines are; therefore, suitable for various high-performance adhesives and composites.

2.3 Acrylonitrile-Butadiene Copolymer Rubber

Acrylonitrile-Butadiene copolymer rubber (NBR) is commonly considered the workhorse of the industrial and automotive rubber products industries. NBR is actually a complex family of unsaturated copolymers of acrylonitrile and butadiene. By selecting an elastomer with the appropriate acrylonitrile content in balance with other properties, the rubber compounder can use NBR in a wide variety of application areas requiring oil, fuel, and chemical resistance. In the automotive area, NBR is used in fuel and oil handling hose, seals and grommets, and water handling applications. With a temperature range of – 40^{o}C to 125^{o}C, NBR materials can withstand all but the most severe automotive applications. On the industrial side NBR finds uses in roll covers, hydraulic hoses, conveyor belting, graphic arts, oil field packers, and seals for all kinds of plumbing and appliance applications.

NBR is produced in an emulsion polymerization system. The water, emulsifier/soap, monomers (butadiene and acrylonitrile), radical generating activator, and other ingredients are introduced into the polymerization vessels. The emulsion process yields a polymer latex that is coagulated using various materials (e.g. calcium chloride, aluminum sulfate) to form crumb rubber that is dried and compressed into bales. Some specialty products are packaged in the crumb form. NBR producers vary polymerization temperatures to make "hot" and "cold" polymers. Acrylonitrile (ACN) and butadiene (BD) ratios are varied for specific oil and fuel resistance and low temperature requirements. Specialty NBR polymers which contain a third monomer (e.g. divinyl benzene, methacrylic acid) are also offered. Some NBR elastomers are hydrogenated [5] to reduce the chemical reactivity of the polymer backbone, significantly improving heat resistance, i.e. hydrogenated acrylonitrile butadiene rubber (HNBR). Each modification contributes uniquely different properties.

Amine terminated butadiene–acrylonitrile copolymer is a family of butadiene-acrylonitrile copolymer with amine (NH_2) functionality at the chain ends as shown in Fig. 2.4.

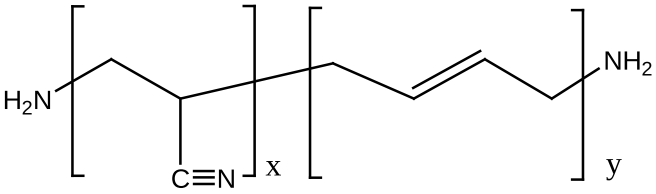

Fig. 2.4 Amine terminated butadiene–acrylonitrile copolymer

In addition, amine terminated butadiene–acrylonitrile copolymer used predominately with other amine functional compounds to improve product performance when added to thermoset resin systems, i.e. enhances the toughness/flexibility of thermoset resins, improves adhesion with difficult to bond substrates, increases low temperature mechanical properties, increases impact and wear resistance. In general, it used for structural adhesive paste, composites, coatings and linings for corrosion resistance, construction joint sealers, crack injection resins and Mastics, end uses include aerospace, automotive, construction, industrial and composites [ref]

Table 2.2 ATBN (Hycar®ATBN 1300X16) specification

Property	**Value**
Brookfield viscosity, mPa.s or cP@27°C	200,000±50,000
Amine equivalent weight	900±100

2.4 Tribology

Tribology is now universally applied to the emerging science of friction, wear, and lubrication involved at moving contacts. In its broad scope, it involves mechanical, chemical, and material technology. Usual tasks in tribology are reduction of friction and wear to conserve energy, enabling faster and more precise motions, increased productivity, and reduced maintenance. Recently, fundamental interest in tribology exists for lubricant formulation, industrial operations, aerospace and transportation equipment, material shaping and machining, computers and electronic devices, power generation, and almost all phases of life where motion is encountered. The friction characteristics of a brake material make up its coefficient of friction. If the coefficient of friction is too high, the brakes will work too well and cause the wheels to lock up. If the coefficient of friction is too low, the brake pedal would require excessive force to stop the vehicles [19]. In general, for tribo-engineering materials, friction and wear are responses of a tribo-system. Coefficient of friction (COF) and wear rate are parameters describing the state of contact of bodies in a tribo-system, and they are not material constants of the bodies in contact [20, 21]. It is well recognized recently that the coefficient of friction and wear rate are not material properties but two kinds of responses *of a* tribo-system. However, they may be treated as material properties for technical conveniences with an engineering sense only in some special states of contact.

2.4.1 Coefficient of Friction [22]

From Fig. 2.5, coefficient of friction (COF) or friction coefficient (μ) mean friction is always present between two materials that slide against each other. The coefficient of friction is the amount of friction that can be produced as two materials slide across each other. The coefficient of friction is simple to find ratio of friction force to normal force.

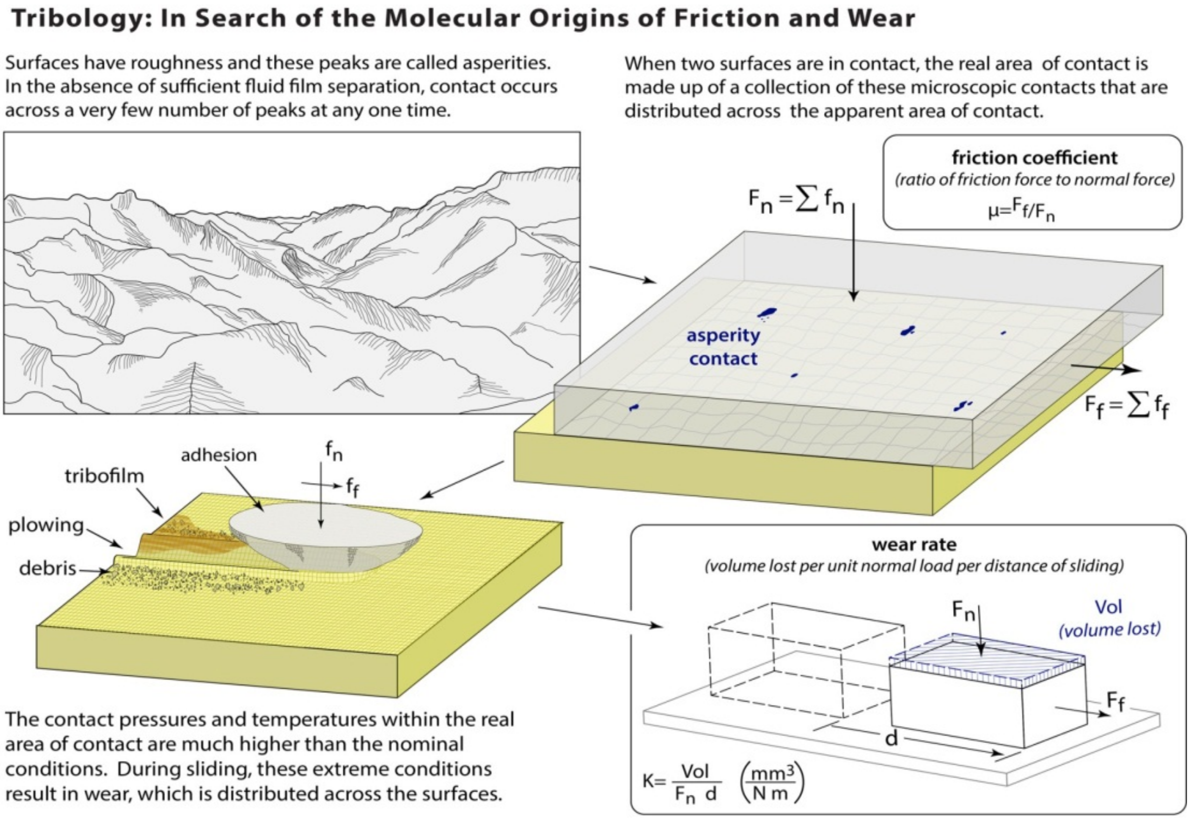

Fig. 2.5 Tribology theory [23].

The friction force is the force exerted by a surface when an object moves across it (kinetic or sliding friction force) - or makes an effort to move across it (static friction force).

Note that static coefficients are somewhat higher than the kinetic or sliding coefficients. The frictional force can be expressed as can be seen in Equation (2.1).

$$F_f = \mu F_n \tag{2.1}$$

Where F_f = Frictional force (N, lb), μ = Static (μ_s) or kinetic (μ_k) frictional coefficient (or Coefficient of friction, COF) and F_n = Normal force (N, lb)

For an object pulled or pushed horizontally as seen in Figure 1(d), the normal force (F_n) is simply the weight:

$$F_n = mg \tag{2.2}$$

Where m = Mass of the object (kg, slugs)

g = Acceleration of gravity (9.81 m/s^2, 32 ft/s^2)

For friction material manufacturers, Society of Automotive Engineers (SAE) [24] classified coefficient of friction of brake pads, based on data obtained from tests conducted in accordance with SAE J661 shown in Table 2.3. Generally the code will include of two letters reflecting the friction coefficients, the first letter will represent normal friction coefficient and the second will represent hot friction coefficient. Example, a lining having a normal friction coefficient of 0.29 and a hot friction coefficient of 0.42 would be coded “EF”.

Table 2.3 Standard Code Letter for Friction Materials [24]

Code letter	Friction coefficient (COF)
C	COF < 0.15
D	0.15 < COF < 0.25
E	0.25 < COF < 0.35
F	0.35 < COF < 0.45
G	0.45 < COF < 0.55
H	0.55 < COF
Z	Unclassified

2.4.2 Wear Rate [25]

The inevitable consequence of friction in a sliding contact is wear. Wear of polymers is a complex process and the explanation of the wear mechanism can be most efficiently given if we follow one of the three systems of classification. Depending on the classification, wear of a polymer sliding against a hard counterface may be termed as interfacial, cohesive, abrasive, adhesive, chemical wear, etc. [26]. It is to be noted that, similar to the case of friction, polymer wear is also greatly influenced by the type (elastomer, amorphous, semi-crystalline) of the polymer. Of particular importance are the properties such as the elastic modulus, tensile strength and the percentage elongation at failure (toughness), which changes drastically as we move from one type of polymer to another. As aforementioned that wear is a kind of responses from a tribo-system and it is not material property. Wear rate is strongly influenced by the operating conditions. Specifically, normal loads and sliding speeds play a pivotal role in determining wear rate. Furthermore, tribo-chemical reaction is also important in order to understand the wear behavior [27]. In the wear test, the differences in weight measured before and after tests gives wear of the materials. The following relation is used to investigate the specific wear rate which is [28]:

$$\text{Specific wear rate}\left(\mathrm{mm}^3/\mathrm{Nm}\right)=\frac{\left[\left(\mathrm{W}_1-\mathrm{W}_2\right)\times\dfrac{10^3}{\rho}\right]}{\mathrm{P}vt} \qquad (2.3)$$

Where W_1 is the weight before test (g), W_2 is the weight after test (g), ρ density (g/cm^3), P is the applied normal load (N), v is the relative sliding velocity and t is the experimental time.

2.5 Tribology Polymers [5, 29-31]

Tribology of materials deals with relative motion of surfaces that is involved with friction, wear, scratching and rubbing. Friction is the resistance to motion that occurs whenever one solid body is in contact with another solid body, while wear represents a surface damage or removal of material from one or both sides of solid surfaces that are in contact during motion. Almost all machines lose their durability and reliability due to wear, and the possibilities of new advanced machines are reduced because of wear problems. Therefore, wear control has become a strong need for the advanced and reliable technology of the future. However, wear and friction are not material properties, but they are a system response. They change drastically even with a relatively small change in a tribosystem, which is composed of dynamic parameters, environmental parameters and material parameters. The purpose of the research in tribology is to minimize and remove losses that occur due to friction and wear at all levels, where rubbing, grinding, polishing and cleaning of surfaces take place. Tribological parameters include surface roughness, mechanisms of adhesion, friction and wear, and physical and chemical interactions of lubricants (if present). Interacting surfaces must be understood for optimal function and long-term reliability of components and devices and economic viability.

The wear and friction of non-metallic solids have some significant differences to that of metals: the wear mechanisms involved and the level of friction or wear which occurs. The most important factors which determining level of wear due to sliding friction and magnitude of the coefficient of sliding friction are hardness and surface roughness of the paired materials, contact pressure, traversed distance, temperature of the sliding surfaces and lubrication. The difference of application of polymers in frictional contacts in comparison to metals and ceramic materials relates mainly to the chemical and physical structures as well as to the surface and bulk properties. Polymers show very low surface free energy and also have visco-elastic properties. It effects in drastic tribological differences when we consider adhesive and mechanical components of fiction force. The steel-on-polymer frictional tribosystem is the most popular and also practically confirmed as the best tribological combination. Relatively low friction coefficient and often sufficiently high wear resistance can be achieved in these systems by proper selection of the polymer and steel to be use. The inevitable consequence of friction in a sliding contact is wear. Wear of the polymer is the result of material removal by physical separation due to microfracture, by chemical dissolution, or by melting at the contact interface. Wear of a polymer sliding against a hard counterface may be termed as adhesive, abrasive, fatigue and corrosive as can be seen in Fig. 2.6. The dominant wear mode may change from one to another for reasons that include changes in surface material properties and dynamic surface responses caused by frictional heating, chemical film formation and wear.

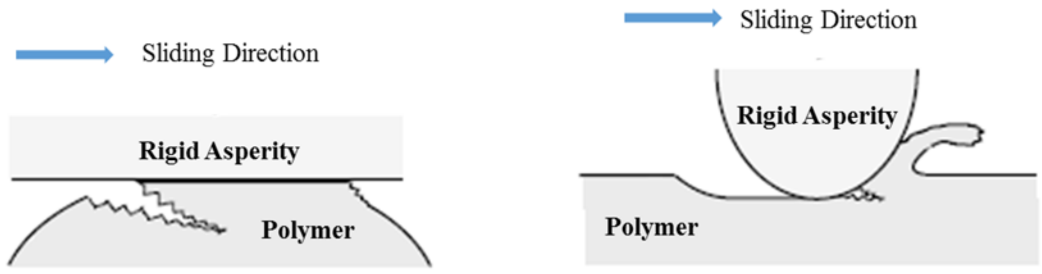

Adhesive Wear

Abrasive Wear

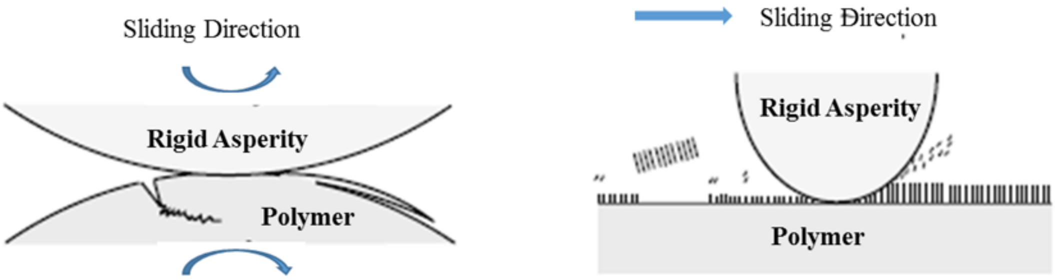

Fatigue Wear

Corrosive Wear

Fig. 2.6 Schematic images of four representative wear modes adapted from Ref 29.

2.5.1 Adhesive Wear

If the contact interface between two surfaces under plastic contact has enough adhesive bonding strength to resist relative sliding, large plastic deformation caused by dislocation is introduced in the contact region under compression and shearing. As a result of such large deformation in the contact region, a crack is initiated and is propagated in the combined fracture mode of tensile and shearing. When the crack reaches the contact interface, a wear particle is formed and adhesive transfer is completed. This type of wear, which occurs when there is enough adhesive bonding at the contact interface, is called adhesive wear.

2.5.2 Abrasive Wear

If the contact interface between two surfaces has interlocking of an inclined or curved contact, ploughing takes place in sliding. As a result of ploughing, a certain volume of surface material is removed and an abrasive groove is formed on the weaker surface. This type of wear is called abrasive wear. Here, we assume a single contact point model where a hard, sharp abrasive is indented against the flat surface and forms a groove on it by ploughing. When wearing material has a ductile property, a ribbonlike, long wear particle is generated by the mechanism of microcutting. In the case of brittle material, however, a wear particle is generated by a crack propagation.

2.5.3 Fatigue Wear

Repeated cycles of contact are not necessary in adhesive and abrasive wear for the generation of wear particles. There are other cases of wear where a certain number of repeated contacts are essential for the generation of wear particles. Wear generated after such contact cycles is called *fatigue wear*. When the number of contact cycles is high, the high-cycle fatigue mechanism is expected to be the wear mechanism. When it is low, the low-cycle fatigue mechanism is expected.

2.5.4 Corrosive Wear

When sliding takes place, especially in corrosive liquids or gases, reaction products are formed on the surface mainly by chemical or electrochemical interactions. If these reaction products adhere strongly to the surface and behave like the bulk material, the wear mechanism should be almost the same as that of the bulk material. In many cases, however, such reaction products behave very differently from the bulk material. Therefore, wear is quite different from that of the bulk material, and is dominated by the reaction products formed by the interaction of solid materials with the corrosive environment. This kind of tribochemical wear accelerated by corrosive media is called *corrosive wear*.

In corrosive wear, tribochemical reaction produces a reaction layer on the surface. At the same time, such layer is removed by friction. Therefore, relative growth rate and removal rate determine the wear rate of the reaction layers and, as a result, of the bulk material. Therefore, models of the reaction layer growth and those of the layer removal become very important.

Literature Reviews

Ning and Ishida [32, 33] investigated the synthesis of bifunctional benzoxazine precursors. These polyfunctional benzoxazine were found to exhibit excellent mechanical and thermal properties with good handling capability for resin processing and composite manufacturing, e.g., tensile modulus of 3.2 GPa, and tensile strength of 58 MPa. In addition, they offered greater flexibility than conventional phenolic resins in terms of molecular design. They do not release by-products during curing reactions and there is no solvent needed in the resin production. Polybenzoxazines can find applications in areas where polyesters, vinyl esters, epoxies, phenolics, bis-maleimides, cyanate esters, and polyimides are currently used.

Ishida and Allen [34] studied the properties of polybenzoxazine thermosetting resins based on the ring-opening polymerization of benzoxazine precursors (B-a, B-m). They can be synthesized from inexpensive raw materials and polymerize by a ring opening addition reaction to yield no reaction by-product. Benzoxazine resins cure without the aid of the strong acid catalysts normally required by phenolic materials. Dynamic mechanical analysis revealed high moduli and high glass transition temperature with low crosslink densities, i.e., flexural modulus ca. 3.8-4.5 GPa, flexural strength ca. 103-126 MPa, and Tg ca. 170-180^{o}C. Polybenzoxazines have significantly higher tensile moduli than both phenolics and epoxies yet maintain adequate tensile strength and impact resistance. In addition, low water absorption and good dielectric properties allow these materials to perform well in electronic applications.

Ishida [5] demonstrated that benzoxazine-based resins are expected to yield significant advantages over many other thermosetting materials. The molecular structure of polybenzoxazine offers superb design flexibility and allows properties of the cured materials to be controlled for specific requirements of a wide variety of individual applications. Polybenzoxazines can be synthesized from a wide selection of raw materials consisting of phenolic derivatives and primary amines. The mechanical properties of regioselective benzoxazine resins based on bisphenolic-A and substituted anilines was reported in Table 3.1.

Table 3.1 The mechanical properties of regioselective benzoxazine resins based on bisphenolic-A and substituted anilines [11]

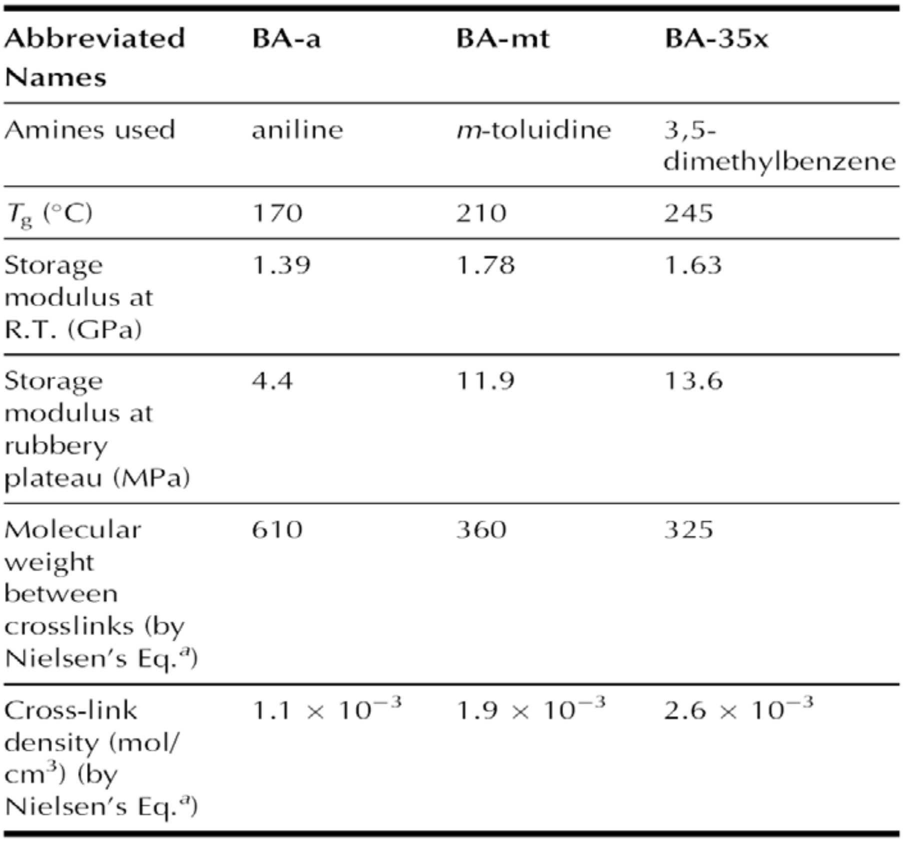

Abbreviated Names	BA-a	BA-mt	BA-35x
Amines used	aniline	*m*-toluidine	3,5-dimethylbenzene
T_g (°C)	170	210	245
Storage modulus at R.T. (GPa)	1.39	1.78	1.63
Storage modulus at rubbery plateau (MPa)	4.4	11.9	13.6
Molecular weight between crosslinks (by Nielsen's Eq.[a])	610	360	325
Cross-link density (mol/cm^3) (by Nielsen's Eq.[a])	1.1×10^{-3}	1.9×10^{-3}	2.6×10^{-3}

[a]Nielsen's Eq. [29,30]

As a relatively low a-stage viscosity, one of the most useful properties of benzoxazine resins results in an ability of the resins to accommodate relatively large quantity of filler while still maintaining their good processability. Ishida and Rimdusit [35] developed highly thermally conductive molding compounds for electronic packing application based on polybenzoxazine system. The authors investigated thermal conductivity of boron nitride-filled benzoxazine resin as a function of filler content and particle size. The investigators used large aggregates of flake-like boron nitride crystals and were able to make a composite with a maximum boron nitride content of 78.5 % by volume (Fig. 3.1) with a corresponding thermal conductivity value of 32.5 W/mK and the glass transition of 225°C (Fig. 3.2). The remarkably high thermal conductivity value was obtained using the well-recognized concept of thermal management in composite materials by maximizing the formation of conductive networks while minimizing the thermal barrier resistance along the heat-flow path. The concept was accomplished by using highly thermally conductive filler with a matrix resin which has low melt viscosity and good adhesion to the filler. Water absorption at room temperature of this composite is also very low, i.e. at 85 % by weight of boron nitride having 0.02 % at 24 hr (ASTM D570).

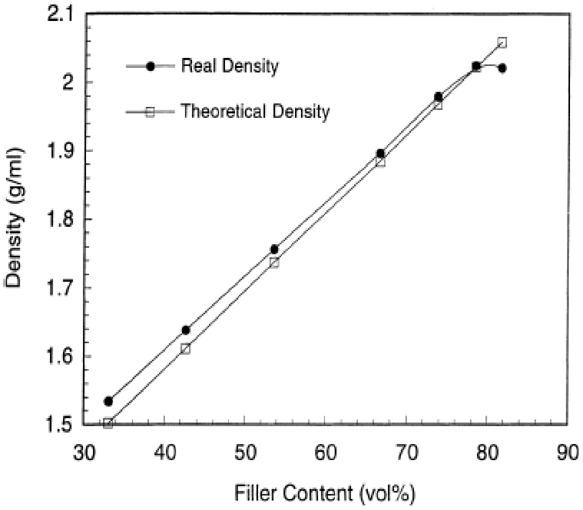

Fig. 3.1 The maximum packing density of boron nitride-filled polybenzoxazine using boron nitride grade HCJ48. (□) theoretical density, (●) experimental density.

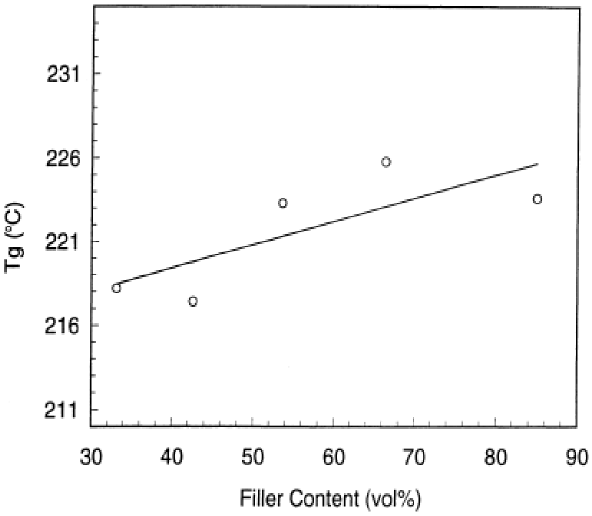

Fig. 3.2 The effect of filler loading on glass-transition temperature of boron nitride-filled polybenzoxazine.

Jang and Seo [17] studied the mechanical properties such as the fracture toughness, flexural modulus, and flexural strength of poly(butadiene-co-acrylonitrile)-modified polybenzoxazine. They reported that the fracture toughness and flexural strength of amine-terminated butadiene acrylonitrile rubber (ATBN) is more effective than carboxyl-terminated butadiene acrylonitrile rubber (CTBN) as shown in Fig. 3.3 and Fig. 3.4, respectively, because ATBN-modified polybenzoxazine showed better distribution of rubber particles in binder phase than did CTBN-modified polybenzoxazine. However, the addition of ATBN and CTBN rubber modification caused a decrease in the thermal property, i.e., glass transition temperature of the polybenzoxazine.

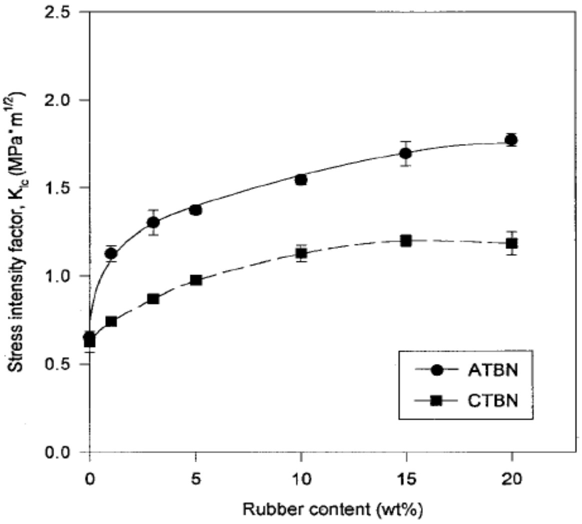

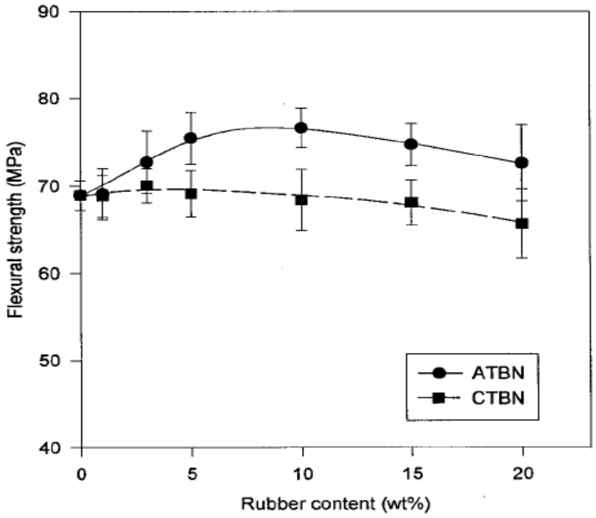

Fig. 3.3 Stress intensity factor, K_{Ic}, of rubber-toughened polybenzoxazine as a function of rubber content.

Fig. 3.4 Yield strength change as a function of rubber content.

Furthermore, in recent years, tribo-engineering materials based on polymer and polymer composites have been finding greatly increased potentials for applications in industry including self-lubricating materials, industrial equipment, automotive and aerospace. In case of friction materials, the materials normally contain multiple ingredients in varying composition, and they are classified as fibres, fillers, binders and property modifiers [36]. Fillers are important in modifying brake friction material characteristics. A good selection of fillers normally depends on the specific components of the friction material. Organic filler, like rubber is commonly used in brake materials due to its superior characteristics. Therefore, rubber is usually incorporated in to brake pads to reduce brake noises [37]. In addition, an enhancement of wear, tribology, mechanical, electrical, optical and other properties of elastomer, thermoplastics and polymer blends reinforced with alumina nanoparticles has been reported. Recently, semi-metallic brake friction materials based polybenzoxazine have been studied [38]. In this work, the effects of epoxidized natural rubber alumina nanoparticles abbreviated as ENRAN in semi-metallic friction composites (SMFCs) were investigated for tribological properties. The compounding ingredients for the SMFC were ENRAN, steel wool (as the main fiber reinforcement), graphite (as a lubricant), and benzoxazine resin (as a binder). Detailed formulations of the SMFCs are given in Table 3.5.

Table 3.5 Ingredient Content for SMFCs

Ingredients (vol%)	Formula				
	A	B	C	D	E
Benzoxazine resin	23	14	18.5	23	14
ENRAN	20	29	31.5	34	43
Steel wool	50	50	41	32	32
Graphite	7	7	9	11	11

The average coefficient of friction and the specific wear rate as functions of ENRAN content is illustrated in Fig. 3.5. From this figure, the average friction coefficient value (~ 0.45) was found to be in almost a constant state with an increase of ENRAN content up to 30% by volume. Further investigation on adding higher volume percentage of ENRAN, greater than 30% by volume, it can be seen that both friction coefficient and specific wear rate of the SMFCs was reduced. This behavior was most likely due to the low volume percentage of the steel wool content as stated in the formulation. Therefore, from the tribological properties, it can conclude that the inclusion of ENRAN in the brake pad formulation presents great potential as friction materials for the semi-metallic friction composites as prevent by it friction coefficient value approximately 0.437 with low specific wear rate of 0.27×10^{-4} mm^3/Nm by addition of 29 vol% ENRAN.

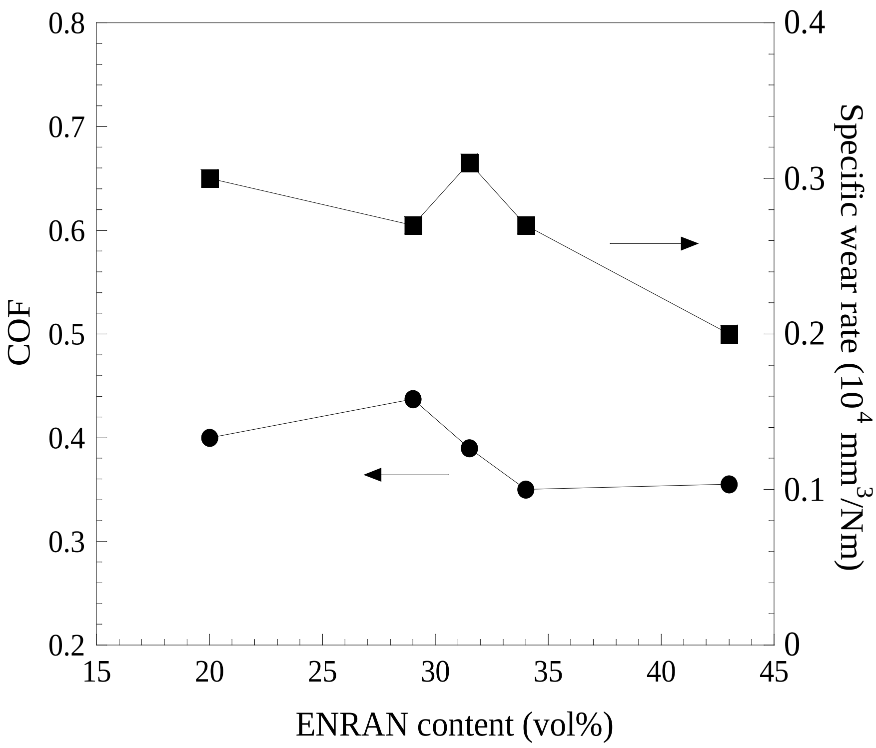

Fig. 3.5 Trobological properties of semi-metallic friction composites at different ENRAN content: (●) Average friction coefficient (■) Specific wear rate. (Adapted from Ref. 38)

As it known that the accumulation of heat in during braking process for brake friction materials will cause high surface temperature, typically in the range 300-400°C on the brake lining materials. The degradation in binder integrity during higher temperatures may cause brake fade which would lead to the loosening of the frictional characteristics of the friction materials. In case of phenolic resin, it based automotive friction material has been extensively investigated [37, 39-41]. However, in nature, the phenolic resins is brittle and is not resistant to high temperature, which often results in wear loss and fade under 350°C for the friction materials [42, 43]. Therefore, it is possible that the polybenzoxazines exhibited the outstanding thermal stability of the polybenzoxazine such as high degradation temperature (339°C) and char yield (38%) [5] can be used as a binder for friction materials as purposed by Wu et al. [44]. The authors have been investigated the effect glass-rubber transition of thermosetting resin matrix on the friction and wear properties of friction materials. Since glass-to-rubber transition of polymer often leads to substantial change in mechanical properties, i.e stiffness and strength and other properties of polymeric materials. However, very little research has been focused on the effect of thermal transition behavior of resin matrix on the resultant wear performance of composite friction materials. In fact, the relationship between thermal transition characteristic of the thermosetting polymers and tribological behaviors of friction materials should attract much attention, because thermosetting resins were mostly utilized as binder matrix in the field of friction composites. Therefore, Wu et al. [44] have reported the effect of temperature on friction coefficient and the specific wear rate of thermosetting polymer binders, i.e. phenolic resin, benzoxazine resin, phenolic/benzoxazine resin and phenolic/benzoxazine/nitrile butadiene rubber filled with ingredients as listed in Table 3.6.

Table 3.6 Formulation of Friction Materials based on Thermosetting Polymer Binders.

Ingredients	Formula			
(vol%)	A	B	C	D
Phenolic resin	24	0	12	9.6
Benzoxazine resin	0	24	12	9.6
Nitrile butadiene rubber	0	0	0	4.8
Ceramic fiber	20	20	20	20
Potassium titanate	10	10	10	10
Friction modifiers graphite, coke, alumina, etc.	26	26	26	26
Filler barium sulfate, calcium carbonate, etc.	20	20	20	20

Fig. 3.6 presents the coefficient of friction (COF) as a function of temperature for all composite friction materials. It was found that the COF values increased to reach the maximum value with the temperature in the range of 100-250^{o}C, and then decreased at higher temperature, i.e. 250-350^{o}C. This drop in coefficient *of* friction is due to the degradation of resin which is associated with the loos of its binding ability to the fiber and other ingredients around 300^{o}C.

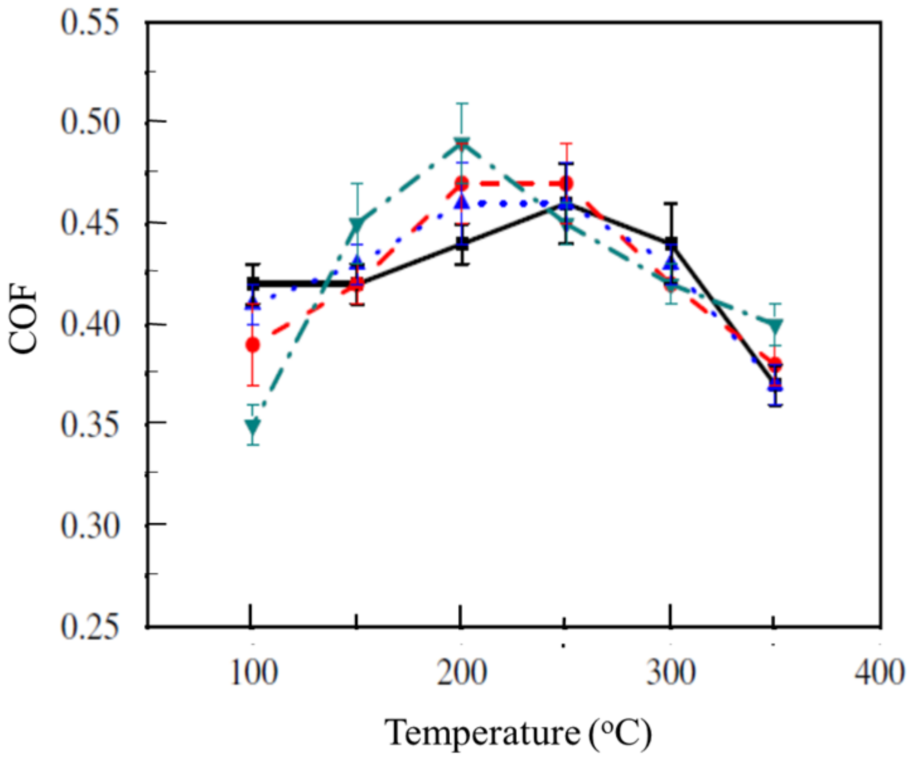

Fig. 3.6 Friction coefficient as a function of temperature for friction materials based on thermosetting polymer binder: (■) phenolic/benzoxazine/nitrile rubber copolymer, (●) phenolic/benzoxazine resins (▲) phenolic resin, (▼) benzoxazine resin. (Adapted from Ref. 44)

Furthermore, the relationship between tribological behavior and the mechanical property has been investigated. At temperature of 100°C, below the glass transition temperature obtained from the peak temperature of loss tangent from dynamic mechanical analysis (DMA) of all polymer binder, i.e. 250°C, 203°C, 225°C and 230°C for phenolic resin, benzoxazine resin, phenolic/benzoxazine resins and phenolic/benzoxazine/nitril rubber, respectively, the COF increased in the order of composites based on benzoxazine resin < phenolic/benzoxazine resins < phenolic resin < phenolic/benzoxazine/nitrile rubber. On the contrary, the storage modulus decreased in the order of composites based on benzoxazine resin > phenolic/benzoxazine resins > phenolic resin > phenolic/benzoxazine/ nitrile rubber at the same temperature as can be seen in Fig. 3.7.

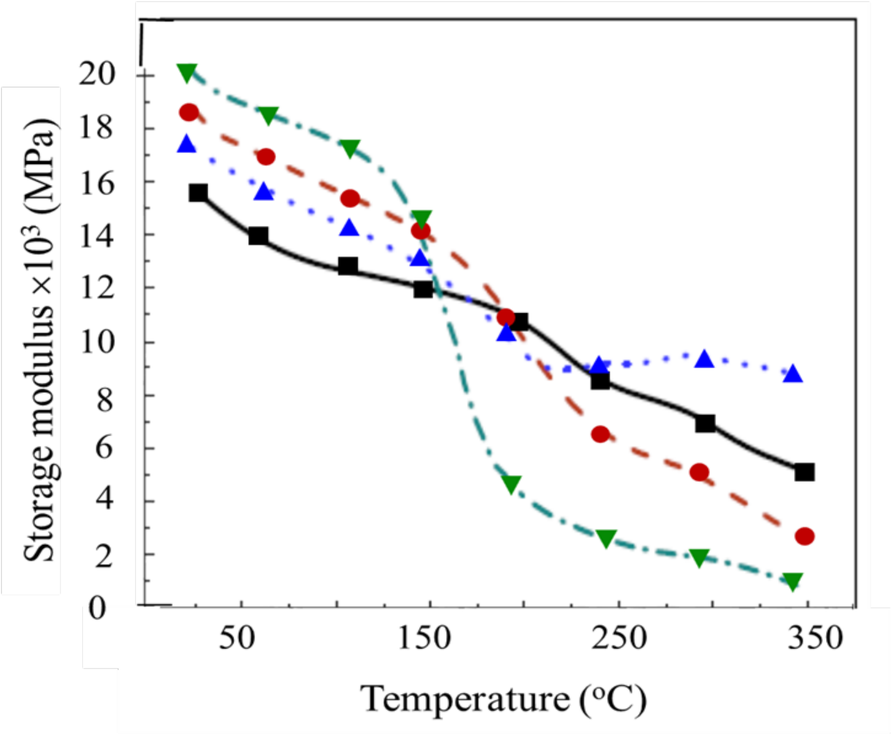

Fig. 3.7 Storage modulus as a function of temperature for friction materials based on thermosetting polymer binders: (■) phenolic/benzoxazine/nitrile rubber copolymer, (●) phenolic/benzoxazine resins (▲) phenolic resin, (▼) benzoxazine resin. (Adapted from Ref. 44)

This behavior was attributed to segmental motions of the polymer chains restricted significantly at 100°C (its glassy state). It is difficult for the polymer matrix to deform and conform to the counterface. Therefore, friction composites with relatively lower storage modulus tended to deform easily, and had relatively larger real contact area between two contact surfaces, which resulting in relatively higher COF.

The specific wear rate as a function of temperature for friction materials based on thermosetting polymer binders was depicted in Fig. 3.8. It can be seen that the specific wear rate for all friction composites increased slowly with increasing of temperature to 200°C or 250°C, and then increased dramatically when temperature was above 250°C. The adhesive resin decomposed to lose its ability to bind with the ingredients around 300°C, resulting in the wear resistance to dramatically decrease.

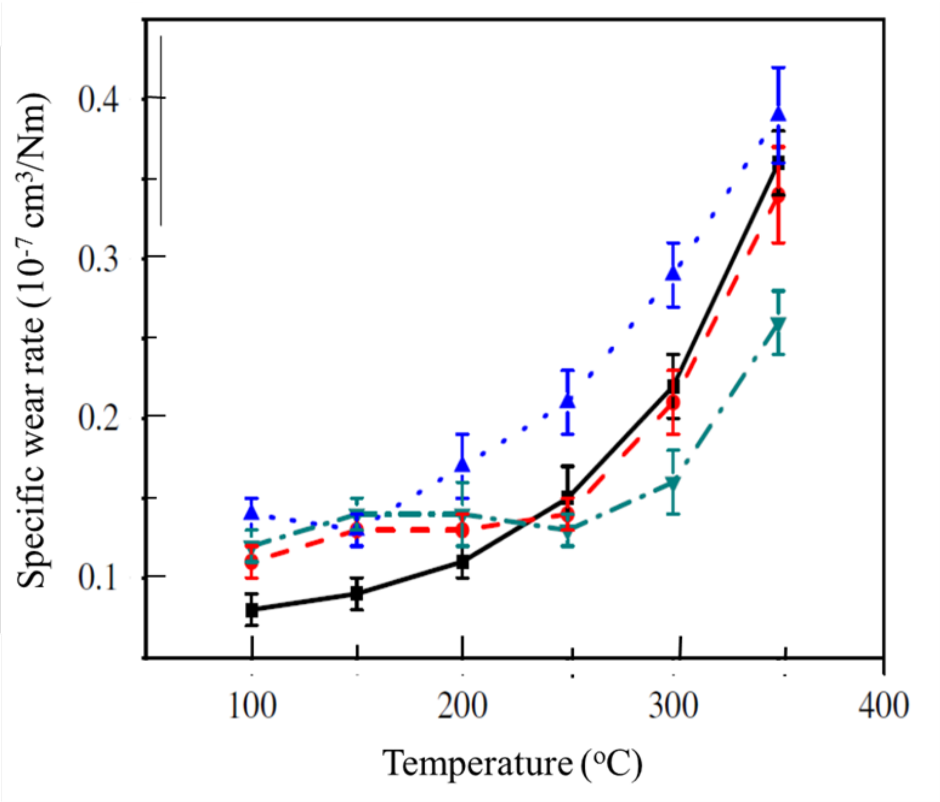

Fig. 3.8 Specific wear rate as a function of temperature for friction materials based on thermosetting polymer binder: (■) phenolic/benzoxazine/nitrile rubber copolymer, (●) phenolic/benzoxazine resins (▲) phenolic resin, (▼) benzoxazine resin. (Adapted from Ref. 44)

Therefore, from storage modulus and tribological behaviors confirmed that glass-to-rubber thermal transition of the thermosetting polymer binders influenced significantly the tribological properties of the composite friction materials. There was a significant increasing tendency in friction coefficient and specific wear rate values of all friction composites when brake temperature increased to 200°C or 250°C, accompanying the polymer matrix converted from glass state to rubbery state. For all composite friction materials, it is worth nothing that the composite based on phenolic/benzoxazine/nitrile rubber occupied relatively higher glass-rubber transition temperature, resulting in better ability to stabilize the friction coefficient and specific wear rate under relatively higher braking temperature.

Lu [45] has been investigated effect of ingredients on friction performance of polybenzoxazine filled with soft (graphite, MoS_2 and Twaron/aramid pulp) and hard (aluminium, oxide and steel wool) additives for automotive friction materials. The authors reported that the addition of either aluminium oxide or steel wool to polybenzoxazine initially causes and increase in friction coefficient (μ), i.e., 0.78 for aluminium oxide and 0.73 for steel wool while the addition of graphite reduced the initial friction coefficient of polybenzoxazine from 0.5 to a value of 0.26 and the average friction coefficient of Twaron filled polybenzoxazine is around 0.35 as shown in Fig. 3.9.

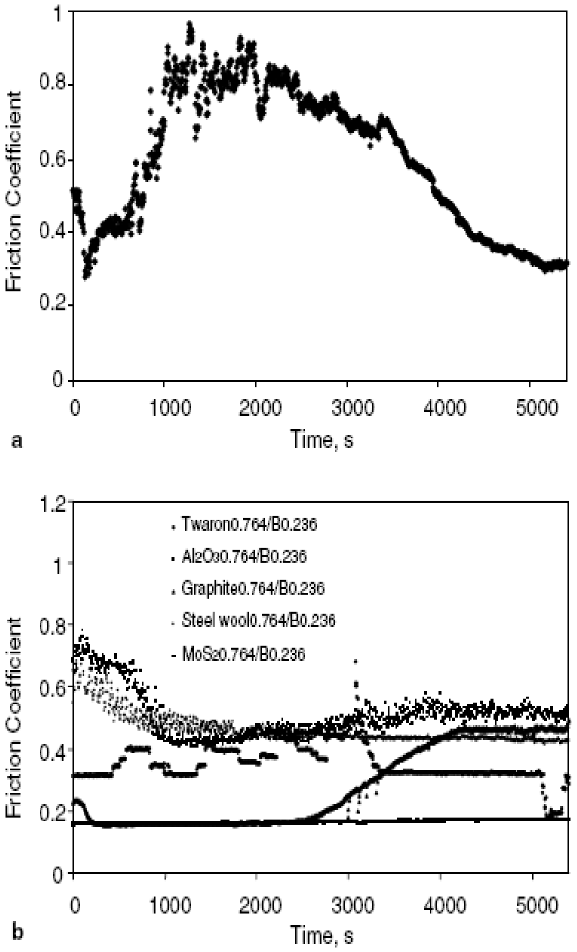

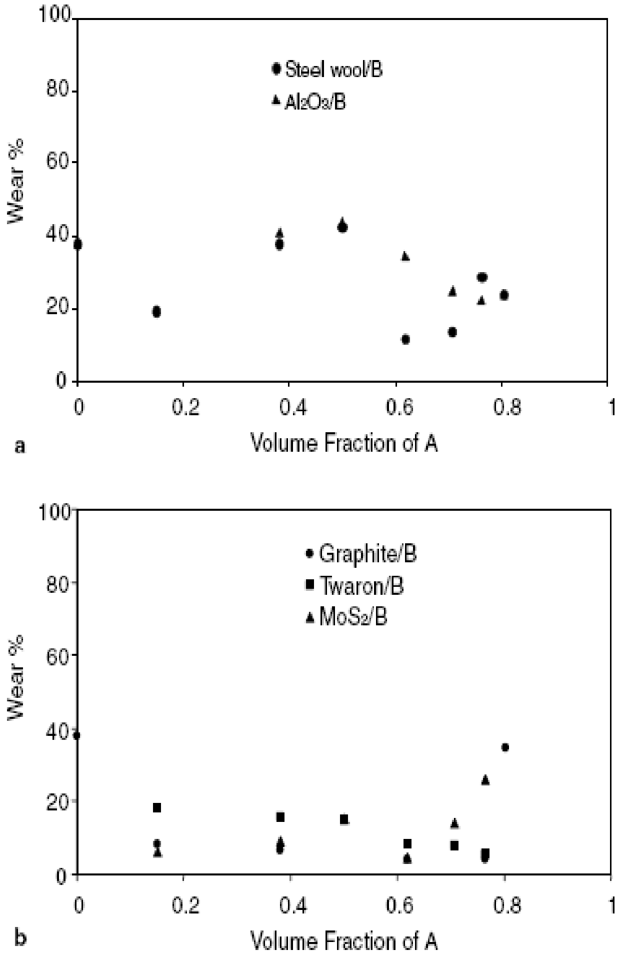

Fig. 3.9 Friction Assessment and Screening Test (FAST) curves of (a) polybenzoxazine and (b) the components of polybenzoxazine filled with soft and hard additives.

Fig.3.10 Wear-composition relationships of (a) hard maters/polybenzoxazine (B) and (b) soft metters/polybenzoxazine (B)

*A is soft and hard additives

Furthermore, the wear-composition relationships of the polybenzoxazine filled with soft and hard additives was depicted in Fig. 3.10. From the figure, the lowest wear and minimum volume of polybenzoxazine are 22.26% and 0.236, respectively, for polybenzoxazine filled with aluminium oxide and 11.53% and 0.382, respectively, for polybenzoxazine filled with steel wool. The parameter of the minimum volume of polybenzoxazine binder reflects the adhesion action between the additives and the binder. In the polybenzoxazine filled with soft additive, the lowest wear is 5.38% for polybenzoxazine filled with Twaron. However, in general, the role of Twaron or aramid pulp in friction materials may enhance the mechanical strength and reduce the thermal conductivity.

Nakamura et al., [46] have investigated non-asbestos friction materials as brake linings, disc pads, clutch facings and the like in automobiles, heavy duty trucks, railroad cars, and various types of industrial equipment. The non-asbestos friction materials were produced by molding and curing a composition comprised of a acrylonitrile-butadiene rubber-modified phenolic resin, a fibrous base, a binder, and a filler. The inventors have suggested the non-asbestos friction materials compositions made by providing a binder with the amount of the binder ca. 3 to 30wt%, wherein the acrylonitrile-butadiene rubber in the rubber-modified phenolic resin is from 10 to 40wt%. In addition, the amount of the fibrous base in the form of short fibers or a powder, i.e., inorganic fibers; alumimum fiber, potassium titanate fibers and organic fibers; aramid fibers, polyimide fibers, and acrylic fibers is 1 to 50wt%, and preferably 5 to 40wt%. The amount of the filler, i.e., inorganic fillers; calcium carbonate, barium sulfate, magnesium oxide, graphite, calcium hydroxide and organic fillers; cashew dust, nitrile rubber dust (vulcanized product) is 20 to 96wt%, based in on the overall weight of the friction material. The presented friction material compositions in this investigation showed in Table 3.7.

Table 3.7 Formulation of the friction materials

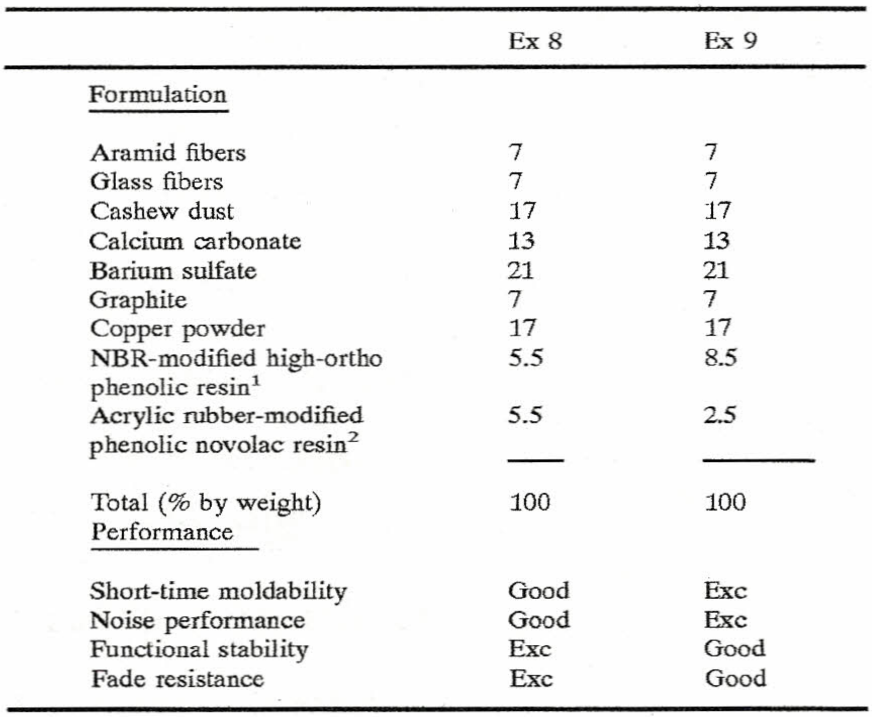

	Ex 8	Ex 9
Formulation		
Aramid fibers	7	7
Glass fibers	7	7
Cashew dust	17	17
Calcium carbonate	13	13
Barium sulfate	21	21
Graphite	7	7
Copper powder	17	17
NBR-modified high-ortho phenolic resin[1]	5.5	8.5
Acrylic rubber-modified phenolic novolac resin[2]	5.5	2.5
Total (% by weight)	100	100
Performance		
Short-time moldability	Good	Exc
Noise performance	Good	Exc
Functional stability	Exc	Good
Fade resistance	Exc	Good

The inventors have reported that the friction material has a 100 Hz vibration damping factor (tan δ) at 300°C minus tan δ at 50°C value of at least -0.030 which is advantageous for noise suppression. In addition, the resulting friction materials have an excellent and long-lasting noise performance, and good wear resistance, and fade resistance.

Experimental

4.1 Raw Materials

BA-a type benzoxazine resin based on bisphenol-A, formaldehyde and aniline was synthesized based on solventless condition as described elsewhere.[8,9] The BA-a resin is a yellow clear solid at room temperature. Bisphenol-A (polycarbonate grade) was provided by Thai PolycarbonateCo., Ltd. Paraformaldehyde and aniline wereobtained from Merck Co. and Fluka Chemical Co., respectively. The end-functionalized liquid rubber, i.e. amine terminated butadiene–acrylonitrile copolymer, Hycar ATBN 1300X16 (BF-Goodrich) with 18% acrylonitrile content and with a nominal molecular weight of 1760 g/molwas provided by UBE Co. (Japan). All chemicals were used as-received.Kevlar short fiber (1 mm in length) was used as reinforcing fiber. The fiber was kindly provided by Du Pont K.K.-Japan. Alumina, Al_2O_3 (A32), used as the abrasive was purchased from Nippon Light Metal Co., Ltd. The density is 3.90 g/cm^3 and an average diameter of particles of the alumina is approximately 1 μm. Graphite powder (particle size ~ 1 mm) was supported byCompact International (1994) Co., Ltd. (Thailand). Calcium carbonate ($CaCO_3$) with 6-9 μm in diameter used as filler was kindly provided by Surintomya Chemical (Thailand) Co., Ltd.

4.2 Preparation of ATBN-modified PBA-a Copolymers and Their Composites

BA-a/ATBN mixtures at various liquid ATBN contents of 5, 10 and 20 wt% was heated to about 80°C in an aluminum pan and was mixed mechanically for 15 min to obtain homogeneous mixture before undergoing a step cure in an air-circulating oven. Then, the mixture was cured sequentially at 150°C/1h, 180°C/3h, 200°C/1hr and 220°C/1h to guarantee complete curing of PBA-a/ATBN copolymers. The PBA-a/ATBN copolymers were finally left to cool down to room temperature before their characterizations.

BA-a/ATBN compounds consisted of 30wt% BA-a/ATBN mixture at different ATBN contents (5, 10 and 20 wt%),filled with 5wt% Kevlar short fiber, 10wt% Al_2O_3 powder, 10wt% graphite powder, and 45wt% $CaCO_3$powder were prepared by mechanical mixing at 80°C for at least 15 min to ensure ingredients wet-out by the BA-a/ATBN mixture. Then, the compounds were cured at 200°C for 2 h in the hydraulic press with hydraulic pressure of 300 kPa. After having been left to cool down to room temperature, the PBA-a/ATBN composites were ready for further characterizations.

4.3 Sample Characterizations

4.3.1 Rheometer

Dynamic shear viscosity measurements were performed on a parallel plate rheometer using HAAKE RheoStress model RS600. Disposable aluminum plates having 20 mm in diameter were preheated for 30 min with the gap zeroed at the testing temperature. The void-free monomer mixture, which was liquefied at 80°C, was then poured onto the lower plate and the gap was set to 0.5 mm. The temperature was immediately equilibrated at the set point for about 180s and the test was then started.

4.3.2 Fourier Transform Infrared Spectroscopy (FTIR)

Fourier transform infrared spectra of fully cured samples were acquired at room temperature using a JASCO spectrophotometer (model FT/IR-420). All spectra were taken with 64 scans at a resolution of 4 cm^{-1} and in a spectral range of 4000-400 cm^{-1}.

4.3.3 Differential Scanning Calorimetry (DSC)

A differential scanning calorimeter model DSC 6000 from PerkinElmer, Inc. was employed to study the exothermic curing reactions. The samples were scanned by non-isothermal method from 30 to 300°C at four different heating rates of 2, 5, 10 and 20°C/min under a constant flow of nitrogen at 50 ml/min.

4.3.4 Density Measurement

A density of each specimen was determined by a water displacement method according to ASTM D 792 (Method A). All specimens were prepared in a rectangular shape (25 mm × 50 mm × 1 mm). The density was calculated by the following equation:
The average value from at least three specimens was calculated.

$$\rho = \left(\frac{A}{A - B} \right) \times \rho_0 \tag{4.1}$$

Where ρ is density of the sample (g/cm^3), A is weight of the sample in air (g), B is weight of the sample in liquid (g), ρ_0 = density of the liquid at the given temperature (g/cm^3)

4.3.5 Dynamic Mechanical Analyzer

Dynamic mechanical analyzer (DMA) from Netzsch Inc. (model DMA 242 C) in three-point bending mode, and a support span of 40 mm was used to examine storage modulus (E') and loss modulus (E'') of the samples. The dimension of each sample in rectangular shape was 10 mm $\times$ 50 mm $\times$ 3mm. The tests were performed in a temperature sweep mode with a fixed frequency of 1 Hz. Each sample was tested using a heating rate of 2^{o}C/min from room temperature (30^{o}C) to about 250^{o}C.The glass transition temperature was taken from the temperature at the maximum point on the loss modulus or the loss tangent curves.

4.3.6 Flexural Property Measurement

Flexural properties were conducted by a Universal Testing Machine, Lloyd Instruments, Model LR 10K. The measurement was carried out in a three-point bending mode, with a support span of 48 mm and at a crosshead speed of 1.2 mm/min. A minimum of five samples with a dimension of 25 mm $\times$ 60 mm $\times$ 3 mm was tested, and the averaged values were determined.

4.3.7 Thermogravimetric Analysis (TGA)

Weight loss of a sample as a function of temperature was monitored using a thermogravimetric analyzer (TGA) from Mettler Toledo (model TGA 1 STARe System). The weight of the sample was measured to be about 8-10 mg. The samples were heated at a rate of 20^{o}C/min from 30^{o}C to 800^{o}C under argon atmosphere at 100 ml/min.

4.3.8 Surface Examination

The worn surface of the samples was observed with a JSM5410LV scanning electron microscopy (SEM) from JEOL Ltd. Using an acceleration voltage of 15 kV. All samples were coated with a thin film of gold to make the surfaces conductive.

Results and Discussion

5.1 Effect of Amine-terminated Acrylonitrile-Butadiene (ATBN) Contents on Properties of Polybenzoxazine Modified with ATBN

5.1.1 Rheological Property of BA-a/ATBN Mixtures

The effect of liquid ATBN contents on liquefying and gelation behaviors via rheological measurement of BA-a/ATBN mixtures is shown in Fig. 5.1. The first major thermal event is called the liquefying point or the liquefying temperature (the left hand side), which is the transition of solid to liquid. At this point, the complex viscosity of the BA-a/ATBN mixtures approaches its minimum value. From the figure, the liquefying temperatures of the BA-a/ATBN mixtures were about 77^{o}C for BA-a, 90^{o}C for BA-a/ATBN (95/5), 115^{o}C for BA-a/ATBN (90/10), and 70^{o}C for BA-a/ATBN (80/20). It can be seen that the liquefying temperature of the samples increased with increasing ATBN contents up to 10 wt%. This is because of the larger molecules having high viscosity of liquid ATBN than that of the BA-a monomer. In the other hand, the liquefying temperature of the BA-a monomer blended with 20 wt% ATBN can be lowered comparing with that of the BA-a monomer. This behavior may be due to the dilution effect of the viscous liquid ATBN in the BA-a. In addition, the room temperature physical appearance of the uncured resins ranged from hard solid in the BA-a, BA-a/ATBN (95/5) and BA-a/ ATBN (90/10), to soft solid in the BA-a/ATBN (80/20). This is due to the fact that the ATBN used is viscous liquid at room temperature while the BA-a monomer is solid at room temperature. An addition of viscous liquid ATBN into the solid BA-a up to 20 wt% thus lowered the liquefying temperature of the resulting mixture. The other reason may be incompatible of BA-a/ATBN mixtures, increasing this phenomenon with ATBN content. The incompatibility traduces into a weak interface. In this case, interlayer slip may occur and, as a result, the viscosity of the BA-a/ATBN (80/20) mixture decreased as similarly observed in polypropylene/NBR system [47].

Furthermore, the second major thermal event on the right hand side is called the gel point, the transition of liquid to solid due to continuous network formation of the resin mixture. The gel temperatures or gel points of the BA-a/ATBN mixtures tended to decrease with increasing ATBN contents, i.e. 185^{o}C for BA-a, 175^{o}C for BA-a/ATBN (95/5) and 168^{o}C for BA-a/ATBN (90/10), except in the case of the BA-a/ATBN (80/20) mixture tended to increase the gel temperature, i.e. 172^{o}C when compared with that of the BA-a/ATBN (90/10) mixture. Remarkably, this characteristic of the samples suggested an additional function of the liquid ATBN as an initiator for benzoxazine curing thus lowering gel temperature of the BA-a. Therefore, the use of the liquid ATBN rubber is attractive because the gel times of the BA-a/ATBN mixtures were shorter. However, an increase of the gel temperature of the BA-a/ATBN (80/20) mixture compared with the gel temperature of the BA-a/ATBN (90/10) mixture was observed. This behavior was also likely due to the dilution effect of the viscous liquid ATBN. In addition, the temperature from the liquefying point to the gel point is called processing window of the resin which is the range of the lowest viscosity useful for polymer compounding or processing. For the BA-a/ATBN mixtures, the processing window was determined to be in a range of 70^{o}C to 175^{o}C which provided sufficient processing window, particularly for the compounding or composite manufacturing process.

5.1.2 Network Formation between BA-a Monomer and ATBN

As discussed above that the liquid ATBN can act as an initiator to lower gel point of theBA-a monomers. Therefore, it can be expected that the primary amino groups may react with the BA-a and accelerate the BA-a homopolymerization. In addition, the chemical reaction between butadiene molecules in the liquid ATBN and hydroxyl groups of the polybenzoxazine (PBA-a) could also occur. Fig. 5.2(a) illustrates IR spectrum of the BA-a with the peak assignments at 1497 and 947 cm^{-1} due to the tri-substituted benzene ring, at 1233 and 1030 cm^{-1} due to the asymmetric stretching of ether linkage (C–O–C), and at 1327 cm^{-1} due to CH_2 wagging in the BA-a ring. After polymerization, IR spectrum of the PBA-a presented the absorption bands of a ring opening of the BA-a to the PBA-a at 1488 and 878 cm^{-1} due to a tetra-substituted benzene ring mode as well as at about 3300 cm^{-1} due to the phenolic hydroxyl group formation [48], while the IR characteristics of the BA-a also disappeared as can be observed in Fig. 5.2(b). For the unsaturation presenting along ATBN backbone, in Fig. 5.2(c), the spectrum clearly showed *trans*-1,4 and 1,2-vinyl characteristic frequencies of the butadiene moieties due to out-of-plane deformation of the =C–H at 970 and 912 cm^{-1}, respectively. Moreover, the peaks at 3320 cm^{-1} (NH_2 stretch) as well as at 1650 and 1580 cm^{-1} (NH_2 deformation) were also observed. In the case of ATBN-modified PBA-a (Fig. 5.2(d)), the characteristic peaks of the BA-a had disappeared by the end of the complete cure accompanied with the appearance of new peaks due to the polymerization of the BA-a. Furthermore, IR spectrum showed a decrease in the absorptions at 970 and 912 cm^{-1} due to the out-of-plane deformation of the =C–H bond of the *trans*-1,4 and vinyl configurations in butadiene [49]. Additionally, the peaks at 1650 and

1580 cm^{-1} due to NH_2 deformation also decreased. These behaviors confirmed that chemical reaction between $-CH=CH_2$ groups of the ATBN and –OH groups of the PBA-a can be formed via ether linkages (C–O–C stretch) at 1110 cm^{-1}. In addition, the BA-a may also undergo primary amino group-activated ring-opening polymerization reaction [50]. Therefore, the possible chemical reaction of the PBA-a and the ATBN according to both reactions above are shown in Fig. 5.3.

One important aspect of a thermosetting polymer is its gel point. The gel points of samples can be accurately estimated by dynamic rheological measurements which are sensitive to degree of crosslinking of the polymers. In principle, elastic modulus and viscous modulus present the same power-law variation with respect to the frequency of oscillation at a gel point as follows Equation (5.1).

$$\tan\delta = G''/G' = \tan(n\pi/2) \tag{5.1}$$

Where G' is storage modulus, G'' is loss modulus and n is the relaxation exponent which is network specific.

The above expression suggests that frequency independent nature of tanδ at gel point by various frequencies crossover each other [51]. As exemplified, tanδ as a function of time (s) at 10 rad/s and 30 rad/s of the BA-a/ATBN(95/5) mixture at 150°C, 160°C, 170°C and 180°C is plotted in Fig. 5.4(a). From this figure, the gel point corresponded to the gel time at each temperature of the mixture was about 3703 s (150°C), 2713 s (160°C), 1508 s (170°C), and 857 s (180°C). It was found that raising the processing temperature increases the rate of crosslinking of the BA-a/ATBN mixture. Consequently, at higher temperature, the mixture reached its gel point more quickly and the gel time was shorter. Furthermore, Fig. 5.4(b) illustrates the gel time at different temperatures of the BA-a/ATBN mixtures at various ATBN contents. At the same temperature, the gel times of the BA-a/ATBN mixtures tended to decrease with increasing of the liquid ATBN content up to 10 wt%, i.e. the gel time at 150°C for the BA-a = 4813 s, the BA-a/ATBN (95/5) = 3703 s and the BA-a/ATBN (90/10) = 3412 s. While, the gel time of the BA-a/ATBN (80/20) = 3480 s which was slightly longer than that of the BA-a/ATBN (90/10) was observed as similarly seen in the gelation behavior in Fig. 5.1. This behavior is possible due to dilution effect of the liquid ATBN. However, these results can also be implied that the curing conversion of the BA-a/ATBN mixtures was raised with increasing of the liquid ATBN content due to its function as the initiator for the

BA-a ring-opening reaction. In some cases, the addition of liquid rubber resulted in a retardancy on gel times of polymer/liquid rubber mixtures, i.e. epoxy resin/hydroxyl-terminated polybutadiene (HTPB). The polymer mixtures showed an increase of gel times with increasing HTPB, i.e. 900 s for epoxy resin/HTPB (95/5) and 1080 s for epoxy resin/HTPB (90/10) at 120°C [52].

5.1.3 Curing Behaviors of BA-a/ATBN Mixtures

Curing behaviors of the BA-a/ATBN mixtures at liquid ATBN contents of 0, 5, 10, 20 and 100 wt% were evaluated by differential scanning calorimetry (DSC). In Fig. 5.5(a), The DSC thermograms of the BA-a/ATBN mixtures at 5, 10 and 20 wt% ATBN displayed the curing exotherms centered at temperature levels of 227°C, 223°C and 223°C, respectively. Those exothermic peaks were lower than that of the BA-a monomers showing a peak at 230°C. This finding implies that the liquid ATBN reveals acceleration effect on the curing process of the monomers. It has been reported that the BA-a ring-opening was stabilized by the lone-pair electron on the terminal amino groups of ATBN, consequently, reduces the cure temperature [17, 49]. On the contrary, the liquid ATBN resulted in no sign of any curing reaction in this temperature range because no initiators or curing agents were added to the liquid ATBN. Instead, the endothermic thermal events in a temperature range of 50–120°C was observed, likely as a result of the evaporation process of some solvent. Moreover, the increase of the liquid ATBN content affected the curing thermograms in such a way to decrease the area under the exothermic peaks, i.e. 243 J/g for BA-a/ATBN (95/5), 216 J/g for BA-a/ATBN (90/10) and 197 J/g for BA-a/ ATBN (80/20). It appeared that the heat of reaction of the BA-a/ATBN curing was lower than that of BA-a monomers, i.e. 276 J/g.

As it was found that the liquid ATBN might act as an initiator of the BA-a, activation energies of a curing process of the BA-a/ATBN mixtures was therefore examined. For example, the heat flows of the BA-a/ATBN (95/5) mixture from the DSC at heating rate of 2, 5, 10 and 20°C/min are illustrated in Fig. 5.5(b), while those of the BA-a, BA-a/ATBN (90/10) and BA-a/ATBN (80/20) at the same heating rate were also investigated (not show here). From Fig. 5(b), the exothermic peaks of the BA-a/ATBN (95/5) mixture shifted to a higher temperature with higher heating rate due to shorter time. In this work, the activation energy of curing reaction of the BA-a/ATBN mixtures was calculated using Kissinger method as can be seen in Equation (5.2) which is an alternative way of estimating the activation energy without assuming any model of kinetic parameters and without integrating the exothermic peak.

$$\ln\left(\frac{\beta}{T_p^2}\right)=\ln\left(\frac{Q_pAR}{E_a}\right)-\frac{E_a}{RT_p} \tag{5.2}$$

Where $Q_p=-[df(\alpha)/d\alpha]_{\alpha=\alpha_p}$, β =dT/dt is a constant heating rate, A is the pre-exponential factor (1/s), E_a is the activation energy (8.314 kJ/mol) and T_p is the peak temperature (K).

The logarithm plots of the heating rates versus the reciprocal of peak temperatures of the BA-a, BA-a/ATBN (95/5), BA-a/ATBN (90/10) and BA-a/ATBN (80/20) is given in Fig. 5.6. A good linear relationship between the heating rates and the reciprocal of peak temperatures was clearly obtained. The average activation energy calculated from the slope of the plot of the BA-a/ATBN (95/5), BA-a/ATBN (90/10) and BA-a/ATBN (80/20) mixtures was 85.4 kJ/mol, 82.3 kJ/mol and 82.7 kJ/mol, respectively, while that of the BA-a was about 88.0 kJ/mol. Therefore, the decrease of the activation energies with increasing of the liquid ATBN for the BA-a/ATBN mixtures was the indication of the acceleration effect, and providing of faster curing reaction. However, the activation energy for the BA-a/ATBN (80/20) mixture was slightly increased comparing with that of the BA-a/ATBN (90/10) combination. A slightly increased energy is to hinder the molecular mobility and to retard the curing reaction due to diluents effect of the liquid ATBN. This behavior is in agreement with the result observed in our rheological measurement and epoxy/CTBN system [53]. For the epoxy/CTBN system, the addition of liquid CTBN in epoxy resin contributed to increase activation energy values of the epoxy resin/CTBN mixtures with increasing the CTBN content, since the reaction between epoxide and anhydride was hindered by the CTBN rubber.

5.1.4 Tribological Behaviors of ATBN-modified PBA-a Copolymers

The effect of liquid ATBN contents on the average friction coefficient ($\mu_{avg.}$) and its extreme values ($\mu_{max.}$ and $\mu_{min.}$) as well as specific wear rate of polybenzoxazine (PBA-a) at 25°C is listed in Table 5.1. The $\mu_{avg.}$ and specific wear rate of the PBA-a was 0.38 and 2.08×10^{-4} mm^3/Nm, respectively. From the result, the $\mu_{avg.}$ of the PBA-a is lower than that of epoxy ($\mu_{avg.}$~ 0.65-0.84) [54], phenolic (μ_{avg} ~ 0.9-1.1) [55] and polyamide66 ~ 0.66 [56]. Therefore, a special characteristic of the PBA-a evidences its self-lubrication ability compared to epoxy, phenolic and polyamide66. Furthermore, the $\mu_{avg.}$ and specific wear rate of the PBA-a decreased with increasing ATBN content up to 5 wt%, i.e. $\mu_{avg.}$ ~ 0.36 and specific wear rate ~ 1.85×10^{-4} mm^3/Nm, which is the most effective to decrease both property of the PBA-a. While with a further increase of ATBN content above 10 wt%, the PBA-a/ATBN copolymers showed a significant increase in its friction coefficient and specific wear rate. These observed trends are in agreement with the finding of previous publications [57-59]. It indicates that the ATBN with softer molecular nature than the PBA-a has good friction-reducing, and anti-wear abilities during sliding of the PBA-a within a mass fraction of 5 wt%. In addition, it is possible that smaller ATBN particle sizes of the PBA-a/ATBN (95/5) copolymer than that of the PBA-a/ATBN (90/10) and PBA-a/ATBN (80/20) copolymers is seen to contribute reduction in friction coefficient and specific wear rate as the finding reported in ZrO_2/PEEK [60] and SiC/epoxy composites [61]. The other reason of improved specific wear rates at low ATBN content provides the toughness enhancement of the ATBN-modified PBA-a. Furthermore, it was expected that the transfer film played a dominant role in determining the tribological behaviors for the PBA-a/ATBN (95/5) copolymer. This will be further discussed below. In the other hand, it could be rationally expected that the PBA-a/ATBN copolymers with the ATBN content above 10 wt% would give poor wear resistance. This behavior may be attributed to the formation of larger ATBN domains at higher proportions and reduction in the hardness of the samples, resulting in fatigue wear. Such wear will be caused by a cycling loading during friction in the softer materials. A comparison of specific wear rate between the PBA-a/ATBN (95/5) copolymer and the liquid carboxyl-terminated poly(butadiene-co-acrylonitrile) (CTBN) rubber-modified epoxy (EP) [57] explained that the specific wear rate of the PBA-a/ATBN copolymer was lower than that of the EP/2.5 wt% CTBN, i.e. 2.5×10^{-4} mm^3/Nm. Therefore, the PBA-a/ATBN (95/5) copolymer was somewhat suitable to act as a matrix for polymer-based bearing and coating materials replacing the thin film epoxy coating on steel, concrete and pipeline. Because the copolymer manifested good wear resistance to abrasion load compared with epoxy resin with specific wear rate value of ~ 5.00×10^{-4} mm^3/Nm [57] and presented the lower friction coefficient than that of the thin film epoxy coating for pipeline, i.e. $\mu_{avg.}$~ 0.51-0.71 [62].

5.1.5 Worn Surface Morphologies of ATBN-modified PBA-a Copolymers

Scanning electron microscope photographs of the worn surface of the PBA-a and the PBA-a/ATBN copolymers at different liquid ATBN contents are illustrated in Fig. 5.7. From this figure, there are remarkable differences in the worn surface morphologies of each sample. In Fig. 5.7(a), wear debris particles were observed. The PBA-a was relatively brittle and it could easily crack and break from the sample surface. These characteristics cause an increase in a specific wear rate of the PBA-a. In the case of the ATBN-modified PBA-a copolymers, a small amount of the ATBN contributed to a reduction of the specific wear rate and friction coefficient of the PBA-a. For the PBA-a/ATBN (95/5) copolymer, the worn surface of the copolymer displayed the scale-like damage, which is apparently generated under repeated loading during sliding as revealed in Fig. 5.7(b). However, the fatigue wear was not observed on the worn surface of the BA-a/ATBN (95/5) copolymer. This behavior can be suggested that the applied load is not higher than the fatigue strength of the copolymer. In addition, it is possible that the friction film on the worn surfaces was formed which creates greater lubricity effect of contact surfaces, consequently lower the frictional response. To compare with wear mode of epoxy (EP) modified by liquid carboxyl-terminated poly(butadiene-co-acrylonitrile) rubber (CTBN) [57], the scale-like damage pattern and the surface peeling off due to the fatigue wear mechanism was found on the tracks of the EP/2.5 wt% CTBN. Therefore, the PBA-a/ATBN (95/5) copolymer showed mild wear mechanisms than the EP/CTBN system. For the worn surface of the PBA-a/ATBN (90/10) and the PBA-a/ATBN (80/20) copolymers are presented in Fig. 5.7(c) and Fig. 5.7(d), respectively. The scale-like damage under a repeating load during sliding was clearly noticed. Also, the more rougher surface having some dimples, and wider damaged areas were found on the worn surface of the PBA-a modified with 10 wt% and 20 wt% ATBN. The cracks inside for the PBA-a/ATBN (90/10) copolymer, and some dimples for the PBA-a/ ATBN (80/20) copolymer were observed. In general, these characteristics corresponded to the fatigue wear mode. Therefore, it can be summarized that the dominant wear mechanisms of the samples were changed from the abrasive wear mode of the PBA-a to the adhesion wear mode for the PBA-a/ATBN (95/5) copolymer, while the wear mode of the PBA-a/ ATBN (90/10) and PBA-a/ATBN (80/20) copolymers is fatigue wear.

5.1.6 Dynamic Mechanical Analysis of ATBN-modified PBA-a Copolymers

Themomechanical properties of PBZ modified with various ATBN contents were tabulated in Table 5.2. Storage moduli at 30°C of PBA-a/ATBN copolymers at ATBN of 5, 10 and 20 wt% exhibited the values of 4,50, 3.64 and 3.11 GPa, respectively, which were lower than that of the poly(BA-a), i.e. 5.50 GPa. It can conclude that the reduction of the storage moduli with addition of the ATBN was about 18.2%, 33.8% and 43.5% for the

PBA-a containing of 5, 10, and 20 wt% ATBN, respectively. The decreases in the modulus were attributed to the presence of low modulus rubber particles in PBA-a matrix. However, the insignificant decrease of the storage moduli of the PBA-a modified with ATBN in a range of 1-5wt% were observed. Therefore, this behavior can confirm that there is a good interfacial bond between ATBN and PBA-a as previously reported that ATBN has amino groups at its chain ends, which can react with imines created during the curing process. This reaction is easy because imine is very elctrophilic and the amino group is very nucleophilic. In addition, the carbon double bonds in ATBN can also form ether linkages with activated phenolic hydroxyl groups in PBA-a. The formation of possible chemical reactions between PBA-a and ATBN was shown in Fig. 5.3.

Glass transition temperatures (T_gs) of poly(BA-a) and their copolymers determined from the maximum of loss modulus (E") or loss tangent (Tanδ) curves in dynamic mechanical analyzer (DMA) experiment are also listed in Table 5.2. The T_g identified from E" curve of the PBA-a was about 173^{o}C and the value was found to be slightly decreased by blending with the ATBN. The T_g of the fully cured PBA-a/ATBN copolymers showed a value ranging from 172^{o}Cto 162^{o}C with increasing ATBN content. The possible effects for this behavior may own to the presence of ATBN rubber dissolved in the PBA-a matrix. Additionally, the T_g of the ATBN phase, i.e. -51^{o}C was also lower that of the PBA-a. Moreover, an increase in free volume caused by the thermal hydrostatic stress applied to the ATBN inclusion was accountable for the decrease of the T_g's copolymers. However, we can see that an incorporation of ATBN into PBA-a has slightly effect on the T_g values for the PBA-a/ATBN copolymers. This indicates that the ATBN rubber particles can perfectly separate in the PBA-a matrix and it can react with the PBA-a.

5.1.7 Mechanical Properties of ATBN-modified PBA-a Copolymers

Flexural properties, i.e. flexural modulus, flexural strength, elongation at break, and area under the stress-strain curves were studied. The flexural moduli were about 3.97, 3.80 and 3.08 GPa for the PBA-a/ATBN copolymers at 5, 10 and 20 wt% ATBN, respectively, which were slightly lower than that of the PBA-a, i.e. 4.68 GPa. This might be related to the fact that the modulus of ATBN rubber is lower than that of the PBA-a. Moreover, the flexural strength of the PBA-a was found to be constant with an addition of the ATBN up to 10 wt%, i.e. 137 and 139 MPa for the PBA-a/ATBN copolymers at 5 and 10 wt% ATBN, respectively, and then that of the PBA-a/ATBN (80/20) copolymer decreased, i.e. 119 MPa. Typically, the flexural strength of the polymer decreased with an addition of rubber following a rule of mixture. However, the ATBN-modified PBA-a copolymers at the ATBN content up to 10 wt% show the opposite characteristic. It is possible that the stress was sufficiently transferred to the rubbery ATBN phase as a result of the good interfacial bond of PBA-a and ATBN. Therefore, the incorporation of ATBN below 10% by weight into the PBA-a was found to be sufficient to improve the flexural strength and to maintain the high modulus of the obtained copolymers. In addition, the elongation at break, i.e. 0.028, 0.034, 0.045 and 0.050% as well as the area under the stress-strain curves, i.e. 1.53, 2.20, 2.84 and 2.86 MPa for the poly(BA-a) modified with ATBN at 0, 5, 10 and 20 wt%, respectively, clearly increased with increasing of the ATBN content. These characteristics are due to an enhanced ability to inhibit the crack growth, absorbing, and dissipating forces in the rigid PBA-a by an addition of the ATBN modifier. Furthermore, ATBN dissolved in the PBA-a matrix phase and rubber particles finely distributed in the matrix contributed to the increase of the toughness the copolymers as a result of the increase of the area under the stress-strain curve.

5.1.8 Thermal Stability of ATBN- modified PBA-a Copolymers

Thermal stabilities, i.e. degradation temperature at 5% weight loss (T_{d5}) and char yield of the PBA-a and ATBN-modified PBA-a copolymers at various ATBN contents are investigated by thermogravimetric analysis (TGA). The T_{d5} of the ATBN-modified PBA-a copolymers at various ATBN contents of 5, 10 and 20 wt% was about 325°C, 322°C and 316°C, respectively, while that of the PBA-a and ATBN was about 339°C and 241°C, respectively. Moreover, the char yield at 800°C decreased from 37% for the PBA-a to 22, 17 and 12% with the incorporation of 5, 10 and 20 wt% ATBN, respectively. From the results, the incorporation of ATBN rubber modifier slightly decreased the thermal stability of the PBA-a. On the other hand, the presence of aromatic structure of the PBA-a in the PBA-a/ATBN copolymers could possibly suppress segmental decomposition via gaseous fragments due to ATBN thermal degradation.

5.2 Effect of Amine-terminated Acrylonitrile-Butadiene (ATBN) Contents on Properties of ATBN-modified Polybenzoxazine Composites

5.2.1 Dynamic Friction and Wear of PBA-a/ATBN Copolymer Based Composites

As previously mentioned that the PBA-a/ATBN copolymer was possible to be a binder for self-lubricating composites because they showed low friction coefficient and anti-wear characteristics compared with those of phenolic and epoxy resins. Table 5.1 summarizes the average friction coefficient ($\mu_{avg.}$) and its extreme values ($\mu_{max.}$ and $\mu_{min.}$) of PBA-a/ATBN composites composed of the PBA-a/ATBN copolymer with different liquid ATBN contents (0-20 wt%), and ingredients (Kevlar short fiber, alumina, graphite and calcium carbonate). From Table 5.1, the $\mu_{avg.}$ of the composites remained in the range of 0.15-0.28. Moreover, the addition of liquid ATBN content about 5 wt% reduced the average friction coefficients of the PBA-a/ATBN composite. However, at the ATBN content greater than 5 wt%, the $\mu_{avg.}$ of the composites tended to increase. These effects of ATBN were similar to those observed in the unfilled PBA-a/ATBN copolymers. The PBA-a/ATBN (95/5) composite had the minimum value of the $\mu_{avg.}$ about 0.15. The decrease in the $\mu_{avg.}$ with an increase in 5 wt% ATBN is due to a strong resistance to fatigue of the ATBN. Moreover, it is possible that the composite which was filled with 5 wt% ATBN could be transferred well to the steel ball and its transfer film was thin, uniform and adhered strongly to the steel ball, which could then act as micro lubrication. While, $\mu_{avg.}$ of larger particle size for 10 and 20 wt% ATBN-filled composites was higher than that of the PBA-a/ATBN (95/5) because the PBA-a/ATBN (90/10) and PBA-a/ATBN (80/20) composites transfer film had poor adhesion the steel ball. In addition, the $\mu_{avg.}$ of the PBA-a/ATBN composites was significantly lower than that of the PBA-a/ATBN copolymers. This characteristic may be due to the additional lubricity and wear resistance of the ingredients in the PBA-a/ATBN binder such as Kevlar short fiber, which was reported to significantly reduce the friction coefficient in hybrid phenolic friction [63] and epoxy composites [64]. The additional cause of this behavior may be the effect of the solid lubricating of graphite as it is known that carbon fillers can serve as a solid material to lubricate the rubbing surface [65].

Specific wear rates of PBA-a/ATBN composites at various liquid ATBN contents are also tabulated in Table 5.1. The specific wear rate of the composites decreased with increasing content of ATBN, i.e. from 7.30×10^{-5} mm^3/Nm for PBA-a composite to 1.64×10^{-5} – 6.07×10^{-5} mm^3/Nm for PBA-a/ATBN composites. Thus, the incorporation of ATBN into PBA-a composite can improve wear resistance of the PBA-a composite. In addition, the PBA-a/ATBN (95/5) composite with lowest friction coefficient showed lower specific wear rate than that of journal bearing based on PA66 filled with 18 wt% self-lubricating PTFE, i.e. 7.50×10^{-5} mm^3/Nm [66]. Moreover, the specific wear rates of the composites tended to be lower than those of the unfilled copolymers because the addition of the ingredients into the PBA-a/ATBN copolymers can reduce the extent of shear stress transferred to the copolymers as expected. From experimental results, the PBA-a/ATBN lubricating composites showed significantly low friction coefficient and specific wear rate. In general, friction coefficient under dry condition of polymer composite bearing is in the range of 0.05-0.15 [67]. Therefore, the PBA-a/ATBN (95/5) composite can be used to increase the service life of machinery and equipment where oil and grease cannot be used.

To investigate wear characteristics of all PBA-a/ATBN composites, SEM worn surfaces are presented in Fig. 5.8. The worn surface showed regions of non-uniform roughness for all samples. In Fig. 5.8(a), the worn surface of the PBA-a composite looks somehow rough. Possibly, as the friction mechanism was attributed to the ploughing, thus a two-body mode of abrasive wear is speculated to be dominant for the composites. For the worn surface of the PBA-a/ATBN (95/5) composite as can be seen in Fig. 5.8(b), there were secondary plateaus that no ingredients could be seen on the worn surface of the composite. Furthermore, resin rich surface layer with less voids and debris on the worn surface of the PBA-a/ATBN (95/5) composite was also observed. This characteristic indicates good interfacial interaction between the ingredients and the copolymer binder for the PBA-a/ATBN (95/5) composite. Moreover, it is possible that the addition of 5 wt% ATBN led to the formation of transfer films on the sliding-ball surface. Lowest friction coefficient of the composite was attributed to the lubricating action of such transferred friction films. Thus, the wear mechanism was mainly the adhesion. The worn surfaces of PBA-a/ATBN (90/10) and PBA-a/ATBN (80/20) composites in Fig. 5.8(c) and Fig. 5.8(d), respectively, were noticed to be very rough with distinct plateaus, while the ploughed grooves were not found on these worn surfaces. There were secondary plateaus and some fine wear debris particles on the worn surface of the composites. Such plateaus play protective role against the wear damage to the underlying material, which are generally responsible for an enhancement of frictional response. Furthermore, the worn surface of PBA-a/ATBN (90/10) and PBA-a/ATBN (80/20) composites also exhibited resin rich surface layer. The presence of resin layer improved the bonding and surface integrity with high ingredient-binder adhesion that resulted in the decrease of specific wear rates of both composites. Therefore, the wear of PBA-a/ATBN (90/10) and PBA-a/ATBN (80/20) composites was could be related to the three-body abrasion. Also the wear morphologies of the PBA-a/ATBN composites in comparison with the PBA-a/ATBN copolymers clearly point out that the addition of ingredients is an effective way to reduce the fatigue wear during the prolonged sliding contact with the steel ball.

5.2.2 Glass Transition Temperature of Lubricating Composites Based on PBA-a/ATBN Copolymers

Loss tangent (Tanδ) plots of the PBA-a/ATBN composites are depicted in Fig. 5.9. The peak in the Tanδ curve is indicative of glass transition temperature (T_g) of the composites. From this figure, the magnitude of T_g for all composites showed the value of ~ 190°C. However, in general, the incorporation of rubbers such as ATBN (T_g ~ -51°C), and hydroxyl-terminated polybutadiene (HTPB) (T_g ~ -75°C) into the polymer leads to decrease in T_g of the polymer as previously reported in epoxy/ATBN blends [68], and epoxy/HTPB blends [52]. In addition, Tanδ factor also indicates damping capacity of the composite materials. It is observed that the highest damping capacity, i.e. 0.420 shown by the PBA-a composite till transition regime gets lower and dominated by the PBA-a/ATBN (95/5) composite at elevated temperature regime, i.e. >210°C. Therefore, the PBA-a composite is most effective in controlling and minimizing the unwanted phenomenon, for example, noise, and vibration to a larger extent dynamically generated during the at temperature near T_g of 190°C, while the PBA-a/ATBN (95/5) composite should be operated at lower and elevated temperatures because it shows better damping capacity behavior than the PBA-a composite.

5.2.3 Flexural Properties of Lubricating Composites Based on PBA-a/ATBN Copolymers

Flexural properties, i.e. strength and modulus of the PBA-a/ATBN composites at different liquid ATBN contents are presented in Fig. 5.10. In this figure, the flexural strengths of the PBA-a/ATBN composites were found to increase with an increase of the ATBN content up to 5 wt%, and then the flexural strengths decreased with further addition of the ATBN. However, all PBA-a/ATBN composites had higher values of flexural strength than that of the PBA-a composite. The flexural strength of the PBA-a/ATBN (95/5) composite, i.e. 47.6±8.0 MPa was about 1.4 times higher than that of the PBA-a composite, i.e. 34.6±3.8 MPa. In addition, the flexural strength value of the PBA-a/ATBN composite was higher than that of linseed oil- and cashew nut shell liquid (CNSL)-modified phenolic resin filled with fibers of glass, steel, polyacrylonitrile (PAN), rock wool, friction modifiers, and a space filler, i.e. 41.2 MPa and 41.0 MPa, respectively [69]. Furthermore, the obtained flexural strength for the PBA-a/ATBN (95/5) composite was similar to the value published by Saffar and Shojaei [70]. It was reported the flexural strength values of the composites based on phenolic/SBR matrix and additives such as coal powder, graphite, $CaCO_3$, iron powder, steel wool, barite, iron oxide, cashew dust, aramid pulp, vermiculite, and alumina was about 47.5 MPa for 7.5vol% SBR. Therefore, in our work, the enhancement in the composite strength with the proper content of the ATBN was possibly due to the good interfacial adhesion between the ingredients and the PBA-a/ATBN copolymer. This characteristic is in agreement with the morphology of worn surface of the PBA-a/ATBN (95/5) composite that exhibited resin rich surface layer with less voids and debris.

The flexural modulus of the PBA-a/ATBN (95/5) composite, i.e. 5.9±0.4 GPa was also found to be higher than that of the PBA-a composite, i.e. 5.4±0.6 GPa as illustrated in Fig. 5.10. At ATBN content greater than 5 wt%, the flexural modulus of the composites was found to decrease with the amount of the ATBN rubber. This behavior could be related to the effect of excessive viscous liquid ATBN with much lower modulus than that of the PBA-a phase. Again, the PBA-a/ATBN(95/5) lubricating composite exhibited the flexural modulus higher than that of linseed oil- and cashew nut shell liquid (CNSL)-modified phenolic resin filled with fibers of glass, steel, polyacrylonitrile (PAN), rock wool, friction modifiers, and a space filler, i.e. 5.3 GPa and 5.7 GPa, respectively [69].

Table 5.1 Tribological properties at 25°Cof ATBN-modified PBA-a copolymers and their composites at various ATBN contents.

PBA-a/ATBN Copolymers (wt%)	Friction coefficient			Specific wear rate (mm^3/Nm)
	μ_{min}	$\mu_{max.}$	$\mu_{avg.}$	
100/0	0.28	0.47	0.38	2.08×10^{-4}
95/5	0.31	0.54	0.36	1.85×10^{-4}
90/10	0.26	0.49	0.38	2.85×10^{-4}
80/20	0.30	0.42	0.51	9.60×10^{-4}

PBA-a/ATBN Composites (wt%)	Friction coefficient			Specific wear rate (mm^3/Nm)
	μ_{min}	$\mu_{max.}$	$\mu_{avg.}$	
100/0	0.16	0.33	0.28	2.43×10^{-5}
95/5	0.11	0.18	0.15	7.07×10^{-5}
90/10	0.12	0.28	0.24	1.64×10^{-5}
80/20	0.16	0.30	0.26	2.51×10^{-5}

Table 5.2 Viscoelastic properties of ATBN-modified polybenzoxazine copolymers at various ATBN contents.

PBA-a/ATBN Compositions (wt%)	E' at 30°C (GPa)	T_g from E" (°C)	T_g from Tan δ (°C)
100/0	5.50	173	192
95/5	4.50	168	182
90/10	3.64	167	180
80/20	3.11	162	175

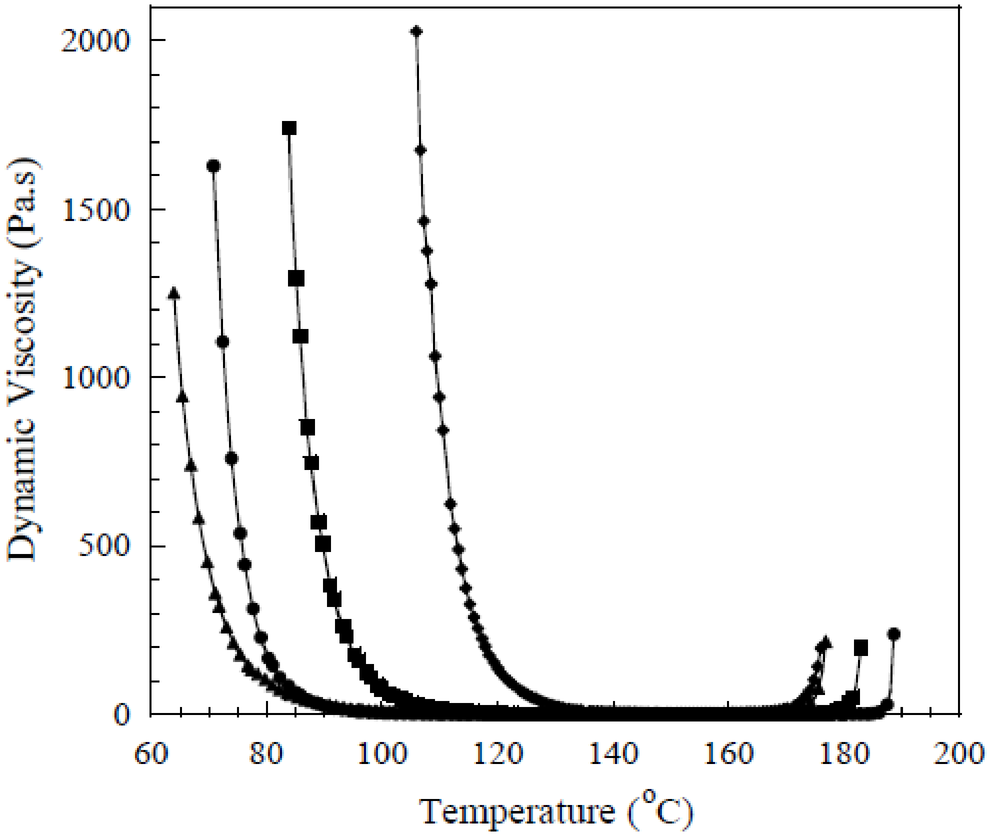

Figure 1: Dynamic viscosity of BA-a/ATBN mixtures at various ATBN mass fractions: (●) BA-a, (■) BA-a/ATBN (95/5), (◆) BA-a/ATBN (90/10), (▲) BA-a/ ATBN (80/20).

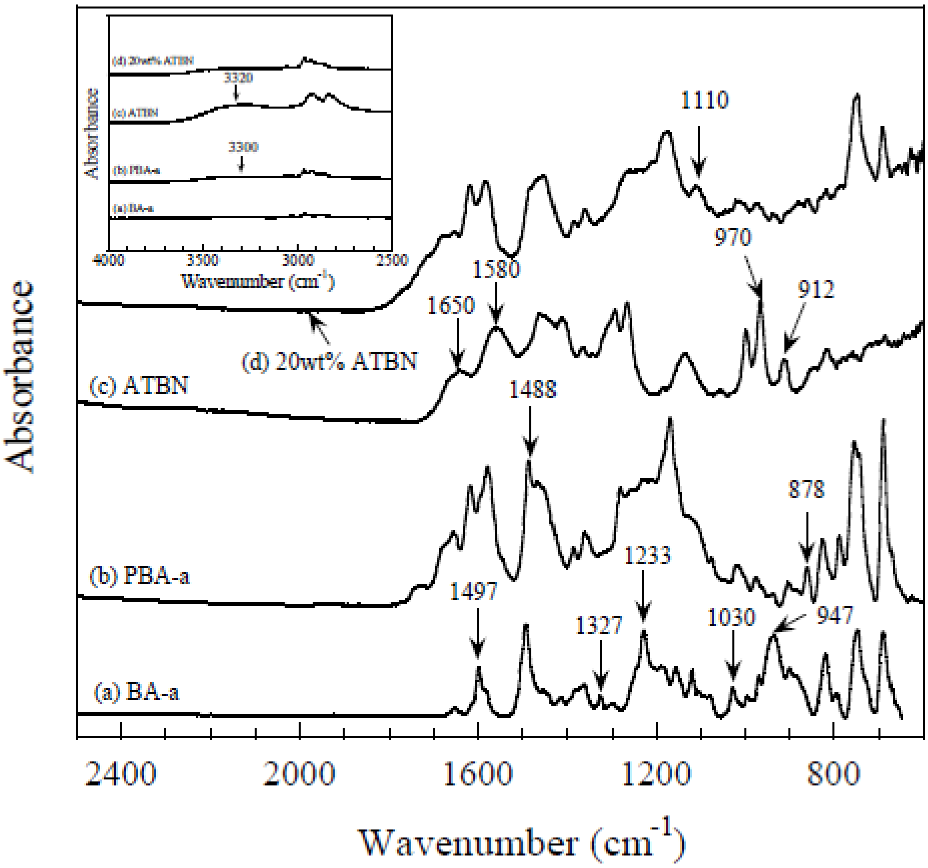

Figure 2: FTIR of BA-a, PBA-a, ATBN and PBA-a/ATBN (80/20) copolymer.

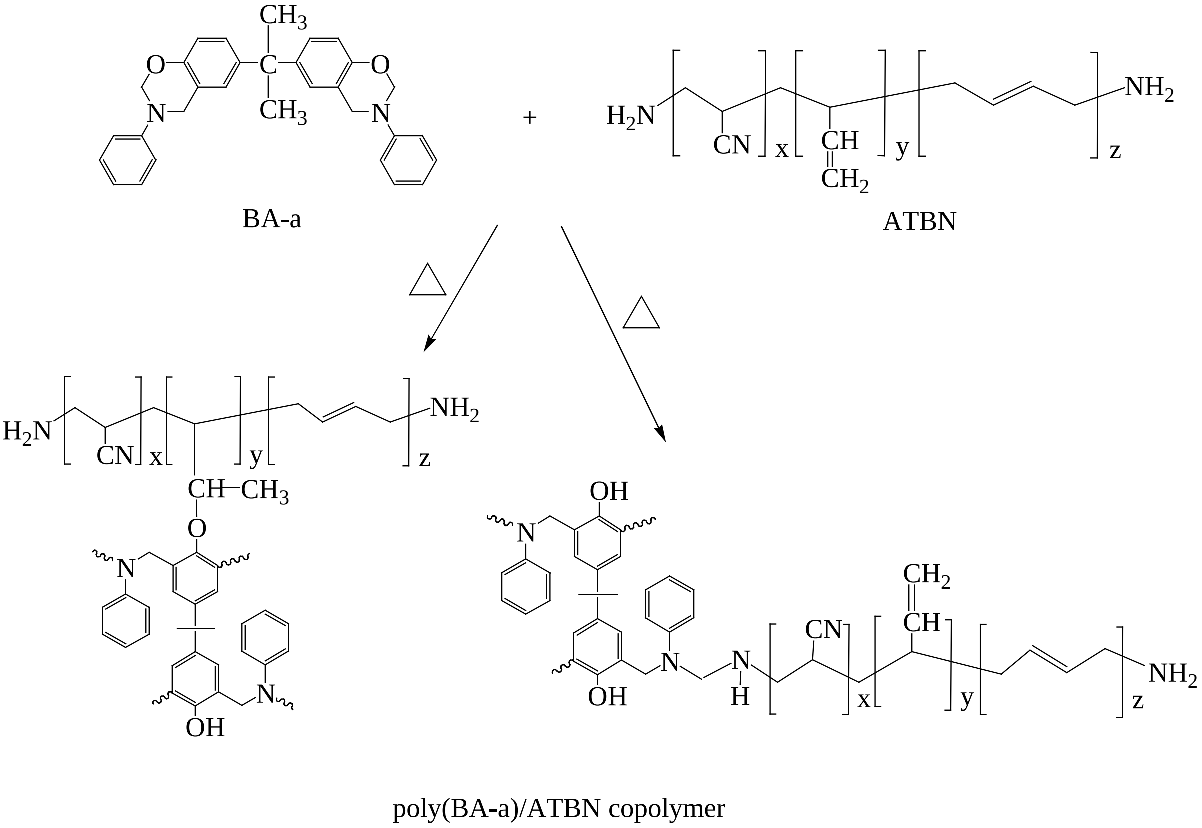

Figure 3: A possible copolymerization between PBA-a and ATBN.

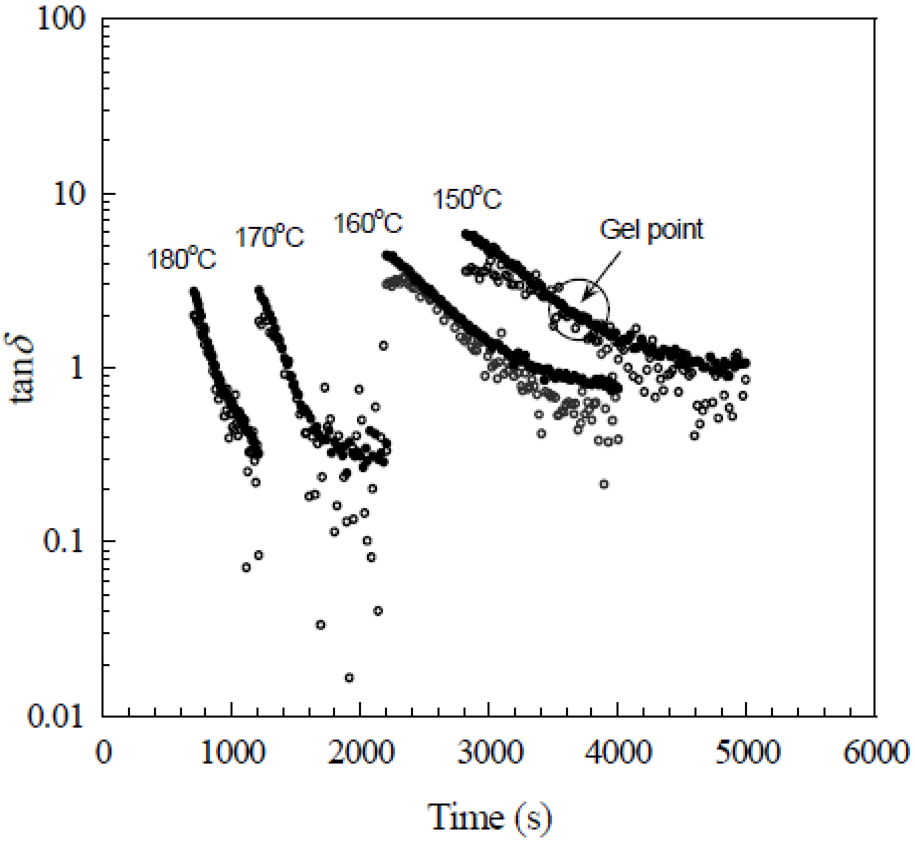

Figure 4(a): Effect of gel temperature on the gel time of BA-*a*/ATBN (95/5) mixture: (○) 10 rad/s, (●) 30 rad/s.

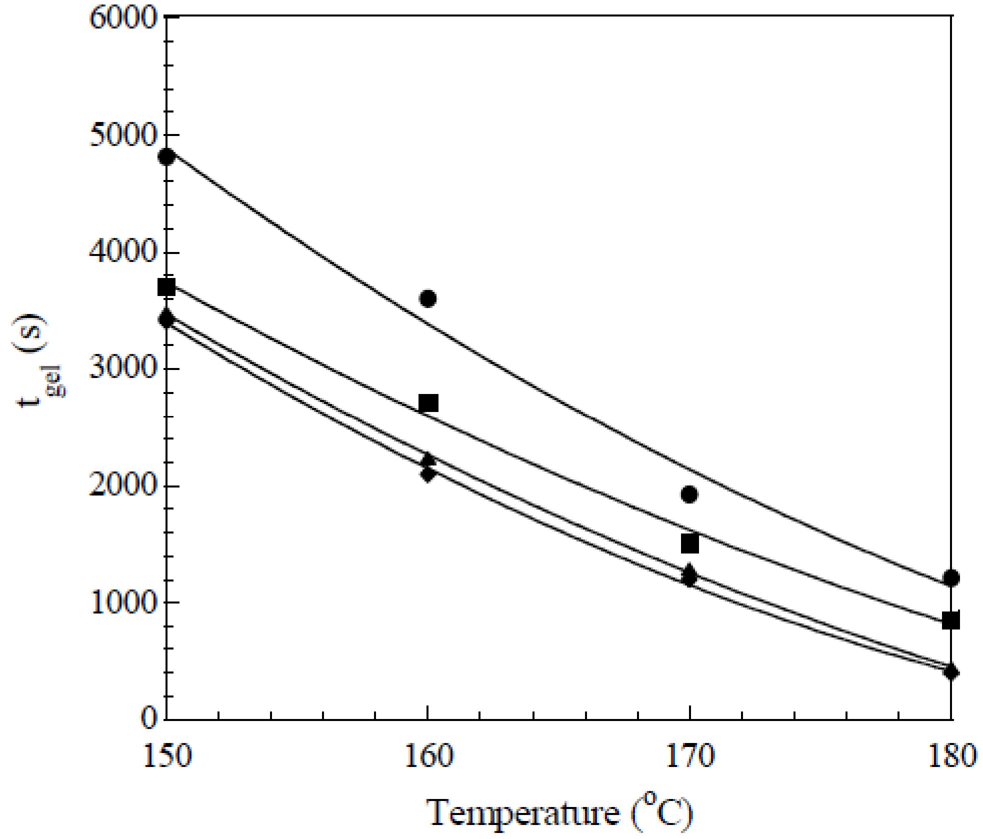

Figure 4(b): The gel times as a function of gel temperature of BA-a/ATBN mixtures at various ATBN contents: (●) BA-a, (■) BA-a/ ATBN (95/5) (◆) BA-a/ATBN (90/10), (▲) BA-a/ATBN (80/20).

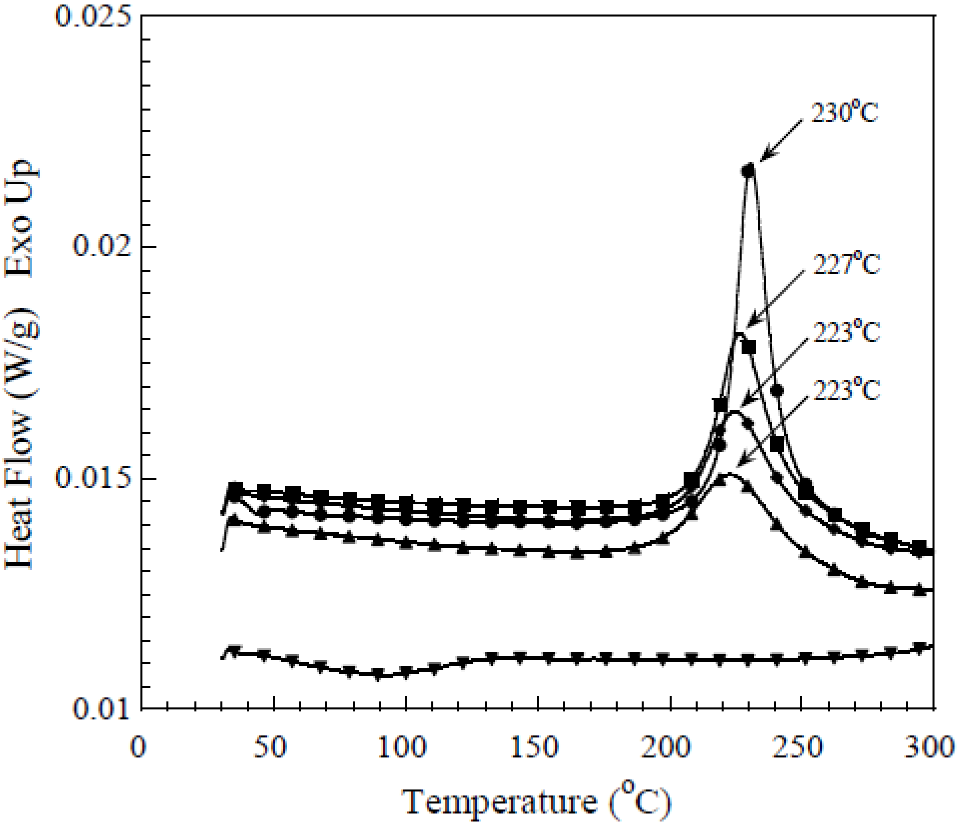

Figure 5(a): DSC thermograms at heating rate 10^{o}C/min of BA-a/ATBN mixtures at different ATBN contents: (●) BA-a, (■) BA-a/ATBN (95/5), (◆) BA-a/ATBN (90/10), (▲) BA-a/ATBN (80/20), (▼) ATBN.

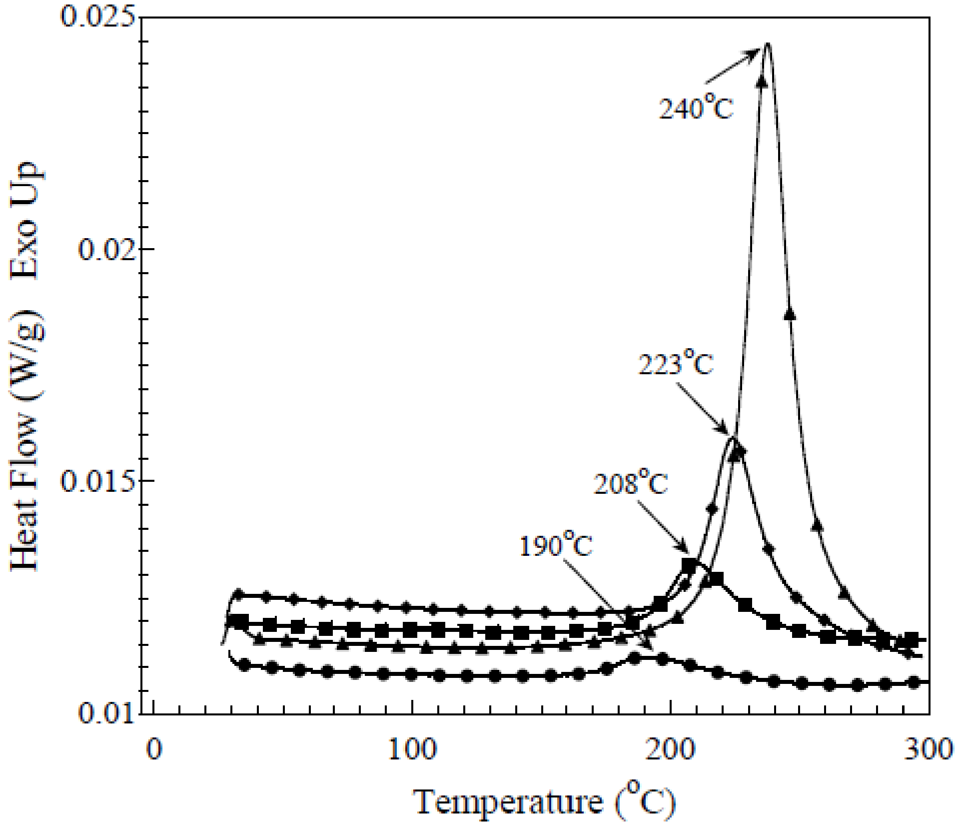

Figure 5(b): DSC thermograms of BA-a/ATBN (95/5) mixture at various heating rates: (●) 2°C/min, (■) 5°C/min, (◆) 10°C/min, (▲) 20°C/min.

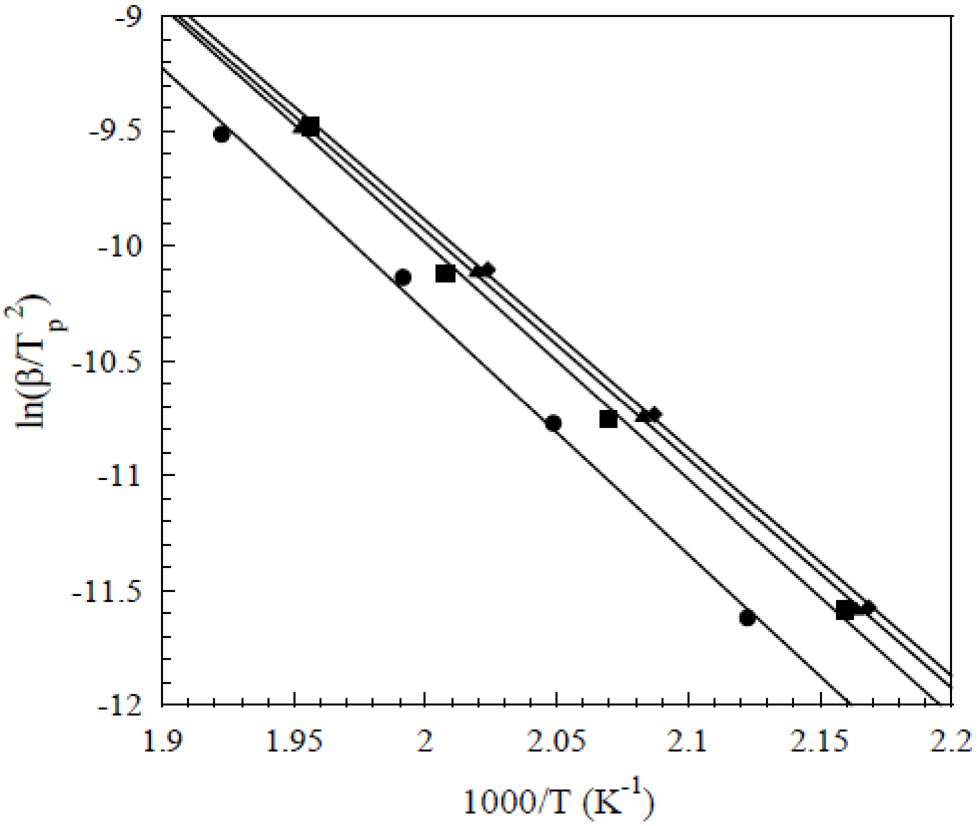

Figure 6: Kissinger method plots for averaged activation energy determination of BA-a/ ATBN mixtures as different ATBN contents: (●) BA-a, (■) BA-a/ATBN (95/5), (◆) BA-a/ATBN (90/10), (▲) BA-a/ATBN (80/20).

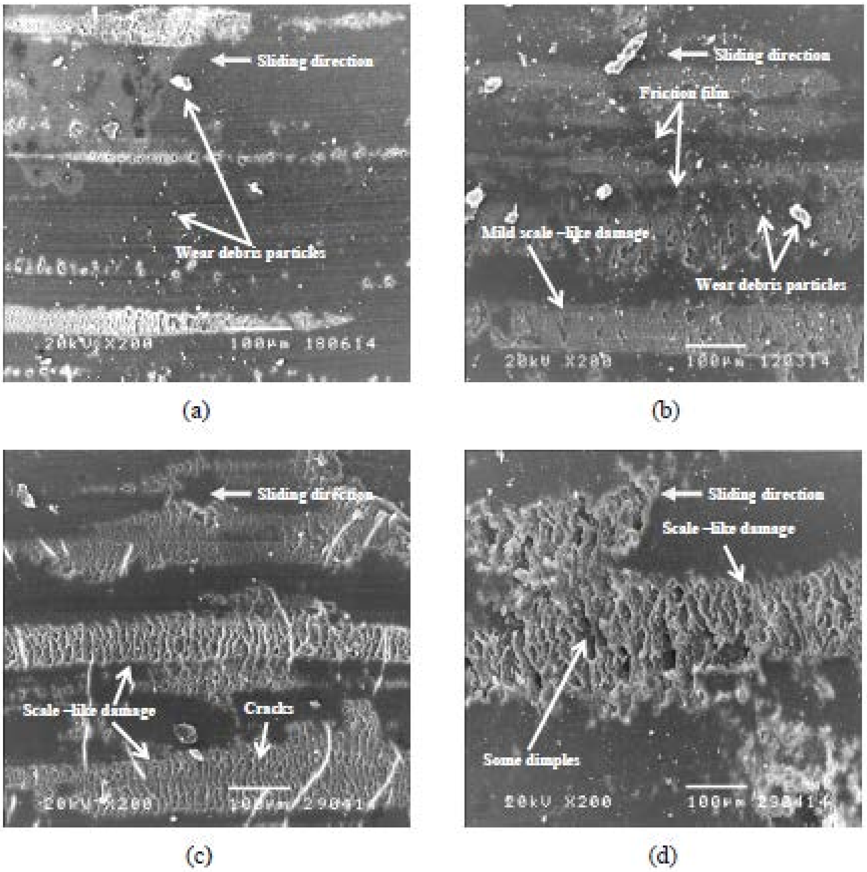

Figure 7: SEM micrographs of worn surfaces of PBA-a/ATBN copolymers at different ATBN contents: (a) PBA-a, (b) PBA-a/ATBN (95/5), (c) PBA-a/ATBN (90/10), (d) PBA-a/ATBN (80/20).

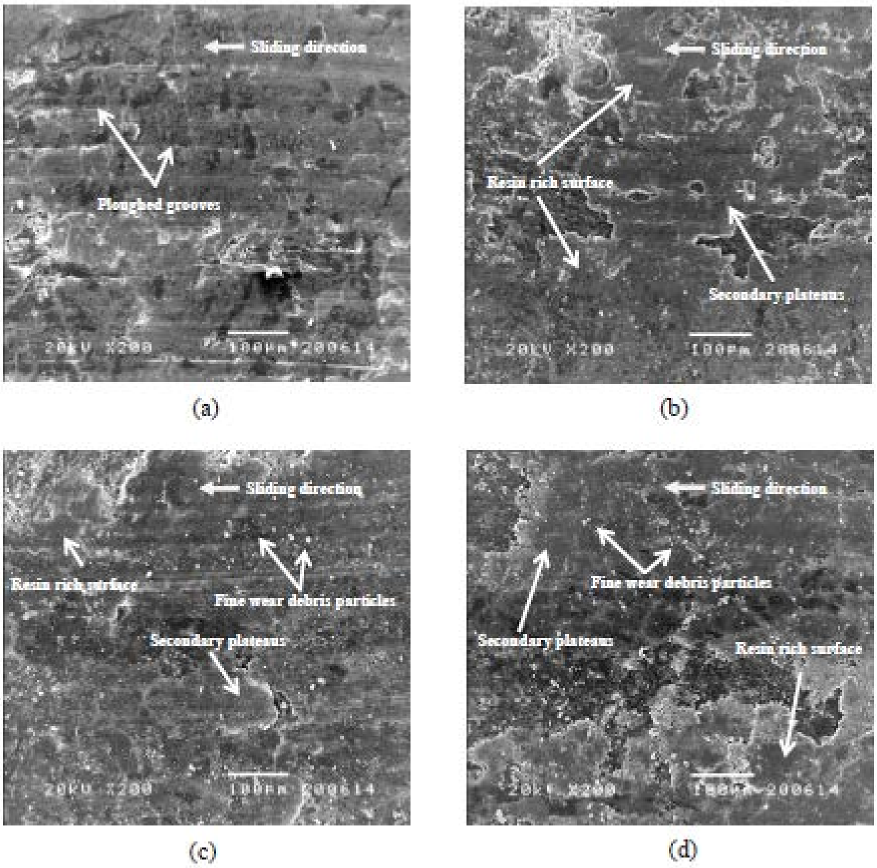

Figure 8: Wear micrographs (SEM) of worn surfaces of PBA-a/ATBN composites at different ATBN contents: (a) PBA-a, (b) PBA-a/ATBN (95/5), (c) PBA-a/ATBN (90/10), (d) PBA-a/ATBN (80/20). Each composite consisted of 30 wt% PBA-a/ATBN, 5 wt% Kevlar short fiber, 10 wt% alumina powder, 10 wt% graphite powder and 45 wt% calcium carbonate powder.

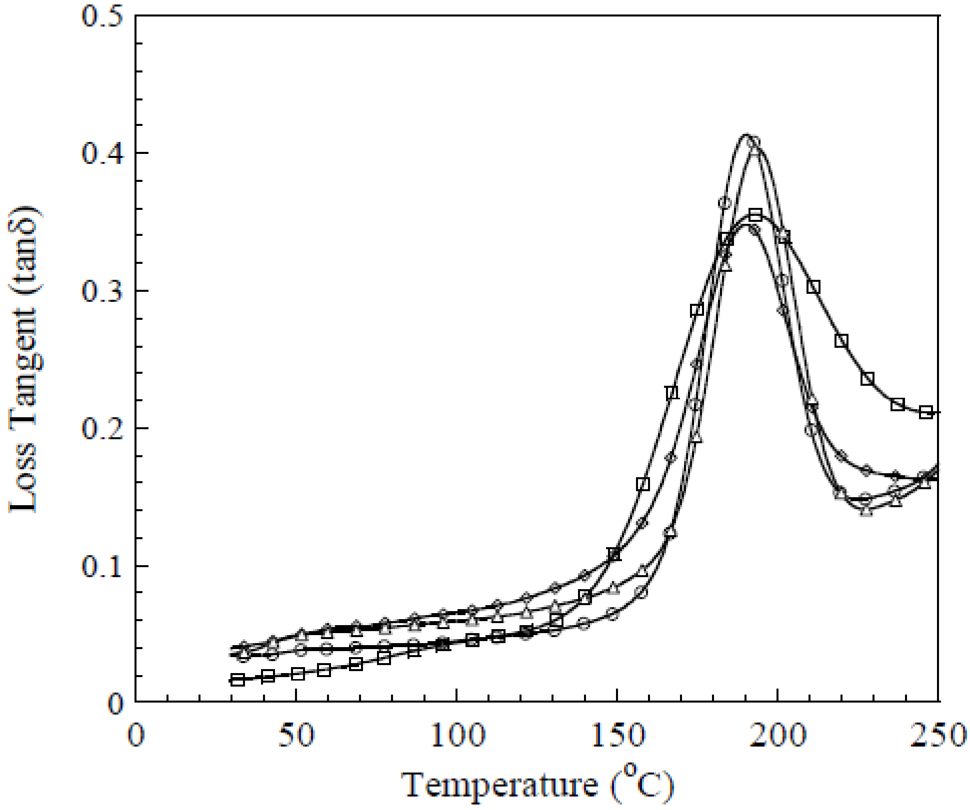

Figure 9: Loss tangent of PBA-a/ATBN composites at different ATBN contents: (○) PBA-a, (□) PBA-a/ATBN (95/5), (◇) PBA-a/ATBN (90/10), (△) PBA-a/ATBN (80/20).

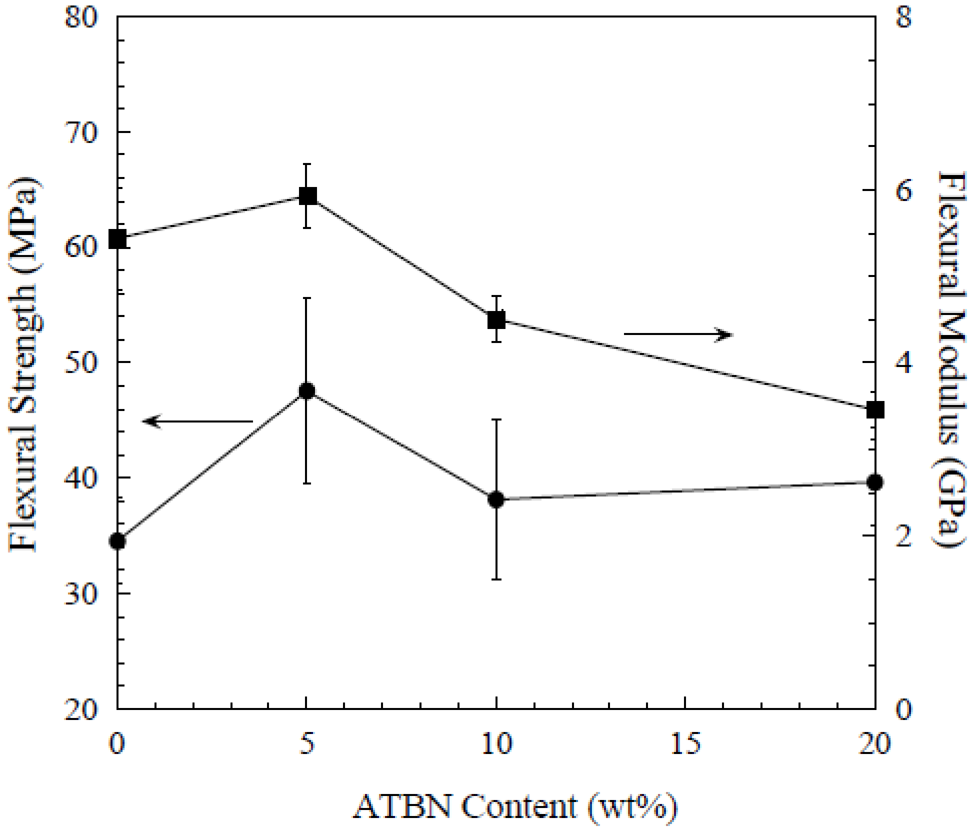

Figure 10: Flexural properties of PBA-a/ATBN composites at various ATBN contents: (●) Flexural strength, (■) Flexural modulus.

Conclusions

The effect of liquid amine-terminated butadiene–acrylonitrile (ATBN) content on the rheological, cure kinetics, triboligical, thermal and mechanical properties of bisphenol-A/aniline-based polybenzoxazine composites can be summarized as follows. An addition of liquid ATBN in benzoxazine resin can substantially reduce the gel time, curing temperature, and curing activation energy of the benzoxazine resin. The copolymers of the polybenzoxazine modified with the ATBN revealed enhancement in the tribological properties, i.e. friction coefficient and wear resistance compared to those of the polybenzoxazine. The friction coefficient for the copolymers was in the range of 0.36-0.39 with 5-10 wt% ATBN contents. Furthermore, it was found that the ATBN-modified polybenzoxazine based self-lubricating composites showed a significantly low friction coefficient value and specific wear rate at the optimal ATBN content of 5 wt%, i.e. 0.15 and 6.07×10^{-5} mm^3/Nm. The mechanical and thermal properties of the composites are still maintained with an addition of ATBN content at less than 10 wt%, i.e. T_g ~ 190°C, σ_f ~ 47.6 MPa and E_f = 5.9 GPa. In addition, the ether bonds formed between the polybenzoxazine and the ATBN is attributed to the significant improvement on thermal and mechanical properties of the resulting polybenzoxazine/ATBN based self-lubricating composites.

References

1. T. Singh, A. Patnaik, B.K. Satapathy, M. Kumar, and B.S. Tomar, Effect of Nanoclay Reinforcement on the Friction Braking Performance of Hybrid Phenolic Friction Composites, J. Mater. Eng. Perform., 2013, 22, p 796–805.
2. J. Xian and L. Xiaomei, Friction and Wear Characteristics of Polymer-Matrix Friction Materials Reinforced by Brass Fibers, J. Mater. Eng. Perform., 2004, 13, p 642–646.
3. J. Li and X.H. Sheng, The Effect of PA6 Content on the Mechanical and Tribological Properties of PA6 Reinforced PTFE Composites, J. Mater. Eng. Perform., 2010, 19, p 342–346.
4. J. Li and X.Z. Li, evaluation of the Tribological Properties of Carbon Fiber Reinforced Poly(vinylidene fluoride) Composites, J. Mater. Eng. Perform., 2010, 19, p 1025–1030.
5. H. Ishida and T. Agag, Handbook of Benzoxazine Resins, New York, Elsevier, 2011.
6. C. Jubsilp, T. Takeichi, S. Hiziroglu, and S. Rimdusit, High Performance Wood Composites based on Benzoxazine-Epoxy Alloys, Biores. Technol., 2008, 99, p 8880–8886.
7. J. Kajohnchaiyagual, C. Jubsilp, I. Dueramae, and S. Rimdusit, Thermal and Mechanical Properties Enhancement Obtained in Highly Filled Alumina-Polybenzoxazine Composites, Polym. Compos., 2014, 35, p 2269–2279.
8. H. Ishida, Polybenzoxazine Nanocomposites of Clay and Method for Making Same, U.S. Patent 6,323,270, November 27, 2001.
9. S. Rimdusit and H. Ishida, Development of New Class of Electronic Packaging Materials based on Ternary Systems of Benzoxazine, Epoxy, and Phenolic Resins, Polymer, 2000, 41, p 7941–7949.
10. S. Rimdusit, C. Jubsilp, and S. Tiptipakorn, Alloys and Composites of Polybenzoxazines: Properties and Applications, Singapore, Springer, 2013.
11. C. Jubsilp, S. Rimdusit, and T. Takeichi, Aniline-based Polybenzoxazine and Their Copolymers or Composites: Molecular Design and Potential Applications, Aniline: Structural/Physical Properties, Reactions and Environmental Effects, K. Hernandez, and M. Holloway eds., New York, Nova Science Publishers, Inc., 2013, p 55–90.
12. S. Rimdusit, S. Pirstpindvong, W. Tanthapanichakoon, and S. Damrongsakkul, Toughening of Polybenzoxazine by Alloying with Urethane Prepolymer and Flexible Epoxy: A Comparative Study, Polym. Eng. Sci., 2005, 45, p 288–296.

13. S. Rimdusit, P. Kunopast, and I. Dueramae, Thermomechanical Properties of Arylamine-based Benzoxazine Resins Alloyed with Epoxy Resin, Polym. Eng. Sci., 2011,51, p 1797–1807.
14. S. Grishchuk, S. Schmitt, O.C. Vorster, and J. Karger-Kocsis, Structure and Properties of Amine-Hardened Epoxy/Benzoxazine Hybrids: Effect of Epoxy Resin Functionality, J. Appl. Polym. Sci., 2012, 124, p 2824–2837.
15. Rimdutsit, S. Bangsen, P. Kasemsiri, Chemorheology and Thermomechanical Characteristics of Benzoxazine-Urethane Copolymers, J. Appl. Polym. Sci., 2011, 121, p 3669–3678
16. C. Jubsilp, C. Panyawanitchakun, S. Rimdusit, Flammability and Thermomechanical Properties of Dianhydride-modified Polybenzoxazine Composites Reinforced with Carbon Fiber, Polym. Compos., 2013, 34, p 2067–2075.
17. J. Jang, and D.J. Seo, Performance Improvement of Rubber-modified Polybenzoxazine, J. Appl. Polym. Sci., 1998, 67, p 1–10.
18. S. Grishchuk, L. Sorochynska, O.C. Vorster, and J. Karger-Kocsis, J. Structure, Thermal, and Mechanical Properties of DDM-Hardened Epoxy/Benzoxazine Hybrids: Effects of Epoxy Resin Functionality and ETBN Toughening, J. Appl. Polym. Sci., 2013, 127, p 5082–5093.
19. F. Findik, Latest progress on tribological properties of industrial materials, Mater. Des 2014, 57, p 218-244.
20. K, Kato, Wear mechanisms, New Dir. Tribol (1997) 39-56.
21. P.J. Blau, Four Great Challenges Conforming Our Understanding and Modeling of Sliding Fricition, D. Dowson ed., Tribology for Energy Conservation (Leeds-Lyon 24), Tribol. Ser 1997, 34, p 117-128.
22. H. Heisler, Advanced Vehicle Technology, H. Heisler ed., Oxford, Butterworth-Heinemann (2002) 450-509.
23. Available from http://web.mae.ufl.edu/tribology/. [Accessed 2014, 24].
24. SAE International, Surface vehicle recommended practice friction coefficient identification system for brake linings (2002).
25. N.C. Wallbridge, D. Dowson, Distribution of wear rate data and a statistical approach to sliding wear theory, Wear 1987, 119, p 295-312.
26. B. J. Briscoe, S. K. Sinha, Wear of polymers. Proc. Inst. Mech. Eng. J. Eng. Tribol 2002, 216, p 401–413.

27. O. Jacobs, B. Schädel, Tribology of Polymeric Nanocomposites, K. Friedrich, A.K. Schlarb eds., Oxford, Butterworth-Heinemann (2013) 307-352.

28. J. Karger-Kocsis, A. Mousa, Z. Major, N. Békési, Dry friction and sliding wear of EPDM rubbers against steel as a function of carbon black conten t, Wear 2008, 264, p 359-367.

29. K. Kato, K. Adachi, Modern Tribology Handbook II Series, B. Bhushan ed., Florida, CRC Press LLC, 2001.

30. B.J. Briscoe, S.K. Sinha, Wear of polymers, Proc. Instn. Mech. Engrs Part J: J Eng. Tribol. 2002, 216, p 401-413.

31. What are the wear mechanisms and what controls them?; American Academy of Orthopaedic Surgeons, 2001.

32. X. Ning and H. Ishida, Phenolic materials via ring-opening polymerization: Synthesis and characterization of bisphenol-A based benzoxazines and their polymers J. Polym. Sci., Polym. Chem. 1994, 32, p 1211-1129.

33. X. Ning and H. Ishida, Phenolic materials via ring-opening polymerization of benzoxazines: Effect of molecular structure on mechanical and dynamic mechanical properties, J. Polym. Sci., Polym. Phys. 1994, 32, p 921-927.

34. H. Ishida and D.J. Allen, Physical and mechanical characterization of near-zero shrinkage polybenzoxazines, J. Polym. Sci. Polym. Phys. 1996, 34, p 1019-1030.

35. H. Ishida and S. Rimdusit, Very high thermal conductivity obtained by boron nitride-filled polybenzoxazine Thermochim. Acta 1998, 320, p 177-186.

36. T. Singh, Tribo-performance evaluation of fibre reinforced and nano-filled composite friction materials, (PhD Thesis), NIT Hamirpur, 2013.

37. D. Chan and G.W. Stachowiak, Review of automotive brake friction materials, J. Automobil. Eng 2004, 218, p 953-966.

38. A. Almaslow, M.J. Ghazali, R.J. Talib, C.T. Ratna, and C.H. Azhari, Effects of epoxidized natural rubber-alumina nanoparticles (ENRAN) composites in semi-metallic brake friction materials, Wear 2013, 302, p 1393-1396.

39. P. Gopal, L.R. Dharani, and D. Blum, Fade and wear characteristics of a glass-fiber-reinforced phenolic friction material, Wear 1994, 174, p 119–127.

40. S.K. Sinha and S.K. Biswas, Friction and wear behavior of continuous fiber as cast kevlar phenolic resin composite, J. Mater. Sci 1992, 27, p 3085–3091.

41. A. Patnaik, M. Kumar, B.K. Satapathy, and B.S. Tomar, Performance sensitivity of hybrid phenolic composites in friction braking: effect of ceramic and aramid fibre combination, Wear 2010, 269, p 891–899.
42. U.S. Hong, S.L. Jung, K.H. Cho, M.H. Cho, S.J. Kim, and H. Jang, Wear mechanism of multiphase friction materials with different phenolic resin matrices, Wear 2009, 266, p 739–744.
43. S.J. Kim and H. Jang, Friction and wear of friction materials containing two different phenolic resins reinforces with aramid pulp. Tribol. Inter. 2000, 33, p 477–484.
44. Y. Wu, M. Zeng, Q. Xu, S. Hou, H. Jin, and L. Fan, Effects of glass-to-rubber transition of thermosetting resin matrix on the friction and wear properties of friction materials, Tribol. Inter 2012, 54, p 51-57.
45. Lu Y, A combinatorial approach for automotive friction materials: effects of ingredients on friction performance, Compos. Sci. Technol. 2006, 66 p 591-598
46. T. Nakamura, T. Nagata, K. Takeuchi, and M. Kobayashi, Non-asbestos friction materials, US Patent 6,596,789 B2, 2003.
47. M. Hermandez, J. Gonzalez, M. Ichazo, D. Lovera, and C. Albano, Rheological Behavior of Modified Polypropylene (PP) with Nitrile Rubber (NBR), May 6-10, 2001 (Dallas, Texas), ANTEC, 2001, p 3554-3557.
48. C. Jubsilp, T. Takeichi, and S. Rimdusit, Property Enhancement of Polybenzoxazine Modified with Dianhydride, Polym. Degrad. Stabil., 2011, 96, p1047–1053.
49. T. Agag and T. Takeichi, Effect of Hydroxyphenylmaleimide on the Curing Behaviour and Thermomechanical Properties of Rubber-Modified Polybenzoxazine, High Perform. Polym., 2001, 13, p S327–S342.
50. S. Grishchuk, S. Schmitt, O.C. Vorster, and J. Karger-Kocsis, Structure and Properties of Amine-Hardened Epoxy/Benzoxazine Hybrids: Effect of Epoxy Resin Functionality, J. Appl. Polym. Sci., 2012, 124, p 2824–2837.
51. H.H. Winter and F. Chambon, Analysis of Linear Viscoelasticity of A Crosslinking Polymer at the Gel Point, J. Rheol. 1986, 30, p 367–382.
52. R. Thomas, D. Yumei, H. Yuelong, Y. Le, P. Moldenaers, Y. Weimin, T. Czigany, and S. Thomas, Miscibility, Morphology, Thermal, and Mechanical Properties of A DGEBA based Epoxy Resin Toughened with A Liquid Rubber, Polymer, 2008, 49, p 278–294.
53. R. Thomas, S. Durix, C. Sinturel, T. Omonov, S. Goossens, G. Groeninckx, P. Moldenaers, and S. Thomas, Cure Kinetics, Morphology and Miscibility of Modified

DGEBA-based Epoxy Resin-Effects of A Liquid Rubber Inclusion, Polymer, 2007, 48, p 1695–1710.

54. G. Xian, R. Walter, and F. Haupert, A Synergistic Effect of Nano-Tio_2 and Graphite on the Tribological Performance of Epoxy Matrix Composites, J. Appl. Polym. Sci., 2006, 102, p 2391–2400.

55. S. Lampman, Characterization and Failure Analysis of Plastics; ASM International, Ohio, 2003; pp 259–264.

56. K.C. Ludema, Friction, Wear, Lubrication: A Textbook in Tribology, New York, CRC Press, 1996.

57. W. Chonkaew, N. Sombatsompop, and W. Brostow, High Impact Strength and Low Wear of Epoxy Modified by A Combination of Liquid Carboxyl Terminated Poly(Butadiene-co-Acrylonitrile) Rubber and Organoclay, Eur. Polym. J., 2013, 49, p 1461–1470.

58. W. Chonkaew, N. Sombatsompop, Mechanical and Triboligical Properties of Epoxy Modified by Liquid Carboxyl Terminated Poly(butadiene-co-acrylonitrile rubber), J. Appl. Polym. Sci., 2012, 125, p 361-369.

59. Yu, H. Hu, J. Ma, and J. Yin, Tribological Properties of Epoxy/Rubber Nanocomposites, Tribol. Inter., 2008, 41, p 1205-1211.

60. Q. Wang, Q. Xue, H. Liu, W. Shen, and J. Xu, The Effect of Particle Size of Nanometer ZrO2 on the Tribological Behaviour of PEEK, Wear, 1996, 198, p. 216-219.

61. X.S. Xing and R.K.Y. Li, Wear Behavior of Epoxy Matrix Composites Filled with Uniform Sized Sub-micron Spherical Silica Particles, Wear, 2004, 256, p. 21-26.

62. E.W. McAllister, Pipeline Rules of Thumb Handbook: A Manual of Quick, Accurate Solutions to Everyday Pipeline Engineering Problem, Massachusetts, Elsevier 2009.

63. P. Gopal, L.R. Dharani, and F.D. Blun, Hybrid Phenolic Friction Composites Containing Kevlar®Pulp Part 1. Enhancement of Friction and Wear Performance, Wear, 1996, 193, p 199–206.

64. J. Wu and X.H. Cheng, Friction and Wear Properties of Kevlar Pulp Reinforced Epoxy Composites Under Dry Sliding Condition, Tribol. Lett., 2006, 22, p 259–263.

65. J.P. Davim and R. Cardoso, Effect of the Reinforcement (Carbon or Glass fibres) on Friction and Wear Behaviour of the PEEK Against Steel Surface at Long Dry Sliding, Wear, 2009, 266, p 795–799.

66. M.T. Demirci and H. Duzcukoglu, Wear Behaviors of PTFE Reinforced PA 66 Journal Bearing, The 10th International Scientific Conference UNITECH, November 19–20, 2010 (Gabrovo, Bulgaria), p 249–253.

67. P.J. Blau, Lubrication to Control Friction, Friction Science and Technology, New York, Marcel Dekker, Inc., 1996, p 285–334.

68. N. Chikhi, S. Fellahi, and M. Bakar, Modification of Epoxy Resin Using Reactive Liquid (ATBN) Rubber, Eur. Polym. J., 2002, 38, p 251–264.

69. J. Bijwe, Nidhi, N. Majumdar, and B.K. Satapathy, Influence of Modified Phenolic Resins on the Fade and Recovery Behavior of Friction Materials, Wear 2005, 259, p 1068–1078.

70. A. Saffar and A. Shojaei, Effect of Rubber Component on the Performance of brake Friction Materials, Wear, 2012, 274-275, p 286–297.

Outputs from This Research

1. ผลงานตีพิมพ์ในวารสารวิชาการนานาชาติ

1.1 . **C. Jubsilp,** R. Taewattana, T. Takeichi and S. Rimdusit, "Investigation on Rubber-modified Polybenzoxazine Copolymers and Their Composites for Lubricating Material Applications", *Accepted for Journal of Materials Engineering and Performance* 2015.

1.2 **C. Jubsilp,** S. Rimdutsit and T. Takeichi, Effect of Rubber Contents on Tribological and Thermomechanical Properties of Polybenzoxazine", *Applied Mechanics and Materials,* 576 (2014), 75-79. (International Conference Publication from The 2nd International Conference on Materials Engineering, ICMEN2014)

1.3 J. Jantaramaha, C. Jubsilp and S. Rimdusit "Thermal and Mechanical Properties of Acrylonitrile-Butadiene Rubber Modified Polybenzoxazine as Frictional Materials" *Key Engineering Materials*, 659 (2015), 511-515. (Intrernational Conference Publication from The 8th International Conference on Materials Science and Technology, MSAT 2014)

2. การนำผลงานวิจัยไปใช้ประโยชน์

เชิงวิชาการ

เป็นการผลิตบุคลากรที่มีทักษะด้านงานวิจัยโดยมีนิสิตระดับปริญญาโท สาขาวิศวกรรมเคมี (จุฬาลงกรณ์มหาวิทยาลัย) จำนวน 1 คน (กำลังศึกษา) และนิสิตระดับปริญญาตรีจำนวน 3 คน สำเร็จการศึกษาจากผลงานวิจัยนี้

3. การเสนอผลงานในที่ประชุมวิชาการระดับนานาชาติ

3.1 **C. Jubsilp**, S. Rimdutsit, T. Takeichi, Effect of Rubber Contents on Tribological and Thermomechanical Properties of Polybenzoxazine" Proceeding of 2nd International Conference on Materials Engineering (ICMEN2014), <u>Oral presentation</u>, 17-18 May 2014, Nanjing, China

3.2 J. Jantaramaha, **C. Jubsilp** and S. Rimdusit "Thermal and Mechanical Properties of Acrylonitrile-Butadiene Rubber Modified Polybenzoxazine as Frictional Materials" Proceeding of 8th International Conference on Materials Science and Technology (MSAT 2014), <u>Oral Presentation</u>, Bangkok, Thailand, 15-16 December 2014.

Appendix

JMEPEG
DOI: 10.1007/s11665-015-1660-5

Investigation on Rubber-Modified Polybenzoxazine Composites for Lubricating Material Applications

Chanchira Jubsilp, Rapiphan Taewattana, Tsutomu Takeichi, and Sarawut Rimdusit

(Submitted January 20, 2015; in revised form July 4, 2015)

Effects of liquid amine-terminated butadiene-acrylonitrile (ATBN) on the properties of bisphenol-A/aniline-based polybenzoxazine (PBA-a) composites were investigated. Liquid ATBN decreased gel time and lowered curing temperature of the benzoxazine resin (BA-a). The PBA-a/ATBN-based self-lubricating composites resulted in substantial enhancement regarding their tribological, mechanical, and thermal properties. The inclusion of the ATBN at 5% by weight was found decreasing the friction coefficient and improved wear resistance of the PBA-a/ATBN composites. Flexural modulus and glass transition temperature of the PBA-a composite samples added the ATBN was constant within the range of 1-5% by weight. A plausible wear mechanism of the composites is proposed based on their worn surface morphologies. Based on the findings in this work, it seems that the obtained PBA-a/ATBN self-lubricating composites would have high potential to be used for bearing materials where low friction coefficient, high wear resistance, and modulus with good thermal property are required.

Keywords dynamic mechanical, organic matrix composites, polymers and plastics, thermal analysis

1. Introduction

Nowadays, a wide range of friction and wear materials serving industries with products suitable for various applications including self-lubricating materials, industrial equipment, automotive, and aerospace industries has been investigated (Ref 1-4). Moreover, polymers and their composites can be used to replace traditional metallic-based self-lubricating materials, particularly in sliding/rolling components such as bearings, rollers, and gears where their self-lubricating properties (low friction coefficient) are exploited to avoid the need for oil or grease lubrication with its attendant problems of contamination. Typically, the most commonly used polymer for the polymer-based self-lubricating material, i.e., bearings is phenolics. However, these resins have various limitations, most notably when used in sufficient concentration to impart strength; the material may become too rigid or brittle for the applications. Therefore, modifications have been made to phenolics to address these limitations including the modification of the phenolic with such moieties as cashew nut shell liquid, epoxy, and various rubbers. In addition, poor shelf life, evolution of harmful volatiles during processing, and shrinkage in final products along with voids are the major problems of the phenolics. In order to overcome those problems, the alternative resins, i.e., benzoxazine resins, were synthesized in the present work to replace currently used phenolics.

Benzoxazine resins, being new types of phenolics, have been synthesized from phenol, formaldehyde, and amine to yield a relatively clean precursor without the need of solvent elimination or monomer purification. After the ring-opening polymerization of benzoxazine monomers, polybenzoxazine overcomes many shortcomings of traditional phenolics such as using acid or base catalyst, and releasing condensation by-products, meanwhile, it can have good thermal properties and flame retardancy of phenolics. Besides, they have a very low melt viscosity, dimensional stability, fast development of mechanical properties as a function of curing conversion, low water absorption, and low dielectric constant (Ref 5). Polybenzoxazines have been used as a matrix for highly filled composites (Ref 6, 7). In addition, polybenzoxazines are used as raw material in automotive (Ref 8), electronic packaging (Ref 9), and aerospace industries (Ref 5). Moreover, an ability of benzoxazine resins to blend with various other resins or polymers results in new resins with a broad range of applications (Ref 5, 10, 11). For example, blending between benzoxazine resins and epoxy resins, polyurethanes, and dianhydrides (Ref 12-16) was considered to be a potentially effective measure to enhance thermal or mechanical properties as well as flammability of the polymers. Furthermore, thermosetting copolymers based on benzoxazine resins and rubbers such as amine-terminated acrylonitrile-butadiene (ATBN) and epoxy-terminated liquid nitrile rubber (ETBN) have been reported to provide various useful characteristics (Ref 17, 18). As an example, the combination of *N*-alkyl benzoxazine resin with ATBN resulted in a significant enhancement of the fracture toughness properties of the polybenzoxazine. The cause of these particular responses is attributed to secondary molecular interactions between the toughening additive and the structural molecules of the polybenzoxazine network. In addition, the presence of rubbery particles creates stress concentration, which acts as initiation sites for plastic shear deformation of the binder/matrix and cavitation of the rubber particles. Consequently, this characteristic provides an additional energy dissipation mechanism.

Chanchira Jubsilp, Department of Chemical Engineering, Faculty of Engineering, Srinakharinwirot University, Nakhonnayok 26120, Thailand; **Rapiphan Taewattana** and **Sarawut Rimdusit**, Polymer Engineering Laboratory, Department of Chemical Engineering, Faculty of Engineering, Chulalongkorn University, Bangkok 10330, Thailand; and **Tsutomu Takeichi**, Department of Environmental and Life Sciences, Toyohashi University of Technology, Tempaku-cho, Toyohashi 441-8580, Japan. Contact e-mail: sarawut.r@chula.ac.th.

Although previous studies have found that the liquid rubber can improve the toughness of the polybenzoxazine (Ref 17, 18), there is very little or no information about the effect of the liquid rubber on the rheology, cure kinetics, and tribological behaviors of the polymer for self-lubricating polymer composites. Therefore, in this work, those behaviors of outstanding liquid rubber-modified polybenzoxazine composites including liquid rubber-modified polybenzoxazine filled with a fiber base, a friction modifier, and filler will be investigated in order to design tribosystems and select materials based on the wear map. A better understanding of wear rate, varieties of wear modes, and wear mechanisms will be provided within the scope of this study.

2. Experimental

2.1 Materials

BA-a-type benzoxazine resin based on bisphenol-A, formaldehyde, and aniline was synthesized in solventless condition (Ref 5). The BA-a resin is a yellow clear solid at room temperature. Polycarbonate type bisphenol-A was provided by Thai Polycarbonate Co., Ltd. Paraformaldehyde and aniline was obtained from Merck Co., and Fluka Chemical Co., respectively. Liquid amine-terminated butadiene-acrylonitrile copolymer, Hycar ATBN 1300X16 (BF-Goodrich) with 18% acrylonitrile content and with a nominal molecular weight of 1760 g/mol, was provided by UBE Co. (Japan). All chemicals were used as-received. Kevlar fiber with a length of 1 mm was used as reinforcing fiber. The fiber was provided by Du Pont K.K. Japan. Alumina, Al_2O_3 (A32), used as the abrasive was purchased from Nippon Light Metal Co., Ltd. The density and an average diameter of particles of the alumina were 3.90 g/cm^3 and 1 μm, respectively. Graphite powder having a particle size approximately 1 mm was supplied by Compact International (1994) Co., Ltd., Thailand. Calcium carbonate ($CaCO_3$) with 6-9 μm in diameter used as filler was provided by Surintomya Chemical Co., Ltd. in Thailand.

2.2 Preparation of ATBN-Modified PBA-a Copolymer Samples and Their Composites

BA-a/ATBN mixtures at liquid ATBN contents of 0, 5, 10, and 20 wt.% were heated to a temperature of 80 °C in an aluminum pan and were mixed mechanically for 15 min to obtain homogeneous mixtures. Then, the mixtures were cured sequentially in an air-circulating oven at 150 °C/1 h, 180 °C/3 h, 200 °C/1 h and 220 °C/1 h to guarantee complete curing of PBA-a/ATBN copolymers. The PBA-a/ATBN copolymers were finally left to cool down to room temperature before their characterizations were carried out.

BA-a/ATBN compounds consisted of 30 wt.% BA-a/ATBN mixture at different ATBN contents, namely 0, 5, 10, and 20 wt.%, filled with 5 wt.% Kevlar short fiber, 10 wt.% Al_2O_3 powder, 10 wt.% graphite powder, and 45 wt.% $CaCO_3$ powder were prepared by mechanical mixing at 80 °C for at least 15 min to ensure ingredients wet-out by the BA-a/ATBN mixture. In the next step, the compounds were cured at 200 °C for 2 h in the hydraulic press using a pressure of 34 MPa. The specimens were kept in a room to cool them to ambient temperature before any tests were carried out.

2.3 Characterizations of Samples

Dynamic shear viscosity measurements were performed on a parallel plate rheometer using HAAKE RheoStress model RS600. Disposable aluminum plates having 20 mm in diameter were preheated for 30 min with the gap zeroed at the testing temperature. The void-free monomer mixture, which was liquefied at 80 °C, was then poured onto the lower plate and the gap was set to 0.5 mm. The temperature was immediately equilibrated at the set point for about 180 s and the test was then started.

A differential scanning calorimeter model DSC 6000 from PerkinElmer, Inc. was employed to study the exothermic curing reactions. The samples were scanned by non-isothermal method from 30 to 300 °C at four different heating rates of 2, 5, 10, and 20 °C/min under a constant flow of nitrogen at 50 ml/min.

Tribological test under dry sliding at room temperature of 25 °C was conducted on a high temperature tribometer having a maximum temperature of 950 °C from CSM Instrument Ltd., Switzerland. Equipment has a ball-on-disk configuration with 6-mm steel ball diameter. The test condition is 10 N for normal load and 0.366 m/s for sliding speed for 1000 m distance.

Dynamic mechanical analyzer (DMA) from Netzsch Inc., model DMA 242 C in three-point bending mode, and a support span of 40 mm was used to examine loss tangent (tanδ) of the samples. The dimension of each sample in rectangular shape was 10 × 50 × 3 mm. The tests were performed in a temperature sweep mode with a fixed frequency of 1 Hz. Each sample was tested using a heating rate of 2 °C/min from 30 °C to about 250 °C.

Flexural properties were conducted by a Universal Testing Machine, Lloyd Instruments, Model LR 10 K. The measurement was carried out in a three-point bending mode, with a support span of 48 mm and at a crosshead speed of 1.2 mm/min. A minimum of five samples with a dimension of 25 × 60 × 3 mm was tested, and the average values for the specimens were determined.

The worn surface of the samples was evaluated with a JSM5410LV scanning electron microscopy (SEM) from JEOL Ltd. using an acceleration voltage of 15 kV. All samples were coated with a thin film of gold to make the surfaces conductive.

3. Results and Discussion

3.1 Rheological Property of BA-a/ATBN Mixtures

The effect of liquid ATBN contents on liquefying and gelation behaviors via rheological measurement of BA-a/ATBN mixtures is shown in Fig. 1. The first major thermal event is called the liquefying point or the liquefying temperature (the left hand side), which is the transition of solid to liquid. At this point, the complex viscosity of the BA-a/ATBN mixtures approaches its minimum value. From the figure, the liquefying temperatures of the BA-a/ATBN mixtures were about 77 °C for BA-a, 90 °C for BA-a/ATBN (95/5), 115 °C for BA-a/ATBN (90/10), and 70 °C for BA-a/ATBN (80/20). It can be seen that the liquefying temperature of the samples increased with increasing ATBN contents up to 10 wt.%. This is because of the larger molecules having high viscosity of liquid ATBN than that of the BA-a monomer. On the other hand, the liquefying temperature of the BA-a monomer blended with 20 wt.% ATBN can be lowered comparing with that of the BA-a

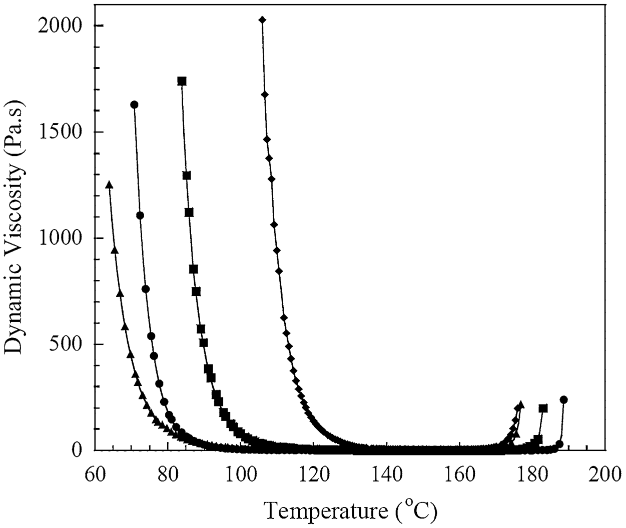

Fig. 1 Dynamic viscosity of BA-a/ATBN mixtures at various ATBN mass fractions: (●) BA-a, (■) BA-a/ATBN (95/5), (♦) BA-a/ATBN (90/10), (▲) BA-a/ATBN (80/20)

monomer. This behavior may be due to the dilution effect of the viscous liquid ATBN in the BA-a. In addition, the room temperature physical appearance of the uncured resins ranged from hard solid in the BA-a, BA-a/ATBN (95/5), and BA-a/ATBN (90/10), to soft solid in the BA-a/ATBN (80/20). This is due to the fact that the ATBN used is viscous liquid at room temperature, while the BA-a monomer is solid at room temperature. An addition of viscous liquid ATBN into the solid BA-a up to 20 wt.% thus lowered the liquefying temperature of the resulting mixture. The other reason may be incompatible of BA-a/ATBN mixtures, increasing this phenomenon with ATBN content. The incompatibility traduces into a weak interface. In this case, interlayer slip may occur and, as a result, the viscosity of the BA-a/ATBN (80/20) mixture decreased as similarly observed in polypropylene/NBR system (Ref 19).

Furthermore, the second major thermal event on the right hand side is called the gel point, the transition of liquid to solid due to continuous network formation of the resin mixture. The gel temperatures or gel points of the BA-a/ATBN mixtures tended to decrease with increasing ATBN contents, i.e., 185 °C for BA-a, 175 °C for BA-a/ATBN (95/5), and 168 °C for BA-a/ATBN (90/10), except in the case of the BA-a/ATBN (80/20) mixture tended to increase the gel temperature, i.e., 172 °C when compared with that of the BA-a/ATBN (90/10) mixture. Remarkably, this characteristic of the samples suggested an additional function of the liquid ATBN as an initiator for benzoxazine curing, thus lowering gel temperature of the BA-a. Therefore, the use of the liquid ATBN rubber is attractive because the gel times of the BA-a/ATBN mixtures were shorter. However, an increase of the gel temperature of the BA-a/ATBN (80/20) mixture compared with the gel temperature of the BA-a/ATBN (90/10) mixture was observed. This behavior was also likely due to the dilution effect of the viscous liquid ATBN as similarly reported in BA-35x/epoxy mixtures (Ref 13). In addition, the temperature from the liquefying point to the gel point is called processing window of the resin which is the range of the lowest viscosity useful for polymer compounding or processing. For the BA-a/ATBN mixtures, the processing window was determined to be in a range of 70-175 °C which provided sufficient processing window, particularly for the compounding or composite manufacturing process.

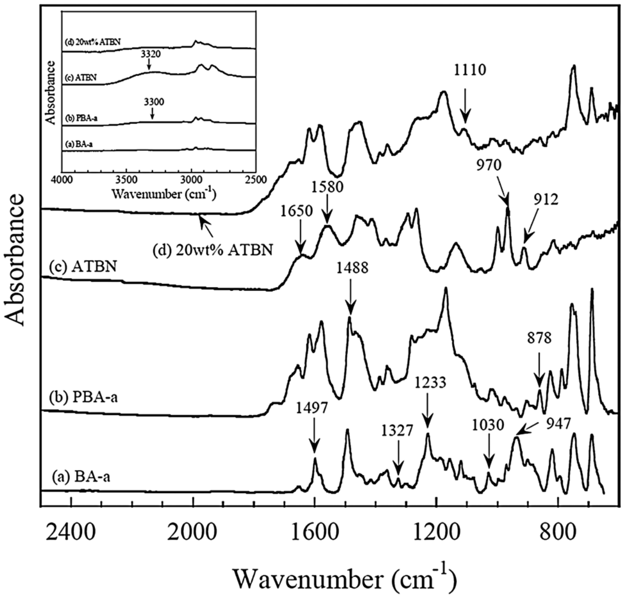

Fig. 2 FTIR of BA-a, PBA-a, ATBN, and PBA-a/ATBN (80/20) copolymer

3.2 Network Formation Between BA-a Monomer and ATBN

As discussed above that the liquid ATBN can act as an initiator to lower gel point of the BA-a monomers. Therefore, it can be expected that the primary amino groups may react with the BA-a and accelerate the BA-a homopolymerization. In addition, the chemical reaction between butadiene molecules in the liquid ATBN and hydroxyl groups of the polybenzoxazine (PBA-a) could also occur. Figure 2(a) illustrates IR spectrum of the BA-a with the peak assignments at 1497 and 947 cm^{-1} due to the tri-substituted benzene ring, at 1233 and 1030 cm^{-1} due to the asymmetric stretching of ether linkage (C-O-C), and at 1327 cm^{-1} due to CH_2 wagging in the BA-a ring. After polymerization, IR spectrum of the PBA-a presented the absorption bands of a ring opening of the BA-a to the PBA-a at 1488 and 878 cm^{-1} due to a tetra-substituted benzene ring mode as well as at about 3300 cm^{-1} due to the phenolic hydroxyl group formation (Ref 20), while the IR characteristics of the BA-a also disappeared as can be observed in Fig. 2(b). For the unsaturation presenting along ATBN backbone, in Fig. 2(c), the spectrum clearly showed *trans*-1,4 and 1,2-vinyl characteristic frequencies of the butadiene moieties due to out-of-plane deformation of the =C-H at 970 and 912 cm^{-1}, respectively. Moreover, the peaks at 3320 cm^{-1} (NH_2 stretch) and at 1650 and 1580 cm^{-1} (NH_2 deformation) were also observed. In the case of ATBN-modified PBA-a (Fig. 2d), the characteristic peaks of the BA-a had disappeared by the end of the complete cure accompanied with the appearance of new peaks due to the polymerization of the BA-a. Furthermore, IR spectrum showed a decrease in the absorptions at 970 and 912 cm^{-1} due to the out-of-plane deformation of the =C-H bond of the *trans*-1,4 and vinyl configurations in butadiene (Ref 21). Additionally, the peaks at 1650 and 1580 cm^{-1} due to NH_2 deformation also decreased. These behaviors confirmed

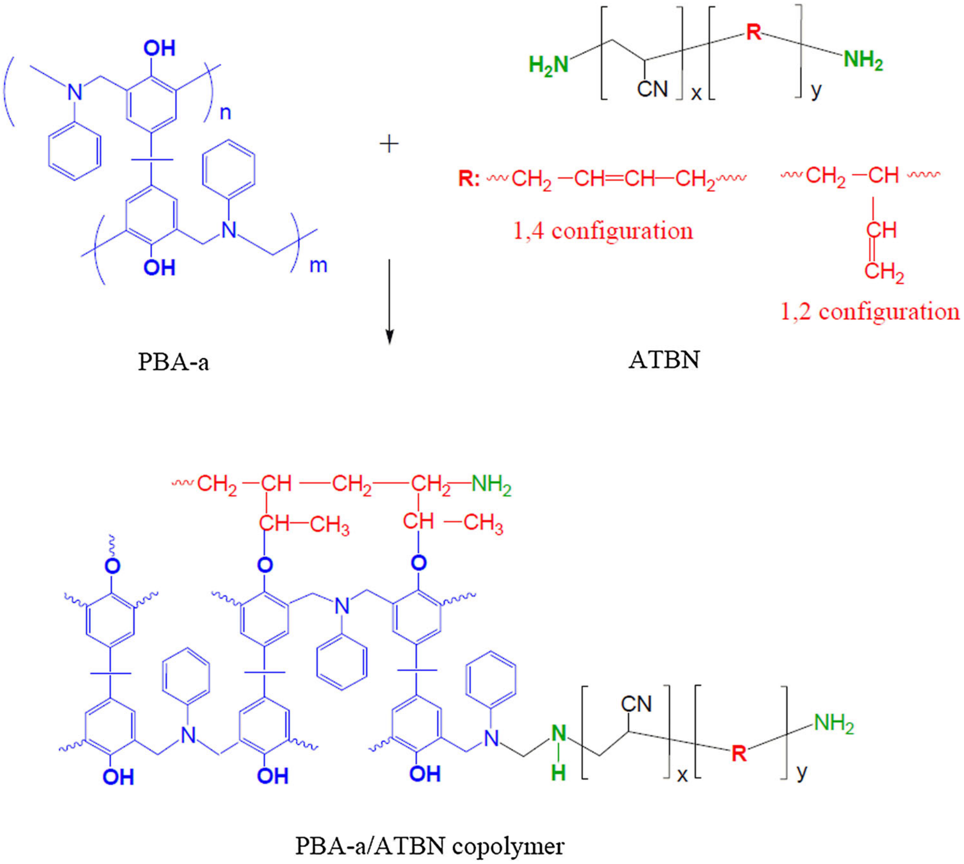

Fig. 3 A possible copolymerization between PBA-a and ATBN

that chemical reaction between -$CH=CH_2$ groups of the ATBN and -OH groups of the PBA-a can be formed via ether linkages (C-O-C stretch) at 1110 cm^{-1}. In addition, the BA-a may also undergo primary amino group-activated ring-opening polymerization reaction (Ref 14). Therefore, the possible chemical reaction of the PBA-a and the ATBN according to both reactions above are shown in Fig. 3.

One important aspect of a thermosetting polymer is its gel point. The gel points of samples can be accurately estimated by dynamic rheological measurements which are sensitive to degree of crosslinking of the polymers. In principle, elastic modulus and viscous modulus present the same power-law variation with respect to the frequency of oscillation at a gel point as follows Eq 1.

$$\tan\delta = G''/G' = \tan(n\pi/2), \quad \text{(Eq 1)}$$

where G' is storage modulus, G'' is loss modulus, and n is the relaxation exponent which is network specific.

The above expression suggests that frequency independent nature of tanδ at gel point by various frequencies crossover each other (Ref 22). As exemplified, tanδ as a function of time (s) at 10 rad/s and 30 rad/s of the BA-a/ATBN(95/5) mixture at 150, 160, 170, and 180 °C is plotted in Fig. 4(a). From this figure, the gel point corresponded to the gel time at each temperature of the mixture was about 3703 s (150 °C), 2713 s (160 °C), 1508 s (170 °C), and 857 s (180 °C). It was found that raising the processing temperature increases the rate of crosslinking of the BA-a/ATBN mixture. Consequently, at higher temperature, the mixture reached its gel point more quickly and the gel time was shorter as similarly observed in BA-a/epoxy mixtures (Ref 13, 15). Furthermore, Fig. 4(b) illustrates the gel time at different temperatures of the BA-a/ATBN mixtures at various ATBN contents. At the same temperature, the gel times of the BA-a/ATBN mixtures tended to decrease with increasing of the liquid ATBN content up to 10 wt.%, i.e., the gel time at 150 °C for the BA-a = 4813 s, the BA-a/ATBN (95/5) = 3703 s, and the BA-a/ATBN (90/10) = 3412 s, while the gel time of the BA-a/ATBN (80/20) = 3480 s which was slightly longer than that of the BA-a/ATBN (90/10) was observed as similarly seen in the gelation behavior in Fig. 1. This behavior is possible due to dilution effect of the liquid ATBN. However, these results can also be implied that the curing conversion of the BA-a/ATBN mixtures was raised with increasing of the liquid ATBN content due to its function as the initiator for the BA-a ring-opening reaction. In some cases, the addition of liquid rubber resulted in a retardancy on gel times of polymer/liquid rubber mixtures, i.e., epoxy resin/hydroxyl-terminated polybutadiene (HTPB). The polymer mixtures showed an increase of gel times with increasing HTPB, i.e., 900 s for epoxy resin/HTPB (95/5) and 1080 s for epoxy resin/HTPB (90/10) at 120 °C (Ref 23).

3.3 Curing Behaviors of BA-a/ATBN Mixtures

Curing behaviors of the BA-a/ATBN mixtures at liquid ATBN contents of 0, 5, 10, 20, and 100 wt.% were evaluated by differential scanning calorimetry (DSC). In Fig. 5(a), the

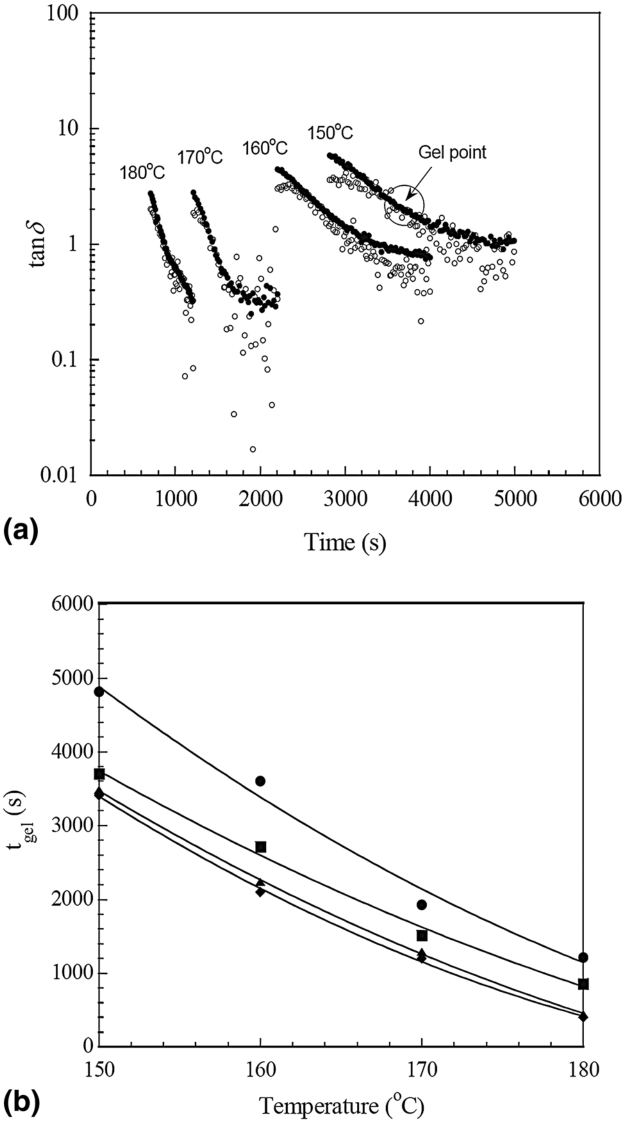

Fig. 4 (a) Effect of gel temperature on the gel time of BA-a/ATBN (95/5) mixture: (○) 10 rad/s, (●) 30 rad/s. (b) The gel times as a function of gel temperature of BA-a/ATBN mixtures at various ATBN contents: (●) BA-a, (■) BA-a/ATBN (95/5) (♦) BA-a/ATBN (90/10), (▲) BA-a/ATBN (80/20)

DSC thermograms of the BA-a/ATBN mixtures at 5, 10, and 20 wt.% ATBN displayed the curing exotherms centered at temperature levels of 227, 223, and 223 °C, respectively. Those exothermic peaks were lower than that of the BA-a monomers showing a peak at 230 °C. This finding implies that the liquid ATBN reveals acceleration effect on the curing process of the monomers. It has been reported that the BA-a ring-opening was stabilized by the lone-pair electron on the terminal amino groups of ATBN and, consequently, reduces the cure temperature (Ref 17, 21) On the contrary, the liquid ATBN resulted in no sign of any curing reaction in this temperature range because no initiators or curing agents were added to the liquid ATBN. Instead, the endothermic thermal events in a temperature range of 50-120 °C was observed, likely as a result of the evaporation process of some solvent. Moreover, the increase of the liquid ATBN content affected the curing thermograms in such a way to decrease the area under the exothermic peaks, i.e., 243 J/g for BA-a/ATBN (95/5), 216 J/g for BA-a/ATBN (90/10), and 197 J/g for BA-a/ATBN (80/20). It appeared that the heat of reaction of the BA-a/ATBN curing was lower than that of BA-a monomers, i.e., 276 J/g.

As it was found that the liquid ATBN might act as an initiator of the BA-a, activation energies of a curing process of the BA-a/ATBN mixtures was therefore examined. For example, the heat flows of the BA-a/ATBN (95/5) mixture from the DSC at heating rate of 2, 5, 10, and 20 °C/min are illustrated in Fig. 5(b), while those of the BA-a, BA-a/ATBN (90/10), and BA-a/ATBN (80/20) at the same heating rate were also investigated (not show here). From Fig. 5(b), the exothermic peaks of the BA-a/ATBN (95/5) mixture shifted to a higher temperature with higher heating rate due to shorter time. In this work, the activation energy of curing reaction of the BA-a/ATBN mixtures was calculated using Kissinger method as can be seen in Eq 2 which is an alternative way of estimating the activation energy without assuming any model of kinetic parameters and without integrating the exothermic peak.

$$\ln\left(\frac{\beta}{T_{\mathrm{p}}^{2}}\right) = \ln\left(\frac{Q_{\mathrm{p}}AR}{E_{\mathrm{a}}}\right) - \frac{E_{\mathrm{a}}}{RT_{\mathrm{p}}}, \qquad \text{(Eq 2)}$$

where $Q_{\mathrm{p}} = -[df(\alpha/d\alpha)]_{\alpha=\alpha_{\mathrm{p}}}$, $\beta = dT/dt$ is a constant heating rate, A is the pre-exponential factor (1/s), E_{a} is the activation energy (8.314 kJ/mol), and T_{p} is the peak temperature (K).

The logarithm plots of the heating rates versus the reciprocal of peak temperatures of the BA-a, BA-a/ATBN (95/5), BA-a/ATBN (90/10), and BA-a/ATBN (80/20) is given in Fig. 6. A good linear relationship between the heating rates and the reciprocal of peak temperatures was clearly obtained. The average activation energy calculated from the slope of the plot of the BA-a/ATBN (95/5), BA-a/ATBN (90/10), and BA-a/ATBN (80/20) mixtures was 85.4 kJ/mol, 82.3 kJ/mol, and 82.7 kJ/mol, respectively, while that of the BA-a was about 88.0 kJ/mol. Therefore, the decrease of the activation energies with increasing of the liquid ATBN for the BA-a/ATBN mixtures was the indication of the acceleration effect, and providing of faster curing reaction. However, the activation energy for the BA-a/ATBN (80/20) mixture was slightly increased comparing with that of the BA-a/ATBN (90/10) combination. A slightly increased energy is to hinder the molecular mobility and to retard the curing reaction due to diluents effect of the liquid ATBN. This behavior is in agreement with the result observed in our rheological measurement and epoxy/CTBN system (Ref 24). For the epoxy/CTBN system, the addition of liquid CTBN in epoxy resin contributed to increase activation energy values of the epoxy resin/CTBN mixtures with increasing the CTBN content, since the reaction between epoxide and anhydride was hindered by the CTBN rubber.

3.4 Tribological Behaviors of ATBN-Modified PBA-a Copolymers

The effect of liquid ATBN contents on the average friction coefficient ($\mu_{\mathrm{avg.}}$) and its extreme values ($\mu_{\mathrm{max.}}$ and $\mu_{\mathrm{min.}}$) as well as specific wear rate of polybenzoxazine (PBA-a) at 25 °C is listed in Table 1. The $\mu_{\mathrm{avg.}}$ and specific wear rate of the PBA-a was 0.38 and 2.08×10^{-4} mm^3/Nm, respectively. From the result, the $\mu_{\mathrm{avg.}}$ of the PBA-a is lower than that of epoxy ($\mu_{\mathrm{avg.}} \sim 0.65$-$0.84$) (Ref 25), phenolic ($\mu_{\mathrm{avg}} \sim 0.9$-$1.1$) (Ref 26),

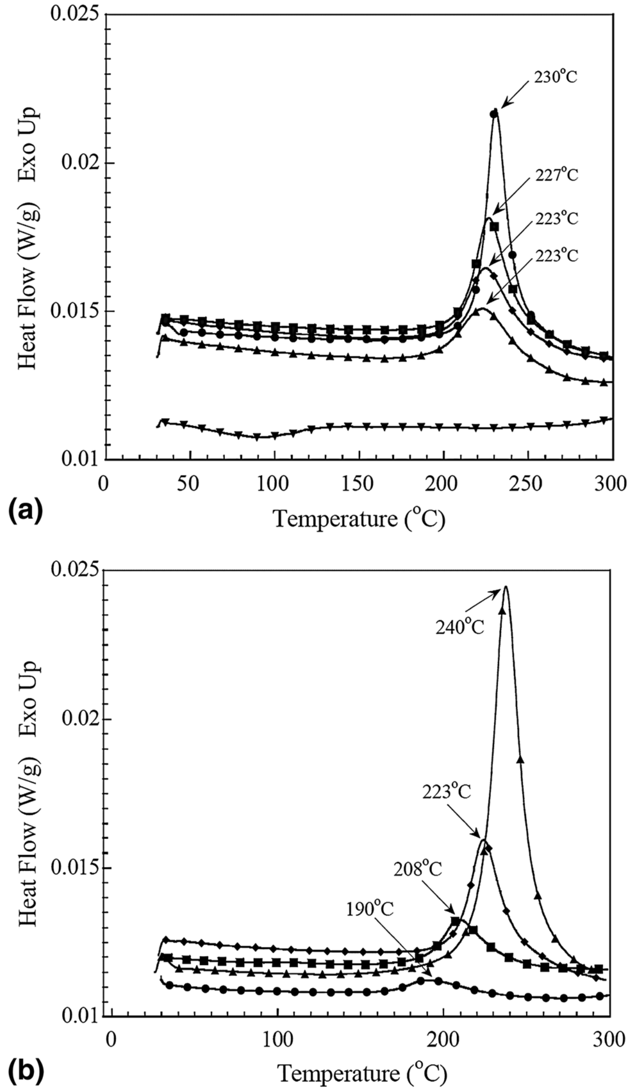

Fig. 5 (a) DSC thermograms at heating rate 10 °C/min of BA-a/ATBN mixtures at different ATBN contents: (●) BA-a, (■) BA-a/ATBN (95/5), (♦) BA-a/ATBN (90/10), (▲) BA-a/ATBN (80/20), (▼) ATBN. (b) DSC thermograms of BA-a/ATBN (95/5) mixture at various heating rates: (●) 2 °C/min, (■) 5 °C/min, (♦) 10 °C/min, (▲) 20 °C/min

and polyamide66 ~ 0.66 (Ref 27). Therefore, a special characteristic of the PBA-a evidences its self-lubrication ability compared to epoxy, phenolic, and polyamide66. Furthermore, the $\mu_{avg.}$ and specific wear rate of the PBA-a decreased with increasing ATBN content up to 5 wt.%, i.e., $\mu_{avg.} \sim 0.36$ and specific wear rate $\sim 1.85 \times 10^{-4}$ mm^3/Nm, which is the most effective to decrease both property of the PBA-a. While with a further increase of ATBN content above 10 wt.%, the PBA-a/ATBN copolymers showed a significant increase in its friction coefficient and specific wear rate. These observed trends are in agreement with the finding of previous publications (Ref 28-30). It indicates that the ATBN with softer molecular nature than the PBA-a has good friction-reducing and anti-wear abilities during sliding of the PBA-a within a mass fraction of 5 wt.%. In addition, it is possible that smaller ATBN particle sizes of the PBA-a/ATBN (95/5) copolymer than that of the PBA-a/ATBN (90/10) and PBA-a/ATBN (80/20) copolymers are seen to contribute reduction in friction coefficient and specific wear rate as the finding reported in ZrO_2/PEEK (Ref 31) and SiC/epoxy composites (Ref 32). The other reason of improved specific wear rates at low ATBN content provides the toughness enhancement of the ATBN-modified PBA-a. Furthermore, it was expected that the transfer film played a dominant role in determining the tribological behaviors for the PBA-a/ATBN (95/5) copolymer. This will be further discussed below. On the other hand, it could be rationally expected that the PBA-a/ATBN copolymers with the ATBN content above 10 wt.% would give poor wear resistance. This behavior may be attributed to the formation of larger ATBN domains at higher proportions and reduction in the hardness of the samples, resulting in fatigue wear. Such wear will be caused by a cycling loading during friction in the softer materials. A comparison of specific wear rate between the PBA-a/ATBN (95/5) copolymer and the liquid carboxyl-terminated poly(butadiene-co-acrylonitrile) (CTBN) rubber-modified epoxy (EP) (Ref 28) explained that the specific wear rate of the PBA-a/ATBN copolymer was lower than that of the EP/2.5 wt.% CTBN, i.e., 2.5×10^{-4} mm^3/Nm. Therefore, the PBA-a/ATBN (95/5) copolymer was somewhat suitable to act as a matrix for polymer-based bearing and coating materials replacing the thin film epoxy coating on steel, concrete, and pipeline. Because the copolymer manifested good wear resistance to abrasion load compared with epoxy resin with specific wear rate value of $\sim 5.00 \times 10^{-4}$ mm^3/Nm (Ref 28) and presented the lower friction coefficient than that of the thin film epoxy coating for pipeline, i.e., $\mu_{avg.} \sim 0.51$-0.71 (Ref 33).

3.5 Worn Surface Morphologies of ATBN-Modified PBA-a Copolymers

Scanning electron microscope photographs of the worn surface of the PBA-a and the PBA-a/ATBN copolymers at different liquid ATBN contents are illustrated in Fig. 7. From this figure, there are remarkable differences in the worn surface morphologies of each sample. In Fig. 7(a), wear debris particles were observed. The PBA-a was relatively brittle, and it could easily crack and break from the sample surface. These characteristics cause an increase in a specific wear rate of the PBA-a. In the case of the ATBN-modified PBA-a copolymers, a small amount of the ATBN contributed to a reduction of the specific wear rate and friction coefficient of the PBA-a. For the PBA-a/ATBN (95/5) copolymer, the worn surface of the copolymer displayed the scale-like damage, which is apparently generated under repeated loading during sliding as revealed in Fig. 7(b). However, the fatigue wear was not observed on the worn surface of the BA-a/ATBN (95/5) copolymer. This behavior can be suggested that the applied load is not higher than the fatigue strength of the copolymer. In addition, it is possible that the friction film on the worn surfaces was formed which creates greater lubricity effect of contact surfaces, consequently lower the frictional response. To compare with wear mode of epoxy (EP) modified by liquid carboxyl-terminated poly(butadiene-co-acrylonitrile) rubber (CTBN) (Ref 28), the scale-like damage pattern and the surface peeling off due to the fatigue wear mechanism was found on the tracks of the EP/2.5 wt.% CTBN. Therefore, the PBA-a/ATBN (95/5) copolymer showed mild wear mechanisms than the EP/CTBN system. For the worn surface of the PBA-a/ATBN (90/10) and the PBA-a/ATBN (80/20), copolymers are presented in Fig. 7(c) and (d), respectively. The scale-like damage under a

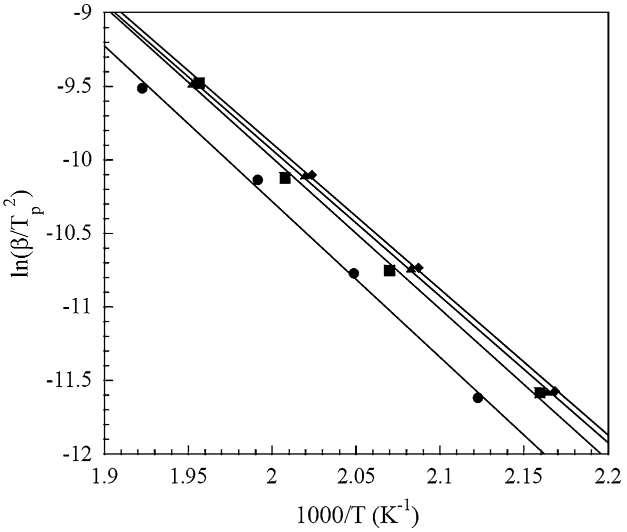

Fig. 6 Kissinger method plots for averaged activation energy determination of BA-a/ATBN mixtures as different ATBN contents: (●) BA-a, (■) BA-a/ATBN (95/5), (♦) BA-a/ATBN (90/10), (▲) BA-a/ATBN (80/20)

repeating load during sliding was clearly noticed. Also, the more rougher surface having some dimples and wider damaged areas were found on the worn surface of the PBA-a modified with 10 wt.% and 20 wt.% ATBN. The cracks inside for the PBA-a/ATBN (90/10) copolymer and some dimples for the PBA-a/ATBN (80/20) copolymer were observed. In general, these characteristics corresponded to the fatigue wear mode. Therefore, it can be summarized that the dominant wear mechanisms of the samples were changed from the abrasive wear mode of the PBA-a to the adhesive wear mode for the PBA-a/ATBN (95/5) copolymer, while the wear mode of the PBA-a/ATBN (90/10) and PBA-a/ATBN (80/20) copolymers is fatigue wear.

3.6 Dynamic Friction and Wear of PBA-a/ATBN Copolymer-Based Composites

As previously mentioned that the PBA-a/ATBN copolymer was possible to be a binder for self-lubricating composites because they showed low friction coefficient and anti-wear characteristics compared with those of phenolic and epoxy resins. Table 1 summarizes the average friction coefficient ($\mu_{avg.}$) and its extreme values ($\mu_{max.}$ and $\mu_{min.}$) of PBA-a/ATBN composites composed of the PBA-a/ATBN copolymer with different liquid ATBN contents (0-20 wt.%), and ingredients (Kevlar short fiber, alumina, graphite, and calcium carbonate). From Table 1, the $\mu_{avg.}$ of the composites remained in the range of 0.15-0.28. Moreover, the addition of liquid ATBN content about 5 wt.% reduced the average friction coefficients of the PBA-a/ATBN composite. However, at the ATBN content greater than 5 wt.%, the $\mu_{avg.}$ of the composites tended to increase. These effects of ATBN were similar to those observed in the unfilled PBA-a/ATBN copolymers. The PBA-a/ATBN (95/5) composite had the minimum value of the $\mu_{avg.}$ about 0.15. The decrease in the $\mu_{avg.}$ with an increase in 5 wt.% ATBN is due to a strong resistance to fatigue of the ATBN. Moreover, it is possible that the composite which was filled with 5 wt.% ATBN could be transferred well to the steel ball and its transfer film was thin, uniform, and adhered strongly to the steel ball, which could then act as micro lubrication. However, $\mu_{avg.}$ of larger particle size for 10 and 20 wt.% ATBN-filled composites was higher than that of the PBA-a/ATBN (95/5) because the PBA-a/ATBN (90/10) and PBA-a/ATBN (80/20) composites transfer film had poor adhesion to the steel ball. In addition, the $\mu_{avg.}$ of the PBA-a/ATBN composites was significantly lower than that of the PBA-a/ATBN copolymers. This characteristic may be due to the additional lubricity and wear resistance of the ingredients in the PBA-a/ATBN binder such as Kevlar short fiber, which was reported to significantly reduce the friction coefficient in hybrid phenolic friction (Ref 34) and epoxy composites (Ref 35). The additional cause of this behavior may be the effect of the solid lubricating of graphite as it is known that carbon fillers can serve as a solid material to lubricate the rubbing surface (Ref 36).

Specific wear rates of PBA-a/ATBN composites at various liquid ATBN contents are also tabulated in Table 1. The specific wear rate of the composites decreased with increasing content of ATBN, i.e., from 7.30×10^{-5} mm^3/Nm for PBA-a composite to 1.64×10^{-5}-6.07×10^{-5} mm^3/Nm for PBA-a/ATBN composites. Thus, the incorporation of ATBN into PBA-a composite can improve wear resistance of the PBA-a composite. In addition, the PBA-a/ATBN (95/5) composite with lowest friction coefficient showed lower specific wear rate than that of journal bearing based on PA66 filled with 18 wt.% self-lubricating PTFE, i.e., 7.50×10^{-5} mm^3/Nm (Ref 37). Moreover, the specific wear rates of the composites tended to be lower than those of the unfilled copolymers because the addition of the ingredients into the PBA-a/ATBN copolymers can reduce the extent of shear stress transferred to the copolymers as expected. From experimental results, the PBA-a/ATBN lubricating composites showed significantly low friction coefficient and specific wear rate. In general, friction coefficient under dry condition of polymer composite bearing is in the range of 0.05-0.15 (Ref 38). Therefore, the PBA-a/ATBN (95/5) composite can be used to increase the service life of machinery and equipment where oil and grease cannot be used.

To investigate wear characteristics of all PBA-a/ATBN composites, SEM worn surfaces are presented in Fig. 8. The worn surface showed regions of non-uniform roughness for all samples. In Fig. 8(a), the worn surface of the PBA-a composite looks somehow rough. Possibly, as the friction mechanism was attributed to the plowing, a two-body mode of abrasive wear is speculated to be dominant for the composites. For the worn surface of the PBA-a/ATBN (95/5) composite as can be seen in Fig. 8(b), there were secondary plateaus where no ingredients could be seen on the worn surface of the composite. Furthermore, resin-rich surface layer with less voids and debris on the worn surface of the PBA-a/ATBN (95/5) composite was also observed. This characteristic indicates good interfacial interaction between the ingredients and the copolymer binder for the PBA-a/ATBN (95/5) composite. Moreover, it is possible that the addition of 5 wt.% ATBN led to the formation of transfer films on the sliding-ball surface. The lowest friction coefficient of the composite was attributed to the lubricating action of such transferred friction films. Thus, the wear mechanism was mainly due to the adhesion. The worn surfaces of PBA-a/ATBN (90/10) and PBA-a/ATBN (80/20) composites in Fig. 8(c) and (d), respectively, were noticed to be very rough with distinct plateaus, while the ploughed grooves were not found on these worn surfaces. There were secondary plateaus and some fine wear debris particles on the worn surface of the

Table 1 Tribological properties at 25 °C of ATBN-modified PBA-a copolymers and their composites at various ATBN contents

	Friction coefficient			
	μ_{min}	μ_{max}	μ_{avg}	Specific wear rate (mm^3/Nm)
PBA-a/ATBN Copolymers, wt.%				
100/0	0.28	0.47	0.38	2.08×10^{-4}
95/5	0.31	0.54	0.36	1.85×10^{-4}
90/10	0.26	0.49	0.39	2.85×10^{-4}
80/20	0.30	0.51	0.42	9.60×10^{-4}
PBA-a/ATBN Composites, wt.%				
100/0	0.16	0.33	0.28	7.30×10^{-5}
95/5	0.11	0.18	0.15	6.07×10^{-5}
90/10	0.12	0.28	0.24	1.64×10^{-5}
80/20	0.16	0.30	0.26	2.51×10^{-5}

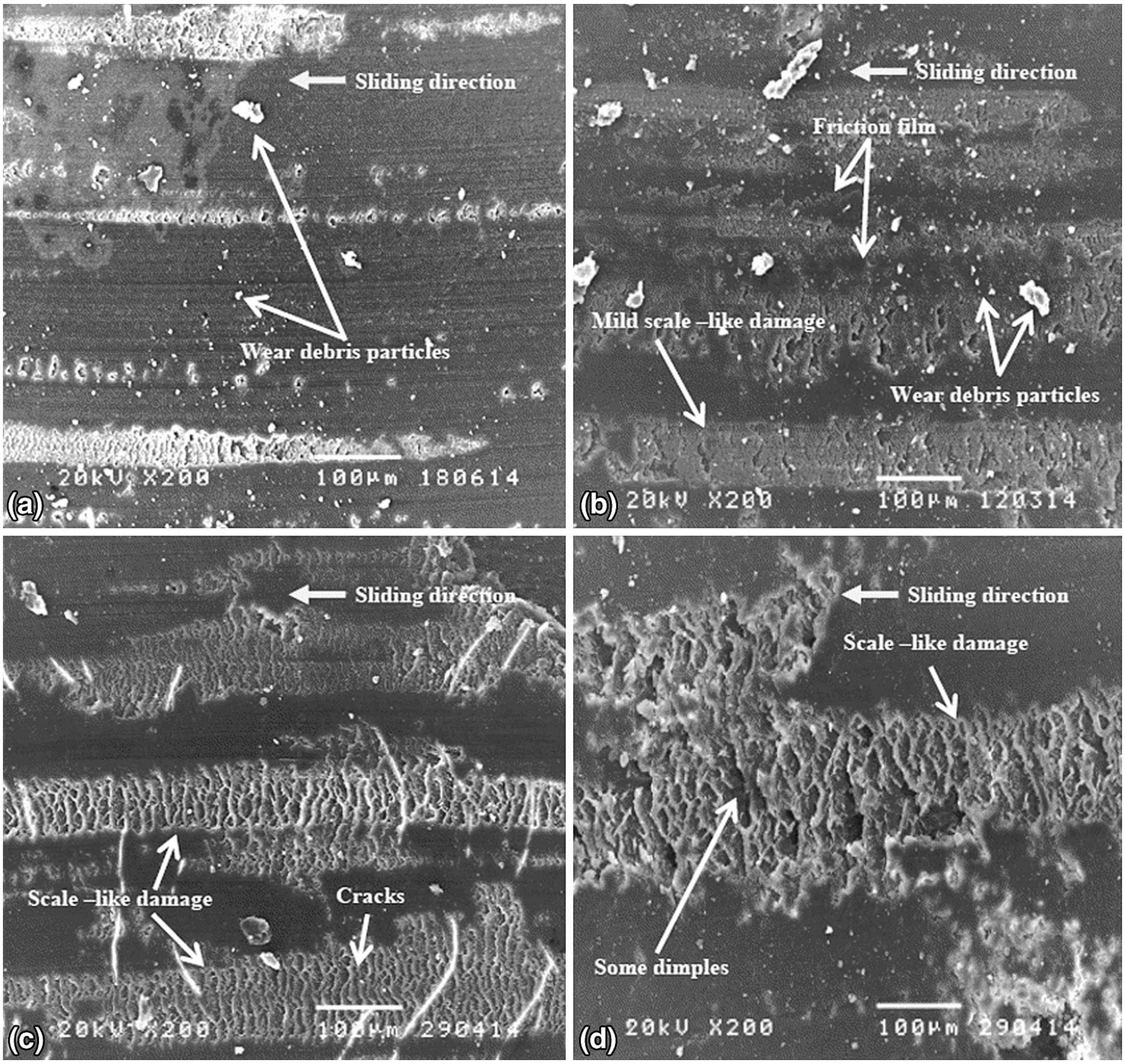

Fig. 7 SEM micrographs of worn surfaces of PBA-a/ATBN copolymers at different ATBN contents: (a) PBA-a, (b) PBA-a/ATBN (95/5), (c) PBA-a/ATBN (90/10), (d) PBA-a/ATBN (80/20)

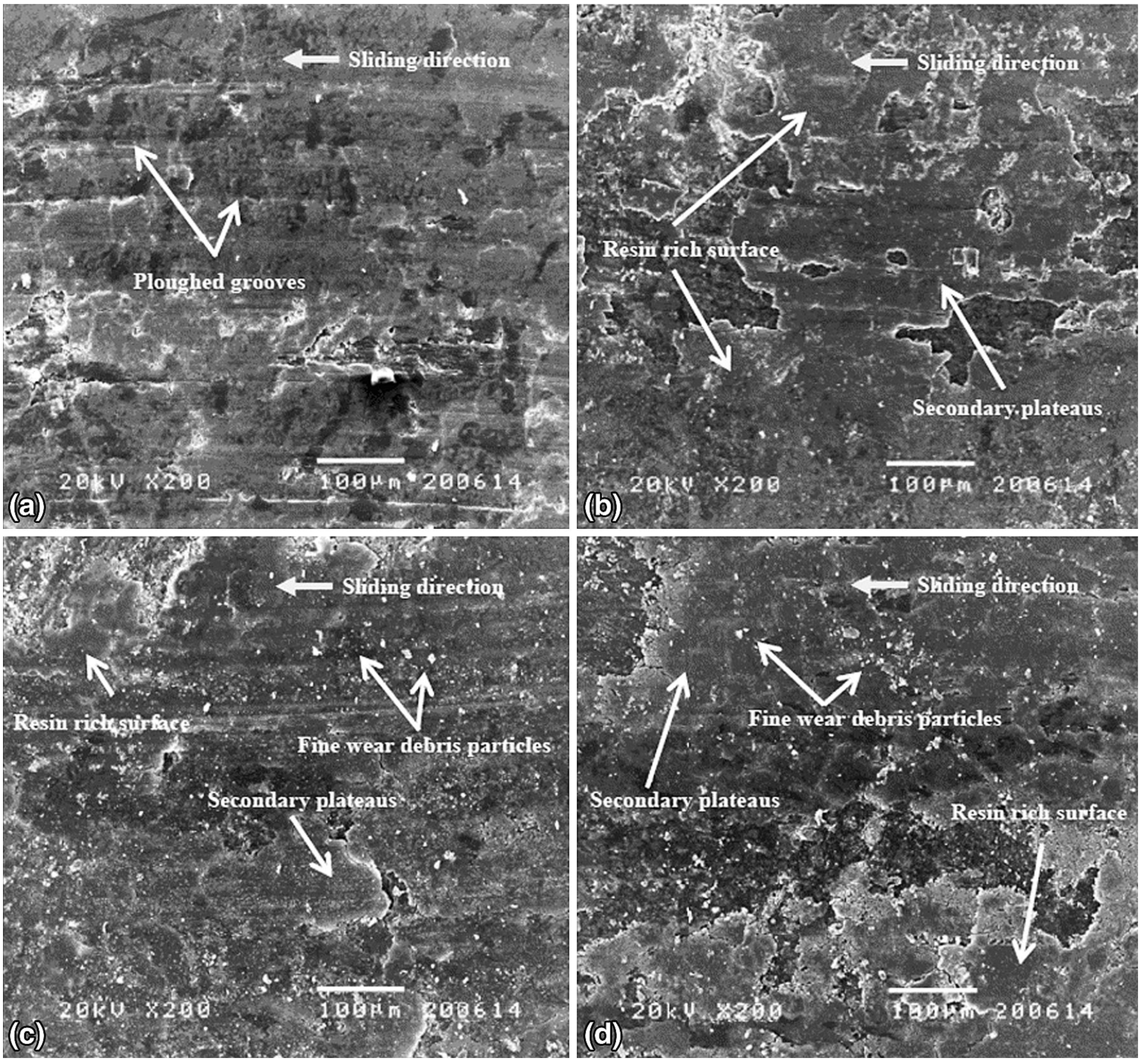

Fig. 8 Wear micrographs (SEM) of worn surfaces of PBA-a/ATBN composites at different ATBN contents: (a) PBA-a, (b) PBA-a/ATBN (95/5), (c) PBA-a/ATBN (90/10), (d) PBA-a/ATBN (80/20). Each composite consisted of 30 wt.% PBA-a/ATBN, 5 wt.% Kevlar short fiber, 10 wt.% alumina powder, 10 wt.% graphite powder, and 45 wt.% calcium carbonate powder

composites. Such plateaus play protective role against the wear damage to the underlying material, which are generally responsible for an enhancement of frictional response. Furthermore, the worn surface of PBA-a/ATBN (90/10) and PBA-a/ATBN (80/20) composites also exhibited resin-rich surface layer. The presence of resin layer improved the bonding and surface integrity with high ingredient-binder adhesion that resulted in the decrease of specific wear rates of both composites. Therefore, the wear of PBA-a/ATBN (90/10) and PBA-a/ATBN (80/20) composites was could be related to the three-body abrasion. Also the wear morphologies of the PBA-a/ATBN composites in comparison with the PBA-a/ATBN copolymers clearly point out that the addition of ingredients is an effective way to reduce the fatigue wear during the prolonged sliding contact with the steel ball.

3.7 Glass Transition Temperature of Lubricating Composites Based on PBA-a/ATBN Copolymers

Loss tangent (Tanδ) plots of the PBA-a/ATBN composites are depicted in Fig. 9. The peak in the Tanδ curve is indicative of glass transition temperature (T_g) of the composites. From this figure, the magnitude of T_g for all composites showed the value of $\sim$190 °C. However, in general, the incorporation of rubbers such as ATBN ($T_g \sim -51$ °C) and hydroxyl-terminated polybutadiene (HTPB) ($T_g \sim -75$ °C) into the polymer leads to decrease in T_g of the polymer as previously reported in epoxy/ATBN blends (Ref 39) and epoxy/HTPB blends (Ref 23). In addition, Tanδ factor also indicates damping capacity of the composite materials. It is observed that the highest damping capacity, i.e., 0.420, was shown by the PBA-a composite till transition regime gets lower and dominated by the PBA-a/ATBN (95/5) composite at elevated temperature regime, i.e. >210 °C. Therefore, the PBA-a composite is most effective in controlling and minimizing the unwanted phenomenon, for example, noise, and vibration to a larger extent dynamically generated during the at temperature near T_g of 190 °C, while the PBA-a/ATBN (95/5) composite should be operated at lower and elevated temperatures because it shows better damping capacity behavior than the PBA-a composite.

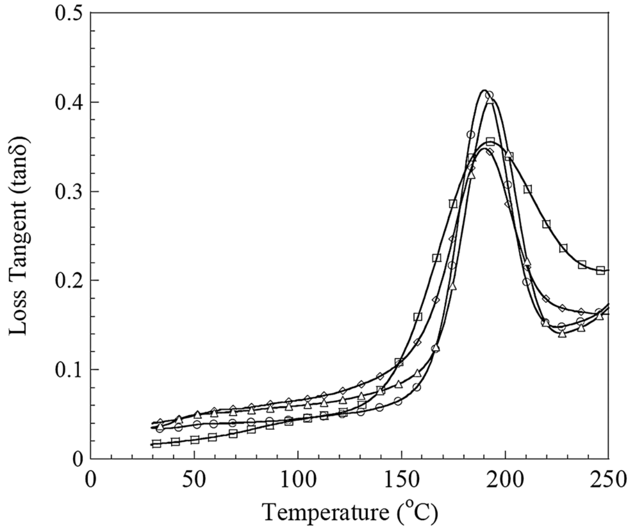

Fig. 9 Loss tangent of PBA-a/ATBN composites at different ATBN contents: (○) PBA-a, (□) PBA-a/ATBN (95/5), (◇) PBA-a/ATBN (90/10), (Δ) PBA-a/ATBN (80/20)

3.8 Flexural Properties of Lubricating Composites Based on PBA-a/ATBN Copolymers

Flexural properties, i.e., strength and modulus of the PBA-a/ATBN composites at different liquid ATBN contents, are presented in Fig. 10. In this figure, the flexural strengths of the PBA-a/ATBN composites were found to increase with an increase of the ATBN content up to 5 wt.%, and then the flexural strengths decreased with further addition of the ATBN. However, all PBA-a/ATBN composites had higher values of flexural strength than that of the PBA-a composite. The flexural strength of the PBA-a/ATBN (95/5) composite, i.e., 47.6 ± 8.0 MPa, was about 1.4 times higher than that of the PBA-a composite, i.e., 34.6 ± 3.8 MPa. In addition, the flexural strength value of the PBA-a/ATBN composite was higher than that of linseed oil- and cashew nut shell liquid (CNSL)-modified phenolic resin filled with fibers of glass, steel, polyacrylonitrile (PAN), rock wool, friction modifiers, and a space filler, i.e., 41.2 MPa and 41.0 MPa, respectively (Ref 40). Furthermore, the obtained flexural strength for the PBA-a/ATBN (95/5) composite was similar to the value published by Saffar and Shojaei (Ref 41). It was reported the flexural strength values of the composites based on phenolic/SBR matrix and additives such as coal powder, graphite, $CaCO_3$, iron powder, steel wool, barite, iron oxide, cashew dust, aramid pulp, vermiculite, and alumina were about 47.5 MPa for 7.5 vol.% SBR. Therefore, in our work, the enhancement in the composite strength with the proper content of the ATBN was possibly due to the good interfacial adhesion between the ingredients and the PBA-a/ATBN copolymer. This characteristic is in agreement with the morphology of worn surface of the PBA-a/ATBN (95/5) composite that exhibited resin-rich surface layer with less voids and debris.

The flexural modulus of the PBA-a/ATBN (95/5) composite, i.e., 5.9 ± 0.4 GPa, was also found to be higher than that of the PBA-a composite, i.e., 5.4 ± 0.6 GPa, as illustrated in Fig. 10. At ATBN content greater than 5 wt.%, the flexural modulus of the composites was found to decrease with the amount of the ATBN rubber. This behavior could be related to the effect of excessive viscous liquid ATBN with much lower modulus than that of the PBA-a phase. Again, the PBA-a/ATBN(95/5)-lubricating composite exhibited the flexural modulus higher than that of linseed oil- and cashew nut shell liquid (CNSL)-modified phenolic resin filled with fibers of glass, steel, polyacrylonitrile (PAN), rock wool, friction modifiers, and a space filler, i.e., 5.3 GPa and 5.7 GPa, respectively (Ref 40).

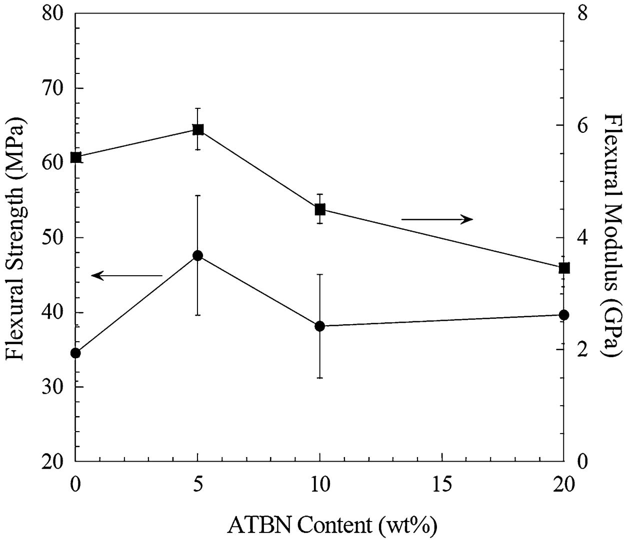

Fig. 10 Flexural properties of PBA-a/ATBN composites at various ATBN contents: (●) Flexural strength, (■) Flexural modulus

4. Conclusions

The effect of liquid amine-terminated butadiene-acrylonitrile (ATBN) content on the rheological, cure kinetics, tribological, thermal, and mechanical properties of bisphenol-A/aniline-based polybenzoxazine composites can be summarized as follows. An addition of liquid ATBN in benzoxazine resin can substantially reduce the gel time, curing temperature, and curing activation energy of the benzoxazine resin. The copolymers of the polybenzoxazine modified with the ATBN revealed enhancement in the tribological properties, i.e., friction coefficient and wear resistance compared to those of the polybenzoxazine. The friction coefficient for the copolymers was in the range of 0.36-0.39 with 5-10 wt.% ATBN contents. Furthermore, it was found that the ATBN-modified polybenzoxazine-based self-lubricating composites showed a significantly low friction coefficient value and specific wear rate at the optimal ATBN content of 5 wt.%, i.e., 0.15 and 6.07×10^{-5} mm^3/Nm. The mechanical and thermal properties of the composites are still maintained with an addition of ATBN content at less than 10 wt.%, i.e., $T_g \sim 190$ °C, $\sigma_f \sim 47.6$ MPa and $E_f = 5.9$ GPa. In addition, the ether bonds formed between the polybenzoxazine and the ATBN is attributed to the significant improvement on thermal and mechanical properties of the resulting polybenzoxazine/ATBN-based self-lubricating composites.

Acknowledgments

This work was supported by a New Researcher's Grant of Thailand Research Fund-Commission on Higher Education (MRG5580101) and Matching Fund, Strategic Wisdom and Research Institute, Srinakharinwirot University 2012-2014 (Contact Grants No. 411/2555), and Srinakharinwirot University Research Fund (Contact Grants No. 171/2556). The authors also greatly acknowledged the National Research University Project, Office of Higher Education Commission, Thailand (WCU-028-AM-57). Additional funding was provided by the Matsumae International Foundation (2012), Japan. Prof. S. Hiziroglu is also acknowledged for his comments on this manuscript.

References

1. T. Singh, A. Patnaik, B.K. Satapathy, M. Kumar, and B.S. Tomar, Effect of Nanoclay Reinforcement on the Friction Braking Performance of Hybrid Phenolic Friction Composites, *J. Mater. Eng. Perform.*, 2013, **22**, p 796–805
2. J. Xian and L. Xiaomei, Friction and Wear Characteristics of Polymer-Matrix Friction Materials Reinforced by Brass Fibers, *J. Mater. Eng. Perform.*, 2004, **13**, p 642–646
3. J. Li and X.H. Sheng, The Effect of PA6 Content on the Mechanical and Tribological Properties of PA6 Reinforced PTFE Composites, *J. Mater. Eng. Perform.*, 2010, **19**, p 342–346
4. J. Li and X.Z. Li, Evaluation of the Tribological Properties of Carbon Fiber Reinforced Poly(vinylidene fluoride) Composites, *J. Mater. Eng. Perform.*, 2010, **19**, p 1025–1030
5. H. Ishida and T. Agag, *Handbook of Benzoxazine Resins*, Elsevier, New York, 2011
6. C. Jubsilp, T. Takeichi, S. Hiziroglu, and S. Rimdusit, High Performance Wood Composites Based on Benzoxazine-Epoxy Alloys, *Bioresour. Technol.*, 2008, **99**, p 8880–8886
7. J. Kajohnchaiyagual, C. Jubsilp, I. Dueramae, and S. Rimdusit, Thermal and Mechanical Properties Enhancement Obtained in Highly Filled Alumina-Polybenzoxazine Composites, *Polym. Compos.*, 2014, **35**, p 2269–2279
8. H. Ishida, Polybenzoxazine Nanocomposites of Clay and Method for Making Same, U.S. Patent 6,323,270, 27 Nov 2001
9. S. Rimdusit and H. Ishida, Development of New Class of Electronic Packaging Materials based on Ternary Systems of Benzoxazine, Epoxy, and Phenolic Resins, *Polymer*, 2000, **41**, p 7941–7949
10. S. Rimdusit, C. Jubsilp, and S. Tiptipakorn, *Alloys and Composites of Polybenzoxazines: Properties and Applications*, Springer, Singapore, 2013
11. C. Jubsilp, S. Rimdusit, and T. Takeichi, Aniline-Based Polybenzoxazine and Their Copolymers or Composites: Molecular Design and Potential Applications, *Aniline: Structural/Physical Properties, Reactions and Environmental Effects*, K. Hernandez and M. Holloway, Ed., Nova Science Publishers Inc, New York, 2013, p 55–90
12. S. Rimdusit, S. Pirstpindvong, W. Tanthapanichakoon, and S. Damrongsakkul, Toughening of Polybenzoxazine by Alloying with Urethane Prepolymer and Flexible Epoxy: A Comparative Study, *Polym. Eng. Sci.*, 2005, **45**, p 288–296
13. S. Rimdusit, P. Kunopast, and I. Dueramae, Thermomechanical Properties of Arylamine-based Benzoxazine Resins Alloyed with Epoxy Resin, *Polym. Eng. Sci.*, 2011, **51**, p 1797–1807
14. S. Grishchuk, S. Schmitt, O.C. Vorster, and J. Karger-Kocsis, Structure and Properties of Amine-Hardened Epoxy/Benzoxazine Hybrids: Effect of Epoxy Resin Functionality, *J. Appl. Polym. Sci.*, 2012, **124**, p 2824–2837
15. S. Rimdutsit and P. Bangsen, Kasemsiri, Chemorheology and Thermomechanical Characteristics of Benzoxazine-Urethane Copolymers, *J. Appl. Polym. Sci.*, 2011, **121**, p 3669–3678
16. C. Jubsilp, C. Panyawanitchakun, and S. Rimdusit, Flammability and Thermomechanical Properties of Dianhydride-modified Polybenzoxazine Composites Reinforced with Carbon Fiber, *Polym. Compos.*, 2013, **34**, p 2067–2075
17. J. Jang and D.J. Seo, Performance Improvement of Rubber-modified Polybenzoxazine, *J. Appl. Polym. Sci.*, 1998, **67**, p 1–10
18. S. Grishchuk, L. Sorochynska, O.C. Vorster, J. Karger-Kocsis, and J. Structure, Thermal, and Mechanical Properties of DDM-Hardened Epoxy/Benzoxazine Hybrids: Effects of Epoxy Resin Functionality and ETBN Toughening, *J. Appl. Polym. Sci.*, 2013, **127**, p 5082–5093
19. M. Hermandez, J. Gonzalez, M. Ichazo, D. Lovera, and C. Albano, Rheological Behavior of Modified Polypropylene (PP) with Nitrile Rubber (NBR), May 6–10, 2001 (Dallas, TX), ANTEC, 2001, p 3554–3557
20. C. Jubsilp, T. Takeichi, and S. Rimdusit, Property Enhancement of Polybenzoxazine Modified with Dianhydride, *Polym. Degrad. Stabil.*, 2011, **96**, p 1047–1053
21. T. Agag and T. Takeichi, Effect of Hydroxyphenylmaleimide on the Curing Behaviour and Thermomechanical Properties of Rubber-Modified Polybenzoxazine, *High Perform. Polym.*, 2001, **13**, p S327–S342
22. H.H. Winter and F. Chambon, Analysis of Linear Viscoelasticity of A Crosslinking Polymer at the Gel Point, *J. Rheol.*, 1986, **30**, p 367–382
23. R. Thomas, D. Yumei, H. Yuelong, Y. Le, P. Moldenaers, Y. Weimin, T. Czigany, and S. Thomas, Miscibility, Morphology, Thermal, and Mechanical Properties of a DGEBA based Epoxy Resin Toughened with a Liquid Rubber, *Polymer*, 2008, **49**, p 278–294
24. R. Thomas, S. Durix, C. Sinturel, T. Omonov, S. Goossens, G. Groeninckx, P. Moldenaers, and S. Thomas, Cure Kinetics, Morphology and Miscibility of Modified DGEBA-Based Epoxy Resin-Effects of a Liquid Rubber Inclusion, *Polymer*, 2007, **48**, p 1695–1710
25. G. Xian, R. Walter, and F. Haupert, A Synergistic Effect of Nano-Tio$_2$ and Graphite on the Tribological Performance of Epoxy Matrix Composites, *J. Appl. Polym. Sci.*, 2006, **102**, p 2391–2400
26. S. Lampman, *Characterization and Failure Analysis of Plastics*, Ohio, ASM International, 2003, p 259–264
27. K.C. Ludema, *Friction, Wear, Lubrication: A Textbook in Tribology*, CRC Press, New York, 1996
28. W. Chonkaew, N. Sombatsompop, and W. Brostow, High Impact Strength and Low Wear of Epoxy Modified by A Combination of Liquid Carboxyl Terminated Poly(Butadiene-co-Acrylonitrile) Rubber and Organoclay, *Eur. Polym. J.*, 2013, **49**, p 1461–1470
29. W. Chonkaew and N. Sombatsompop, Mechanical and Triboligical Properties of Epoxy Modified by Liquid Carboxyl Terminated Poly(butadiene-co-acrylonitrile rubber), *J. Appl. Polym. Sci.*, 2012, **125**, p 361–369
30. S. Yu, H. Hu, J. Ma, and J. Yin, Tribological Properties of Epoxy/Rubber Nanocomposites, *Tribol. Int.*, 2008, **41**, p 1205–1211
31. Q. Wang, Q. Xue, H. Liu, W. Shen, and J. Xu, The Effect of Particle Size of Nanometer ZrO$_2$ on the Tribological Behaviour of PEEK, *Wear*, 1996, **198**, p 216–219
32. X.S. Xing and R.K.Y. Li, Wear Behavior of Epoxy Matrix Composites Filled with Uniform Sized Sub-micron Spherical Silica Particles, *Wear*, 2004, **256**, p 21–26
33. E.W. McAllister, *Pipeline Rules of Thumb Handbook: A Manual of Quick, Accurate Solutions to Everyday Pipeline Engineering Problem*, Elsevier, Waltham, 2009
34. P. Gopal, L.R. Dharani, and F.D. Blun, Hybrid Phenolic Friction Composites Containing Kevlar®Pulp Part 1. Enhancement of Friction and Wear Performance, *Wear*, 1996, **193**, p 199–206
35. J. Wu and X.H. Cheng, Friction and Wear Properties of Kevlar Pulp Reinforced Epoxy Composites Under Dry Sliding Condition, *Tribol. Lett.*, 2006, **22**, p 259–263
36. J.P. Davim and R. Cardoso, Effect of the Reinforcement (Carbon or Glass fibres) on Friction and Wear Behaviour of the PEEK Against Steel Surface at Long Dry Sliding, *Wear*, 2009, **266**, p 795–799
37. M.T. Demirci and H. Duzcukoglu, Wear Behaviors of PTFE Reinforced PA 66 Journal Bearing, The 10th International Scientific Conference UNITECH, November 19-20, 2010 (Gabrovo, Bulgaria), p 249–253
38. P.J. Blau, *Lubrication to Control Friction*, New York, Marcel Dekker Inc, Friction Science and Technology, 1996, p 285–334
39. N. Chikhi, S. Fellahi, and M. Bakar, Modification of Epoxy Resin Using Reactive Liquid (ATBN) Rubber, *Eur. Polym. J.*, 2002, **38**, p 251–264
40. J. Bijwe, Nidhi, N. Majumdar, and B.K. Satapathy, Influence of Modified Phenolic Resins on the Fade and Recovery Behavior of Friction Materials, *Wear*, 2005, **259**, p 1068–1078
41. A. Saffar and A. Shojaei, Effect of Rubber Component on the Performance of Brake Friction Materials, *Wear*, 2012, **274–275**, p 286–297

Applied Mechanics and Materials Vol. 576 (2014) pp 75-79
© (2014) Trans Tech Publications, Switzerland
doi:10.4028/www.scientific.net/AMM.576.75

Effect of Rubber Contents on Tribological and Thermomechanical Properties of Polybenzoxazine

Chanchira Jubsilp[1, a], Sarawut Rimdusit[2,b] and Tsutomu Takeichi[3,c]

[1]Department of Chemical Engineering, Faculty of Engineering, Srinakharinwirot University,
Nakhonnayok 26120, Thailand

[2]Polymer Engineering Laboratory, Department of Chemical Engineering, Faculty of Engineering,
Chulalongkorn University, Bangkok 10330, Thailand

[3]Department of Environmental and Life Sciences, Toyohashi University of Technology,
Tempaku-cho, Toyohashi 441-8580, Japan

[a]chanchira@swu.ac.th, [b]sarawut.r@chula.ac.th, [c]takeichi@ens.tut.ac.jp

Keywords: Polybenzoxazine, Rubber, Tribological Property.

Abstract. Bisphenol-A/aniline based polybenzoxazine (PBZ) modified with amine terminated butadiene–acrylonitrile (ATBN) were prepared. The tribological and thermomechanical properties as well as thermal stability of the PBZ/ATBN copolymers were investigated by ball-on-disc tribometer, dynamic mechanical analysis (DMA), universal test machine and thermogravimetric analysis (TGA). The inclusion of ATBN at a mass fraction of 5% was found to greatly increase friction coefficient and wear resistance of the copolymers. DMA measurements showed that the storage modulus and the glass transition temperature of the PBZ can be maintained with an addition of ATBN in the range of 1-5wt%. Moreover, flexural property measurements indicated that the flexural strength of the copolymer increased with increasing of ATBN content up to 10wt% whereas TGA results revealed that an increase of the PBZ content can help improve thermal stability of the copolymers.

1. Introduction

Recently, developments in the automotive industry have been accompanied by increases of speed, loads, and engine power. Therefore, the friction materials highly suitable as disc pads are required to fulfill several demands such as high and stable friction coefficient and low wear rate [1-2]. The friction materials in automobiles as the disc pads comprise conventionally a binder and several usual fillers. In the friction material composition for producing the friction material, a pure novolak type phenolic resin is generally used as the thermosetting binder from the viewpoint of overall balance characteristics such as moldability, economy, heat resistance, good mechanical properties, flame resistance, and dielectric insulation property, etc. Furthermore, the phenolic resins compounded with rubber, epoxy resin, and cashew nut shell liquid to act as a binder for the friction materials have been investigated [1-3]. Liu et al., [3] reported that the use of the phenolic resin compound with nano powdered rubber, i.e. styrene butadiene nano powdered rubber and nitrile-butadiene nano powdered rubber, prevails over the use of the pure phenolic resin. However, the phenolic resin releases volatile by-product such as water or ammonia during the curing process, so it is hard to control their micro void. In addition, designing their molecular structure is also difficult besides their inherent shortcomings such as their brittleness and short shelf-life.

Benzoxazine resins are a new type of phenolic resins that are obtained from reaction of phenols, formaldehyde and amines to yield a relatively clean precursor, without the need of solvent elimination or monomer purification. After the ring opening polymerization, polybenzoxazine overcomes many shortcomings of traditional phenolic resins such as using acid or base catalyst and releasing condensation by-products while retaining good thermal properties and flame retardancy of phenolic resins [4-6]. Besides, they also exhibit lots of unique characteristics including low melt viscosity, dimensional stability, fast development of mechanical properties as a function of curing conversion, low water absorption in spite of having prevalent hydrophilic group in the structure, low dielectric constant and excellent mechanical properties. Moreover, an ability of benzoxazine resins to form blends with various other resins or polymers often renders a novel class of resin systems with intriguing properties to provide improved performance in a broad range of applications [7,8]. For example, blending between benzoxazine and epoxy resins [9], polyurethanes [10], polyimides [11], dianhydrides [6] is considered to be a potentially effective measure to enhance thermal or mechanical properties as well as flammability of the polymers. Interestingly, in recent years, thermoset compositions based on benzoxazine resins and amine-terminated acrylonitrile-butadiene copolymer (ATBN) have been reported [12]. As an example, the combination of benzoxazine resin with ATBN results in a significant enhancement of the fracture toughness properties of the resulting cured polybenzoxazine.

Therefore, this work will investigate effects of amine-terminated acrylonitrile-butadiene copolymer (ATBN) contents on tribological, mechanical and thermal properties of polybenzoxazine to be used as a binder for friction materials.

2. Experimental

2.1 Materials. BA-a type benzoxazine resin based on bisphenol-A, formaldehyde, and aniline was synthesized according to the patented solventless technology [13]. The BA-a resin is a yellow clear solid at room temperature. Bisphenol-A (polycarbonate grade) was provided by Thai Polycarbonate Co., Ltd. (TPCC). Paraformaldehyde and aniline was obtained from Merck Co. and Fluka Chemical Co., respectively. The end-functionalised liquid rubber, i.e. amine terminated butadiene–acrylonitrile copolymer, Hycar ATBN 1300X16 (BF-Goodrich) with 18% acrylonitrile content and with a nominal molecular weight of 1760 g/mol from UBE Co. were used as tougheners. All chemicals were used as-received.

2.2Preparation of ATBN-modified PBZ. In this study, the formulations of the bisphenol-A/aniline based polybenzoxazine (PBZ) modified with ATBN were varied with 1, 3, 5, 10, 20, and 30% by weight. The mixture was then heated to about 80°C in an aluminum pan for 15 minutes until the homogeneous mixture was obtained. Then, the mixture was cured sequentially at 150°C to 220°C for 6h.

2.3 Characterizations. The tribological properties were performed by using ball-on-disc test. All tests were conducted at room temperature. Wear tests were conducted with a load of 10 N, sliding distance up to 1000 m and sliding time of 2700s. A dynamic mechanical analyzer (DMA) from Netzsch Inc. (model DMA 242 C) in a bending mode was used to examine storage modulus (E′) and loss modulus (E") of the specimens. The dimension of each specimen was 10 mm × 50 mm × 3 mm. The tests were performed in a temperature sweep mode with a fixed frequency of 1 Hz. Each specimen was tested using a heating rate of 2°C/min from room temperature to about 270°C. The glass transition temperature was taken from the temperature at the maximum point on the loss modulus curve. The weight loss of a specimen as a function of temperature was monitored using a thermogravimetric analyzer (TGA) from Mettler Toledo (model TGA 1 STARe System). The weight of the specimen was measured to be about 8-10 mg. The specimens were heated at a rate of 20°C/min from 30°C to 800°C under argon atmosphere at 100 ml/min. Flexural properties were conducted by a Universal Testing Machine, Lloyd Instruments, Model LR 10K. The measurement was carried out in a three-point bending mode with a support span of 48 mm and at a crosshead speed of 1.2 mm/min. A minimum of five samples with a dimension of 25 mm × 60 mm × 3 mm were tested, and the averaged values were determined.

3. Results and Discussion

3.1 Friction and Wear Behaviors of ATBN-modified Polybenzoxazine. Fig. 1 and Fig. 2 plot the effect of ATBN contents on the coefficients of friction and wear rates of the polybenzoxazine (PBZ) at temperature of 25°C, an applied load of 10 N and a sliding velocity of 0.366 m/s. From the figures, we can see that the coefficients of friction and the wear rates of the PBZ decreased with increasing ATBN content up to 5wt% and then showed a significant increase at a ATBN content above 10wt%, which indicated that ATBN had good friction-reducing and anti-wear abilities of the PBZ at 25°C within a mass fraction of 1-5wt% while showed negative trend to the wear resistance of the ATBN-modified PBZ above a mass fraction of 10wt%. It could be rationally expected that the PBZ copolymers with excess amount of ATBN would have poor wear resistance, owing to the decreased mechanical strength and lubricity.

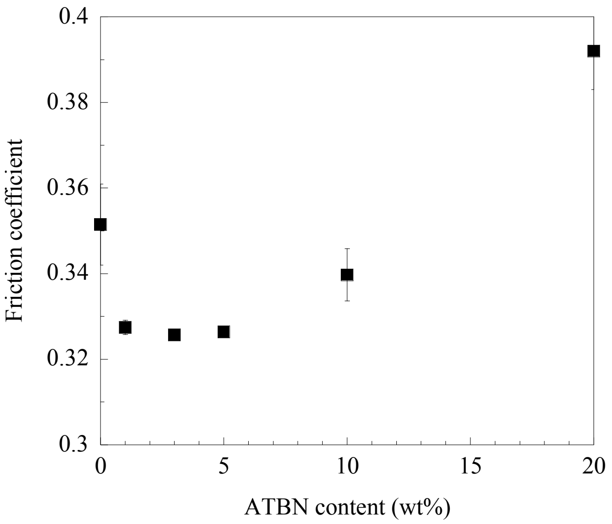

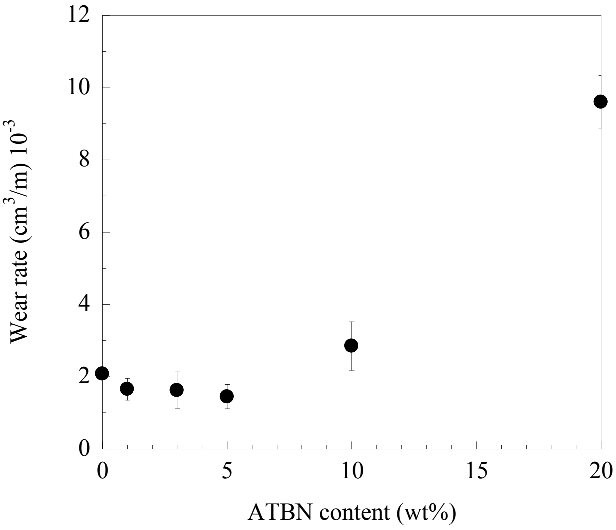

Fig. 1 Friction coefficient of ATBN-modified PBZ **Fig. 2** Wear rate of ATBN-modified PBZ

3.2 Dynamic Mechanical Properties of ATBN-modified Polybenzoxazine. Themomechanical properties of PBZ modified with various ATBN contents measured as a function of temperature were displayed in Fig. 3 and Fig. 4. Generally, the storage modulus of the materials demonstrates the deformation resistances of material when external force were applied sinusoidally. The storage moduli at room temperature (30°C) of BA-a modified with 1, 3, 5, 10, 20 and 30wt% of ATBN exhibited the values of 5.20, 4.64, 4,50, 3,64, 3.11 and 2.11 GPa, respectively, which were lower than that of the neat polybenzoxazine of 5.50 GPa as shown in Fig.3. However, we can see that the storage moduli of 1-5wt% ATBN-modified polybenzoxazine are relatively constant and then significantly decrease.

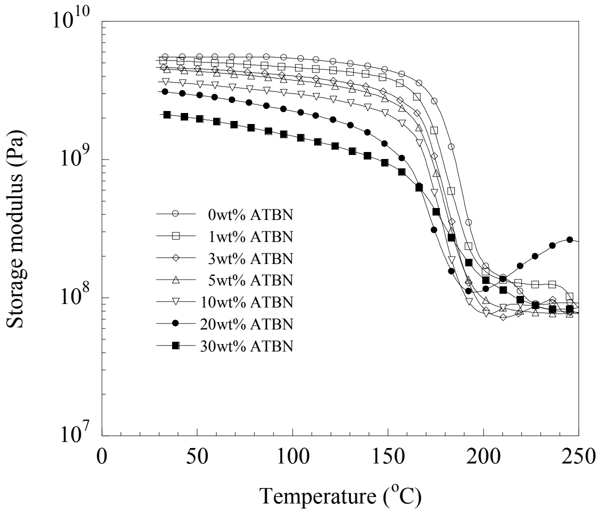

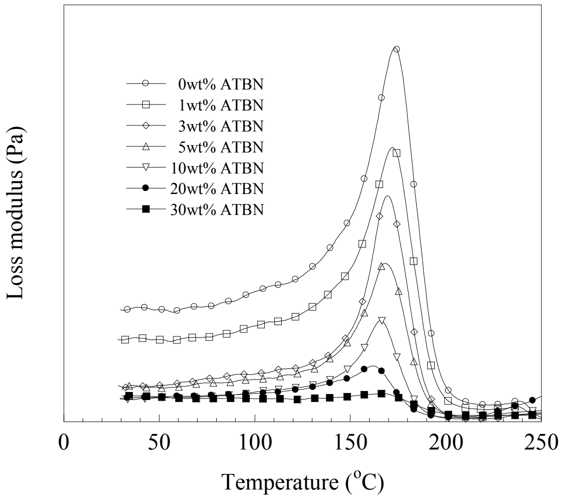

Fig. 3 Storage modulus of ATBN-modified PBZ **Fig. 4** Loss modulus of ATBN-modified PBZ

Fig. 4, the T_g of the polybenzoxazine determined from the maximum of loss modulus curve in DMA experiment was about 171°C and the value was found to be slightly decreased by blending with the ATBN. The T_g of the fully cured PBZ/ATBN copolymer samples showed a value ranging from

172°C to 167°C with increasing ATBN content. This result obviously indicated that the soft ATBN segments can increase the free volume of the copolymer thus reduce glass transition temperature of the polymer hybrids as observed previously in epoxy/ATBN copolymers [14].

3.3 Thermal Stability of ATBN-modified Polybenzoxazine. Thermal stabilities, i.e. degradation temperature at 5% weight loss (T_{d5}) and char yield of PBZ and ATBN-modified PBZ copolymers at various ATBN contents was investigated by thermogravimetric analysis (TGA). The T_{d5} of the ATBN-modified PBZ copolymers at various ATBN contents of 1, 3, 5, 10, 20 and 30wt% was about 338°C, 338°C, 325°C, 322°C, 316°C and 303°C, respectively, while that of the PBZ and the ATBN was about 339°C and 335°C, respectively. Moreover, the char yield decreased from 37% for the PBZ to 28, 23, 22, 17, 12 and 6wt% with the incorporation of ATBN. From the results, the degradation temperature and the char yield of the ATBN-modified PBZ copolymers increased with the PBZ fraction clearly from the more thermally stable of the polybenzoxazine compared to the rubber modifier.

3.4 Mechanical Properties of ATBN-modified Polybenzoxazine. The flexural properties, i.e. flexural modulus, flexural strength, elongation at break, and area under curve were listed in Table 1. From the table, we can see that the flexural modulus of all copolymer specimens were slightly lower than that of PBZ due to addition of soft segments of the ATBN in the hard segments of the PBZ. Interestingly, flexural strength of the PBZ was found to increase with an addition of ATBN up to 10wt% and then decreased. Typically, the flexural strength of the polymer matrix will be decreased with an addition of rubber following a rule of mixture. However, this behavior cannot be observed in ATBN-modified the PBZ system at the ATBN content less than 10wt%. This behavior may be due to reaction formation between the activated phenolic hydroxyl groups in the PBZ and the amino groups in the ATBN. The good interfacial adhesion of the ATBN can adequately support stress transfer from the PBZ matrix [12,15]. Moreover, the elongation at break and area under the stress-strain curves of the ATBN-modified PBZ copolymers clearly increased with the ATBN contents due to an enhanced ability to inhibit the crack growth, absorbing, and dissipating forces in the rigid polybenzoxazine by an addition of flexible molecules of the ATBN.

Table 1. Flexural properties of ATBN-modified polybenzoxazine compolymers

BA-a/ATBN Compositions (wt%)	σ_f (MPa)	E_f (GPa)	Elongation at break (%)	Area under curve (MPa)
100/0	114	4.63	0.028	1.53
99/1	115	4.70	0.028	1.53
97/3	137	4.64	0.033	2.13
95/5	137	3.97	0.034	2.20
90/10	139	3.80	0.045	2.84
80/20	119	3.08	0.050	2.86
70/30	83	1.69	0.065	2.70

4. Conclusion

The effect of amine-terminated butadiene–acrylonitrile (ATBN) content on the triboligical, thermal and mechanical properties of bisphenol-A-aniline based polybenzoxazine can be summarized as follows. The copolymers of polybenzoxazine modified with ATBN showed enhancement in the tribological properties, i.e. friction coefficient and wear resistance compared to those of the neat polybenzoxazine. The coefficients of friction for the ATBN-modified polybenzoxazine copolymers were about 0.32 with the ATBN contents in a range of 1-5wt%. Furthermore, the copolymer's mechanical and thermal properties are still maintained with an addition of ATBN content at less than 10wt%, i.e. T_g = 168-172°C, T_{d5} = 325-338°C, $\sigma_f \sim$ 137 MPa and E_f = 3.97-4.70 GPa.

Acknowledgements

This work is supported by a New Researcher's Grant of Thailand Research Fund-Commission on Higher Education (MRG5580101) and Matching Fund, Strategic Wisdom and Research Institute, Srinakharinwirot University 2012-2014 (Contact Grants No. 411/2555 and 171/2556). Additional funding is from the Matsumae International Foundation (2012), Japan.

References

[1] S. Yosuke, Y. Michinori, T. Yuzo and M. Tadahiro, U.S. Patent 6,(080) (2000),p.230.

[2] T. Nakamura, T. Nagata, K. Takeuchi and M. Kobayashi, U.S. Patent 6,(596) (2003),p.789 B2.

[3] Y. Liu, Z. Fan, H. Ma, Y. Tan and J. Qiao, Wear Vol. 261 (2001), p. 225.

[4] H. Ishida, and T. Agag, eds.: *Handbook of Benzoxazine Resins* (Elsevier, Amsterdam 2011).

[5] S. Rimdusit and H. Ishida, Polymer Vol. 41 (2000), p. 7941.

[6] C. Jubsilp, T. Takeichi and S. Rimdusit, Polym. Degrad. Stabili. Vol. 96 (2011), p. 1047.

[7] S. Rimdusit, C. Jubsilp, and S. Tiptipakorn: *Alloys and Composites of Polybenzoxazine: Properties and Applications* (Springer, Singapore 2013).

[8] S. Rimdusit, S. Tiptipakorn, C. Jubsilp and T. Takeichi: React. Funct. Polym., Vol. 73 (2013), p. 369.

[9] S. Rimdusit, P. Kunopast and I. Dueramae, Polym. Eng. Sci. Vol. 51 (2011), p. 1683.

[10] S. Rimdusit, S. Pirstpindvong, W. Tanthapanichakoon and S. Damrongsakkul, Polym. Eng. Sci. Vol. 45 (2005), p. 288.

[11] T. Takeichi, Y. Guo and S. Rimdusit, Polymer Vol. 46 (2005), p. 4909.

[12] J. Jang and D. Seo, J. Appl. Polym. Sci. Vol. 67 (1998), p. 1.

[13] H. Ishida, U.S. Patent 5,(543) (1996),p.516.

[14] N. Chikhi, S. Fellahi and M. Bakar, Eur. Polym, J. Vol. 38 (2002), p. 251.

[15] T. Agag and T. Takeichi, High Perform. Polym. Vol. 13 (2001), p.S327.

Key Engineering Materials Vol 659 (2015) pp 511-515
© (2015) Trans Tech Publications, Switzerland
doi:10.4028/www.scientific.net/KEM.659.511

Submitted: 2015-01-02
Revised: 2015-03-10
Accepted: 2015-04-01

Thermal and Mechanical Properties of Acrylonitrile-Butadiene Rubber Modified Polybenzoxazine as Frictional Materials

Jakkrit Jantaramaha[1], Chanchira Jubsilp[2] and Sarawut Rimdusit[1*]

[1]Polymer Engineering Laboratory, Department of Chemical Engineering,

Faculty of Engineering, Chulalongkorn University, Bangkok, 10330, THAILAND

[2]Department of Chemical Engineering, Faculty of Engineering, Srinakharinwirot University, Nakhonnayok, 26120, THAILAND

*Corresponding author: sarawut.r@chula.ac.th

Keywords: Polybenzoxazine, Acrylonitrile-butadiene rubber, Frictional composite

Abstract

Frictional composites based on polybenzoxazine (PBA-a) and acrylonitrile-butadiene rubber (NBR) are developed in this study. Mechanical, thermal and tribological properties of the PBA-a/NBR composites at 0, 2, 5, 10 and 15wt% of NBR particle contents are evaluated. Curing behaviors of the NBR-benzoxazine molding compounds are examined by differential scanning calorimetry to show an exothermic peak of about 222°C compared with that of the benzoxazine resin, i.e. 232°C suggesting curing acceleration of the benzoxazine resin due to the presence of the NBR particles. The storage modulus of the NBR-filled PBA-a is observed to systematically decrease from 5.2 GPa of the neat PBA-a to 2.8 GPa with an addition of 15wt% of the rubber particles. Glass transition temperature (T_g) of the composites evaluated by dynamic mechanical analysis increases with increasing of NBR particle contents, i.e. from 172°C for PBA-a to 186°C for PBA-a/15wt% NBR. Furthermore, the friction coefficients of the composites with 2wt% NBR are determined to be 0.603 for static type and 0.528 for kinetic type. Those values are improved from the value of 0.597 and 0.475 for unmodified polybenzoxazine, respectively. Therefore, the obtained outstanding properties, i.e. storage modulus, glass transition temperature and friction coefficient make the polybenzoxazine composites highly attractive to be utilized as friction materials.

Introduction

Organic formulations of brake pad materials generally contain polymers, i.e. phenolics and ingredients such as reinforcing fiber (Kevlar, asbestos and glass fiber), friction additives (alumina and graphite) and fillers ($CaCO_3$). In the past, asbestos was widely used in organic formulation-based brake pads. However, in recent years, it was discovered that breathing dust containing asbestos fibers can cause serious bodily harm [1]. Therefore, nowadays, non-asbestos organic brake pads were developed. The non-asbestos organic formula has four classes of ingredients consisted of binder, reinforcing fiber, frictional additives and fillers [2]. For the binder, it was used to maintain the brake pads structural integrity under mechanical and thermal stresses. Recently, a new thermosetting phenolic resin namely benzoxazine resin (BA-a) is of our interest as a binder of friction materials. The BA-a can be synthesized from phenol, formaldehyde and amine. The resin can undergo ring-opening polymerization without the use of catalysts or curing agents and do not produce by-products upon curing. Polybenzoxazines have outstanding properties such as low melt viscosity before curing, high glass-transition temperature (T_g), high thermal stability as well as excellent mechanical properties. Furthermore, polybenzoxazines possess a relatively good dimensional stability after curing with low water absorption characteristic thus makes these polymers highly useful in vast applications such as highly filled composites [3,4]. In the case of fillers such as rubber, $CaCO_3$ and $BaSO_4$, they act to prevent lining cracking, reduce brake noise and overall cost of brake pads. In particular, rubber particle fillers can be added to suppress brake noise, improve toughness and impact strength of friction materials [5,6]. For reinforcing fibers, i.e.

Kevlar pulp and glass fiber, they were used to improve mechanical strength of the frictional materials. Moreover, frictional additives, i.e. lubricant (graphite) and abrasive (zirconium oxide and silica) were also added into the friction composites to reduce wear behaviors.

This research aims to study effects of NBR powder in a novel polybenzoxazine binder on mechanical, thermal and tribological properties for an application of friction composite materials. Those essential properties include storage modulus, glass transition temperature, curing temperature and friction coefficient to determine friction material performance of the obtained PBA-a/NBR composite systems.

Experimental

Materials

The materials in this research are benzoxazine resin and acrylonitrile-butadiene rubber. Benzoxazine resin (BA-a) is based on bisphenol-A, formaldehyde and aniline. Thai Polycarbonate Co., Ltd. (TPCC) supplied bisphenol-A (polycarbonate grade). Paraformaldehyde (AR grade) was purchased from Merck Company and aniline (AR grade) was obtained from Panreac Quimica SA Company. NBR particle (bound acrylonitrile~34.5%) was purchased from Lanxess emulsion rubber, France. The average particle size of NBR is about 0.12 mm and the density is 1.2 g/cm^3.

Synthesis ofbenzoxazine resin

Benzoxazine resin was synthesized by using bisphenol-A, formaldehyde and aniline in the molar ratio of 1:4:2 at 110°C for 40 min according to a patented solventless method disclosed in U.S. Patent 5,543,516 [7]. The obtained resin is clear-yellowish solid at room temperature and the solid benzoxazine resin is then ground to fine powder and kept in a refrigerator for future-use.

Preparation of polybenzoxazine/NBR rubber composites

The NBR-filled polybenzoxazine composites with NBR contents of 0, 2, 5, 10 and 15wt% were prepared. The NBR particles were mechanically mixed with benzoxazine resin to achieve uniform dispersion of molding compounds by using an internal mixer at about 110°C for 30 min. Then, the molding compounds were thermally cured at 200°C for 2 hours under a hydraulic pressure of 10 MPa using a compression-molder. The fully cured composite samples were air-cooled to room temperature in the open mold before characterizations.

Sample characterizations

Differential scanning calorimetry (DSC). Differential scanning calorimetry (DSC model 2910, TA instruments, USA) was performed in order to study curing behavior of samples. For each experimental, a small amount of the molding compounds ranging from 5 to 10 mg was placed on the aluminum pan with lids. The experiment was performed using a heating rate of 10°C/min from 30°C up to 300°C under nitrogen purging at 50 ml/min.

Dynamic mechanical analysis (DMA). Dynamic mechanical analysis (model DMA242C, Netzsch, Germany) was used to investigate thermomechanical properties of the composites. The dimension of samples was 50 mm × 10 mm × 2.5 mm. The test was achieved under the three-point bending mode. The strain was applied sinusoidally at a frequency of 1 Hz. The temperature was scanned from 30°C to 300°C with a heating rate of 2°C/min at a test frequency of 1 Hz and strain amplitude of 15 μm under nitrogen atmosphere.

Ball-on-disc tribometer. The friction behaviors of polybenzoxazine/NBR friction composites were evaluated using a ball-on-disc tribometer from CSM Instrument Ltd., Switzerland. The dimension of samples was 50 mm in diameter and 6 mm in thickness. The friction tests were conducted at a linear speed of 36.6 cm/s and a load of 10 N at room temperature for distance of 1000 m.

Results and Discussion

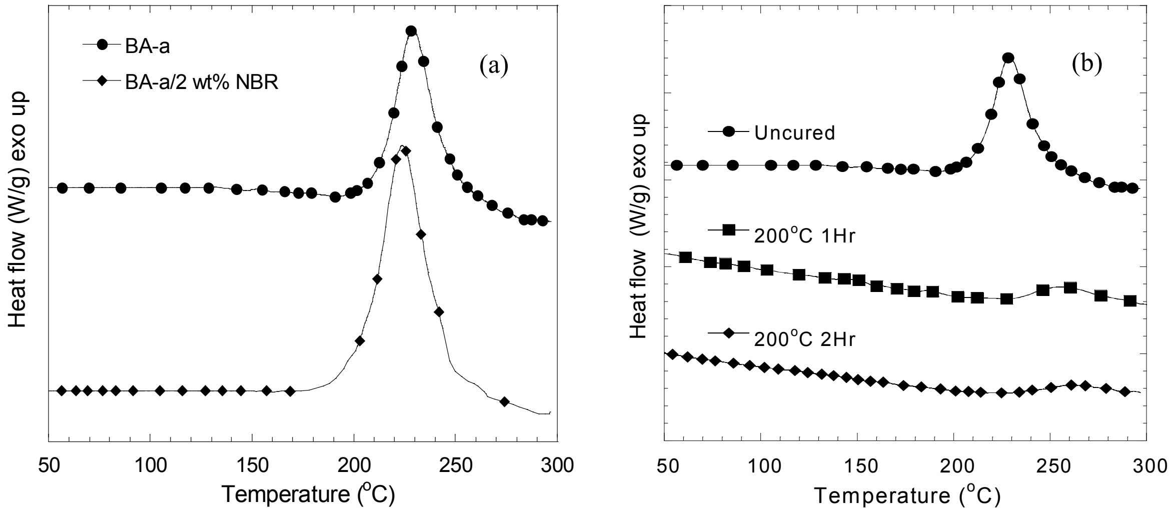

Figure 1 DSC thermograms of (a) BA-a and BA-a/NBR (98/2) compounds and (b) BA-a/NBR (98/2) compound at various curing times.

Curing behaviors of benzoxazine resin and benzoxazine/NBR molding compound

The curing behavior of benzoxazine resin filled with 2wt% NBR content was detected by differential scanning calorimeter in a temperature range of 30°C to 300°C and at a heating rate of 10°C/min is shown in Fig. 1(a). From the figure, the exothermic peak of the neat benzoxazine resin observed at 232°C was attributed to the ring-opening polymerization of its oxazine-ring. Remarkably, the curing peak maximum of the BA-a resin was evidently shifted to lower temperature, i.e. 222°C with the addition of 2wt% NBR. The result indicating that NBR could act as a catalyst for oxazine-ring opening reaction. In addition, area under exothermic peak indicated the heat of reaction of the polymerization from monomer to polymer as seen in Fig. 1(a) was increased with the addition of NBR in the molding compound. The values increased from 277 J/g for the neat BA-a resin to 597 J/g for BA-a/NBR (98/2) molding compound. This expected phenomenon is related to the chemical reaction between NBR and polybenzoxazine as we can observe the polymerization can occur at onset temperature of 190°C for the BA-a/NBR (98/2) compound which is faster than that of the neat BA-a resin, i.e. 210°C. Furthermore, Fig. 1(b) exhibited the DSC thermograms of 2wt% NBR-filled benzoxazine molding compound cured at 200° at curing time of 0, 1 and 2 hours. In theory, the fully cured stage has been reported to provide a polymer with desirable properties including sufficiently high thermal and mechanical integrity. From the figure, the heat of reaction of the uncured BA-a/NBR (98/2) molding compound determined from the area under the exothermic peak was measured to be 597 J/g and the value decreased to 42 J/g and 19 J/g for curing times of 1 hour and 2 hours, respectively, which corresponded to the degree of conversions estimated by Eq. (1) about 92% and 97% after curing at 200°C for 1 hour and 2 hours, respectively. The curing condition at 200°C for 2 hours was therefore used to cure all benzoxazine/NBR molding compounds to prepare the samples for further characterization.

$$\%\ \text{conversion} = \left(1 - \frac{\mathrm{H_{rxn}}}{\mathrm{H_0}}\right) \times 100 \qquad (1)$$

Where H_{rxn} is the heat of reaction of the partially cured samples, H_0 is the heat of reaction of the uncured benzoxazine resin.

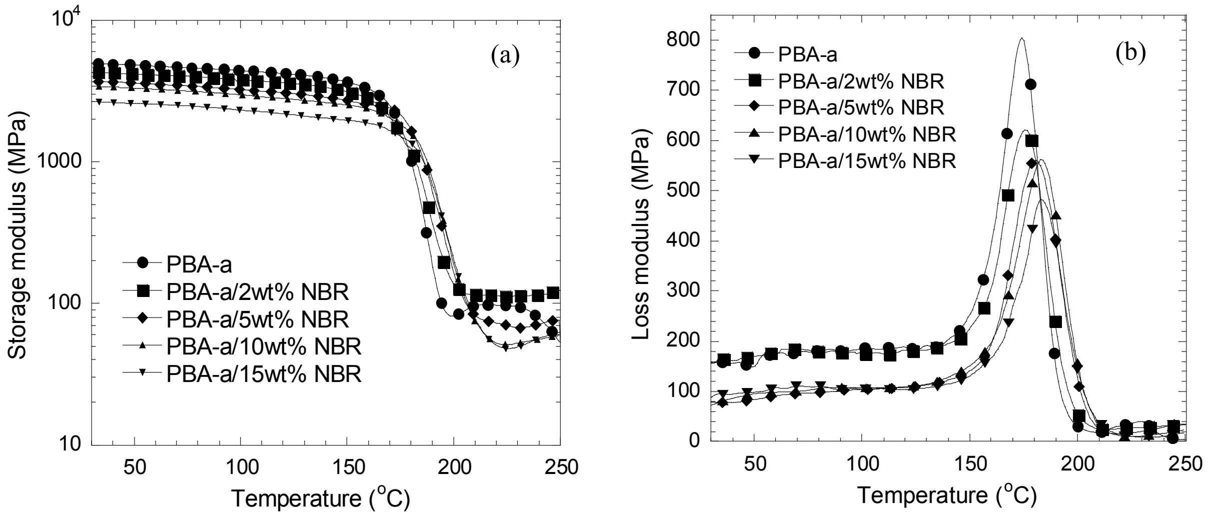

Figure 2 DMA thermograms of PBA-a/NBR composites (a) storage modulus (b) loss modulus.

Dynamic mechanical properties of NBR-filled polybenzoxazine composites

Thermomechanical properties, i.e. storage modulus (E') and loss modulus (E'') of NBR-filled polybenzoxazine (PBA-a) composites with the NBR content ranging from 0 to 15wt% are shown in Fig. 2(a) and Fig. 2(b), respectively. From the results, the storage modulus at room temperature of the composites was decreased from 5.2 GPa of the neat PBA-a to 2.8 GPa at 15wt% of NBR. Furthermore, the minor peak of the neat PBA-a in the rubbery plateau region was observed. This characteristic implied that the fully cure of the PBA-a cannot be achieved under the previous curing condition. However, in the case of PBA-a/NBR composites, the minor peak at the rubbery plateau region of the composites disappeared. Therefore, this behavior indicates that the NBR acts as a catalyst for oxazine ring-opening reaction.

Loss modulus curves of NBR-filled PBA-a at 0-15wt% of NBR contents as a function of temperature were also investigated as depicted in Fig. 2(b). From the figure, glass-transition temperatures (T_g) obtained from the maximum peak of loss modulus curve of the NBR-filled PBA-a composites were reported. The T_g values of the composites were observed to be in the range of 172°C to 186°C which were higher than that of the neat PBA-a as reported to be 172°C. It could be seen that the T_g values systematically increased with increasing of NBR contents in the PBA-a composites. This phenomenon may be due to good interfacial adhesion between the NBR filler and the polybenzoxazine matrix as previously reported by Nair [8].

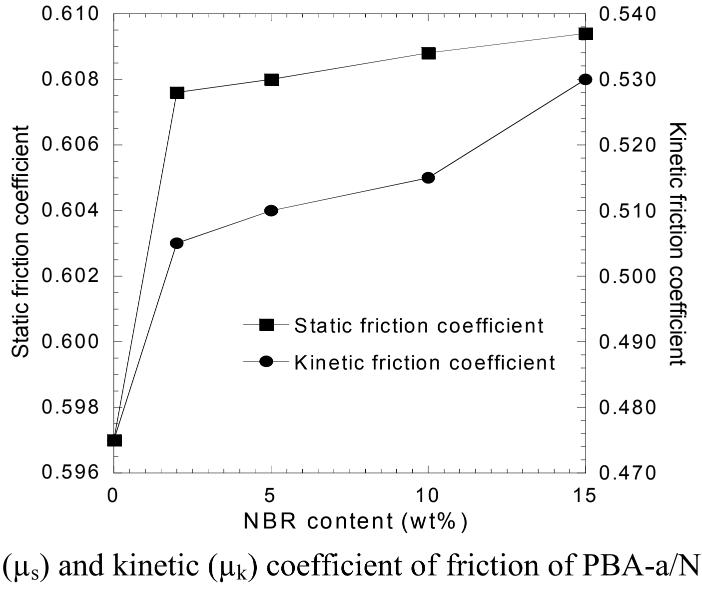

Figure 3 Static (μ_s) and kinetic (μ_k) coefficient of friction of PBA-a/NBR composites.

Friction properties of NBR-filled polybenzoxazine composites

The friction properties of the NBR-filled polybenzoxazine composites are shown in Fig. 3. The results showed that the static friction coefficient (μ_s) is greater than kinetic friction coefficient (μ_k) for all formulations. This behavior means that the force required to initiate sliding (static friction) is larger than the force needed to maintain sliding (kinetic friction) as discussed in Ref. 9. Furthermore, the static friction coefficient of the composites tended to increase with increasing NBR content in the composites. The values of static friction coefficient of the composites were about 0.597, 0.603, 0.604, 0.605 and 0.608 for the addition of NBR content of 0, 2, 5, 10 and 15 wt%, respectively. Moreover, the values of kinetic friction coefficient of PBA-a/NBR composites were also increased from 0.475 for PBA-a to 0.537 for PBA-a/15wt% NBR.

Summary

The curing temperature of the composites was reduced with the addition of NBR in polybenzoxazine composites. The optimal curing condition to obtain the fully-cured specimens of NBR-filled polybenzoxazine was 200°C for 2 hours in a hydraulic hot-pressed machine at 10 MPa. The glass transition temperatures of the obtained composites increased with increasing NBR content, while the storage modulus at room temperature of the composites were decreased with increasing NBR content. Furthermore, the friction coefficient of the polybenzoxazine composites was improved with the addition of NBR.

Acknowledgements

This research has been supported by the Ratchadaphiseksomphot Endowment Fund 2014 of Chulalongkorn University (CU-57-056-EN) and a New Researcher’s Grant of Thailand Research Fund-Commission on Higher Education (MRG5580101) and Matching Fund, Strategic Wisdom and Research Institute, Srinakharinwirot University 2012-2014 (Contact Grants No. 411/2555).

References

[1] M.S. Kanarek, Mesothelioma from Chrysotile Asbestos: Update, Annals of Epidemiology. 21 (2011) 688-697.

[2] J. Bijwe, Composites as friction materials: Recent developments in non-asbestos fiber reinforced friction materials—a review, Polymer Composites. 18(1997) 378-396.

[3] S. Rimdusit, S. Tiptipakorn, C. Jubsilp, T. Takeichi, Polybenzoxazine alloys and blends: Some unique properties and applications, Reactive and Functional Polymers. 73(2013) 369-380.

[4] A. Chernykh, T. Agag, H. Ishida, Novel benzoxazine monomer containing diacetylene linkage: An approach to benzoxazine thermosets with low polymerization temperature without added initiators or catalysts, Polymer. 50(2009) 3153-3157.

[5] Nidhi, J. Bijwe, NBR-modified resin in fade and recovery module in non-asbestos organic (NAO) friction materials, Tribology Letters. 27(2007) 189-196.

[6] J. Liu, T. Agag, H. Ishida, Main-chain benzoxazine oligomers: A new approach for resin transfer moldable neat benzoxazines for high performance applications, Polymer. 51(2010) 5688-5694.

[7] H. Ishida, U.S. Patent 5,543,516 . (1996).

[8] C.P. Nair, Advances in addition-cure phenolic resins, Prog. Polym. Sci. 29 (2004) 401–498.

[9] A.E. Jiménez, M.D. Bermúdez, Friction and Wear, in J.P. Davim (Eds), Tribology for Engineers: A practice guide, first ed., Woodhead Publishing Limited, Cambridge, 2011, pp. 33-63.